INVESTIGATING ALLOSTERIC REGULATION OF ABL AND BCR-ABL KINASES: IMPLICATIONS FOR SMALL MOLECULE INHIBITORS

by

Shoghag B. Panjarian

Bachelor of Science in Clinical Laboratory Sciences, Haigazian University, 1999

Master of Science in Human Physiology, American University of Beirut, 2003

Submitted to the Graduate Faculty of

The University of Pittsburgh School of Medicine in partial fulfillment

of the requirements for the degree of

Doctor of Philosophy

University of Pittsburgh

2012

UNIVERSITY OF PITTSBURGH

SCHOOL OF MEDICINE

This dissertation was presented

by

Shoghag B. Panjarian

It was defended on

November 2nd, 2012

and approved by

Thomas E Smithgall, Ph.D., Major Thesis Advisor, Microbiology and Molecular Genetics

Yu Jiang, Ph.D., Thesis Committee Chair, Pharmacology and Chemical Biology

Billy W. Day, Ph.D., Pharmaceutical Sciences and Chemistry

John R. Engen, Ph.D., Chemistry and Chemical Biology, Northeastern University

Qiming Jane Wang, Ph.D., Pharmacology and Chemical Biology

Jack Yalowich, Ph.D., Pharmacology, Ohio State University

INVESTIGATING ALLOSTERIC REGULATION OF ABL AND BCR-ABL KINASES: IMPLICATIONS FOR SMALL MOLECULE INHIBITORS

Shoghag B. Panjarian, PhD

University of Pittsburgh, 2012

BCR-ABL is the oncogenic protein-tyrosine kinase responsible for the pathogenesis of chronic myelogenous leukemia (CML). Clinical management of CML has been revolutionized by imatinib, a selective ATP-competitive inhibitor of BCR-ABL kinase activity. Despite this clinical success, imatinib is less effective in advanced disease due to the emergence of drug resistant BCR-ABL mutants. Resistant mutations often arise in the drug binding site and include the most recalcitrant gatekeeper mutation, T315I. Other mutations arise outside the active site and allosterically reduce imatinib binding by promoting the active kinase conformation. Recently, a new class of allosteric BCR-ABL inhibitors, of which GNF-2 is the prototype, has been reported that targets the myristate-binding pocket of ABL. These compounds stabilize the inactive conformation of ABL and work in concert with ATP-competitive inhibitors to overcome imatinib resistance. Mounting evidence supports a regulatory influence of the non-catalytic SH3 and SH2 domains on BCR-ABL kinase domain. The major focus of this study was to exploit the intramolecular SH3:linker interaction, to stabilize the downregulated kinase domain conformation of BCR-ABL and sensitize the kinase to both imatinib and GNF-2. To achieve this goal, I engineered High Affinity Linker (HAL) variants of both ABL and BCR-ABL in which SH3:linker interaction was tightened through sequential addition of proline residues to the linker. Enhanced SH3:linker interaction induced long-range suppressive effects on the kinase activity in

c-ABL, allosterically stabilized both the active site and the myristate-binding pocket, and sensitized BCR-ABL to small molecule inhibitors.

Src family kinases (SFKs) are important mediators of BCR-ABL signal transduction and oncogenesis in CML. SFKs also play important roles in clinical resistance to imatinib in the absence of BCR-ABL mutations. In the second part of my project, I explored the effect of SFK-selective inhibitor, pyrazolopyrimidine A-419259, on myeloid cells transformed with clinically relevant imatinib resistant BCR-ABL mutants. While proliferation of cells expressing BCR-ABL E255V and Y253H was inhibited by A-419259, BCR-ABL T315I cells were not. Surprisingly, cells expressing BCR-ABL-T315I maintained SFK activity in the presence of the inhibitor. This observation suggests that BCR-ABL-T315I induces cross-resistance to drugs that inhibit SFKs in CML through direct phosphorylation of the SFKs.

TABLE OF CONTENTS

LIST OF FIGURES

LIST OF ABBREVIATIONS

ABD	Actin binding domain
Abl	Abelson tyrosine kinase
AGP	α1 acid glygoprotein
AKT	v-akt murine thymoma viral oncogene
ARG	Abl-related gene
Bcl-XL	Basal cell lymphoma-extra large
BCR	Breakpoint cluster region
CC	Coiled-coil
CBL	Cas-Br-M (murine) ecotropic retroviral transforming sequence
CD34	Cluster of differentiation 34
CML	Chronic myelogenous leukemia
CRK	v-crk sarcoma virus CT10 oncogene homolog (avian)
CRKL	v-crk sarcoma virus CT10 oncogene homolog (avian)-like
EGFR	Epidermal growth factor receptor
ERK	Extracellular signal-regulated kinase
FYN	FYN oncogene related to SRC, FGR, YES
GMCSF	Granulocyte monocyte colony stimulating factor
GRB2	Growth factor receptor bound protein 2

GSK3	Glycogen synthase kinase 3β
HCK	Hematopoietic cell kinase
HX MS	Hydrogen exchange mass spectrometry
INF-α	Interferon-α
JAK	Janus family of non-receptor tyrosine kinases
KIT	v-Kit Hardy-Zuckerman 4 feline sarcoma viral oncogene homolog
LYN	v-yes-1 Yamaguchi sarcoma viral related oncogene homolog
MAPK	Mitogen-activated protein kinase
PDGFR	Platelet-derived growth factor receptor
Ph	Philadelphia chromosome
PI3K	Phosphatidylinositol-3 kinases
SAXS	Small angle X-ray scattering
SFK	Src family kinase
SH	Src homology
SHP1	SH2 domain-containing protein tyrosine phosphatase
SRC	v-Src avian sarcoma (Schmidt-Ruppin A-2) viral oncogene homolog
STAT	Signal transducer and activator of transcription
STI571	Signal transduction inhibitor 571
TKI	Tyrosine kinase inhibitor

ACKNOWLEDGMENTS

The time has come. Indeed!

This is the time to pause from defining hypotheses, discussing data, significance and future directions. This is the time to pause and focus not on the details (which I am very much prone to do), but to appreciate the picture as a whole. The picture I am referring to is the picture of “my journey as a graduate student”. If I were to freeze my journey in a framed painting, I am sure ***you*** would recognize the strokes of ***your*** paint brush. ***You*** have contributed so much that I am humbled and have trouble seeing my strokes.

My utmost gratitude goes to the person who took on the role of not just adding color to my journey, but took on the role of harmonizing a mixture of different colors. Dr. Thomas Smithgall, my thesis advisor, I thank you for welcoming me to your laboratory and to your research team. I still remember how determined I was to join your laboratory even before my arrival to Pittsburgh. I feel blessed and privileged that I had the chance to get to know you as a scientist and a mentor. I thank you for guiding and leading me in my academic journey. When I think of you and your mentorship, I am reminded of at least two skills that distinguish you as a mentor. First, I think of and thank you for your listening skill which assured me that I can knock on your door at any time and discuss the ups and downs of my research as well as the difficulties of my personal life. Your listening skill has been a great support system that I experienced fully. Second, I think of and thank you for your ability to motivate me. In times of frustration

concerning my research, you always guided me to transition from focusing on the problem to creating the solution. You always believed in me and helped me maximize my potential and outperform my research tasks.

My gratitude and appreciation goes to my dissertation committee members. I would like to thank you, Dr. Billy Day, for the support I received from you early on as my comprehensive exam committee chair. I would like to thank you, Dr. Jane Wang, for your constant enthusiasm about my research work. I would like to thank you, Dr. Yu Jiang, for chairing my dissertation committee. I would like to thank you, Dr. Yalowich, for your commitment to stay on my dissertation committee despite your move. Thank you ***all*** for being part of and for adding color to my journey with your critical questions, constructive advice and support.

I am deeply grateful to our collaborator who supported the dynamic nature of my thesis project- Dr. John Engen. First, I want to thank you for your commitment as a member of my dissertation committee. Thank you for creating the time to help me think critically and constructively about my project. Second, I am grateful for the opportunity to experience some hands-on hydrogen exchange mass spectrometry in your laboratory. Thanks to that experience, I am well aware of and more appreciative of the dynamic nature of proteins. Thank you also for your support and encouragement during the toughest times of my graduate career. I would also like to thank your team: Dr. Shugui Chen who initiated the ABL-HAL project while a graduate student in your laboratory. Drs Roxana Iacob and Thomas Wales. I want to thank you Thomas for introducing me to HX MS and to the data analysis software. I would like to thank you Roxana for running all the HX MS experiments on the different ABL proteins. I appreciate the time and effort you invested in running and analyzing the enormous set of data. Without your

input, we would not have been able to correlate the biological observations with the biophysical data. It has been my privilege to get to know you all and to collaborate with you.

I would like to thank the current members of the Smithgall laboratory: Dr. Lori Emert-Sedlak, Dr. Sabine Hellwig, Dr. Sherry Shu, Dr. Jerrod Poe, Jamie Moroco, Mark Weir, Prerna Grover, Sreya Tarafdar, Xiong Zhang, Kathleen Makielski and Julian Baptiste. Many thanks also to former lab members: Dr. Linda O'Reilly, Dr. Malcom Meyn, Dr. Teodora Pene-Dumitrescu, Dr. Jonathan Shaffer, Dr. Purushottam Narute and Terri Robinson. I want to thank you ***all*** for the moments we shared together-moments of laughter and of sorrow, moments of silence and of support. Thank you for your suggestions and scientific discussions that helped in the development and the progress of my thesis project. Many warm thanks to you, Lori for your support since the beginning of my graduate work. I cherished the moments we had together specially during the most difficult times of our lives. Many thanks to you, Linda, for your support and caring attention. I also want to thank you, Dora (Teodora) first for your friendship and second for your contagious enthusiasm about our research. I also hope that I was able to pass that enthusiasm to the "next generation BCR-ABL researcher", Prerna. Xiong and Prerna, I thank you for your lovely support and for being great friends.

I am certain that all of us who have been on this journey have a special story to tell. We all experienced peaks and valleys, we all got to know that we need to be in the valley to appreciate the peaks, and to know that one cannot exist without the other. However, I could not have appreciated the valleys along this journey and could not have enjoyed the peaks without the support and the unconditional love of my beloved family and friends. I want to thank each one of you, my beloved family, for your sacrifices and for your unconditional love. You believed in me,

you admired me, you lifted me up, you spoiled me and you made me feel special. I see your strokes, aren't the brightest ones yours?

Dear Moms, Nora, Sebouh, Norayr, Arax, Armand, Areen, Ayk, Karine, Sevag, Koko, Hrag, Aram, Armen, Alec and Araz as a token of my gratitude to you all, I would like to dedicate this dissertation to my beloved dad-Boghos. Dad, you inspired me, you passed down on me your determination and your love of life. You sacrificed a lot and I am sure you would have loved to witness this day; however I am sure your spirit is well satisfied and happy. I thank you and I always remember your words after our house got bombarded during the war; you said "I will re-build this house and you will go to school, do not worry". This is for you dad. Cheers!

I would like to thank the person who changed my life forever by her birth, her smile, her innocence, her patience, her energy and her love. Thank you my gem –Araz. Thank you for blessing my life in an unimaginable way.

Last but not least, I would like to thank the love of my life –Alec! Alec, I want to thank you for who you are. Thank you for your noble, gentle, humble and loving spirit. You have been my amazing partner, my true friend, my consultant, my counselor, and the loving father to our daughter. You held my hand and supported me at every step of this journey and by doing so you touched my soul. Thank you for helping me create my stand and thank you for believing in that stand. Thank you for always helping me to look at the bigger picture and not to be carried away by the complexities of the details. Thank you for helping me say ; "Life is Good".

1.0 INTRODUCTION

1.1 THE DISCOVERY OF PHILADELPHIA CHROMOSOME AND THE CLONAL EVOLUTION OF CANCER HYPOTHESIS

In the early nineteen hundreds and even prior to the determination of human chromosome number, Theodore Boveri proposed that tumors result from chromosomal abnormalities that originate in a single cell. The tumor is thus characterized as a genetically unstable cell population that is unresponsive to growth regulation. This hypothesis was later developed and supported as the "clonal evolution" model for tumor development (Boveri, 2008; Nowell, 2007).

With the advancement of cell and tissue culture techniques, the human chromosome number was determined. Furthermore, chromosomal abnormalities were shown to be associated with certain human disorders such as Down syndrome (Harper, 2006). However, the association between specific chromosomal alteration and cancer was made for the first time by David Hungerford and Peter Nowell in 1960 (Nowell, 1962; Nowell, 2007). They identified a characteristic minute chromosome in neoplastic cells from chronic myelogenous leukemia (CML) patients. This minute chromosome was designated as the "Philadelphia (Ph) Chromosome" because it was discovered at the University of Pennsylvania School of Medicine in Philadelphia, where Dr. Nowell was a member of the Pathology faculty. In 1973, Janet Rowley discovered that the Ph chromosome arises from a reciprocal translocation between

chromosome 9 and chromosome 22 (Rowley, 1980). In the 1980s, John Groffen and Nora Heisterkamp showed that the Ph chromosome translocation, now known as t(9;22)(q34;q11), fuses the "breakpoint cluster region gene" (*BCR*) on chromosome 22 with sequences of the c-*ABL* proto-oncogene on chromosome 9. This fusion generates the *BCR-ABL* oncogene that encodes the constitutively active chimeric BCR-ABL protein (Lugo et al., 1990; Heisterkamp and Groffen, 2002) . There are three BCR-ABL variants that are associated with different types of leukemias (Figure 1). The three variants arise from differences in the position of the translocation, which affects the length of the *BCR* gene fused to *ABL* sequences. Splicing at the minor (m), major (M) or micro (μ) breakpoints in *BCR* produces three distinct proteins, p185, p210 and p230 respectively. The three variants differ in the amount of the BCR portion of the protein and are involved in acute lymphocytic leukemia (p185), chronic myelogenous leukemia (p210) and chronic neutrophilic leukemia (p230) (Lugo et al., 1990; Voncken et al., 1995; Advani and Pendergast, 2002). Work described in this thesis is related exclusively to the p210 form of BCR-ABL which is associated with more than 95% of CML cases.

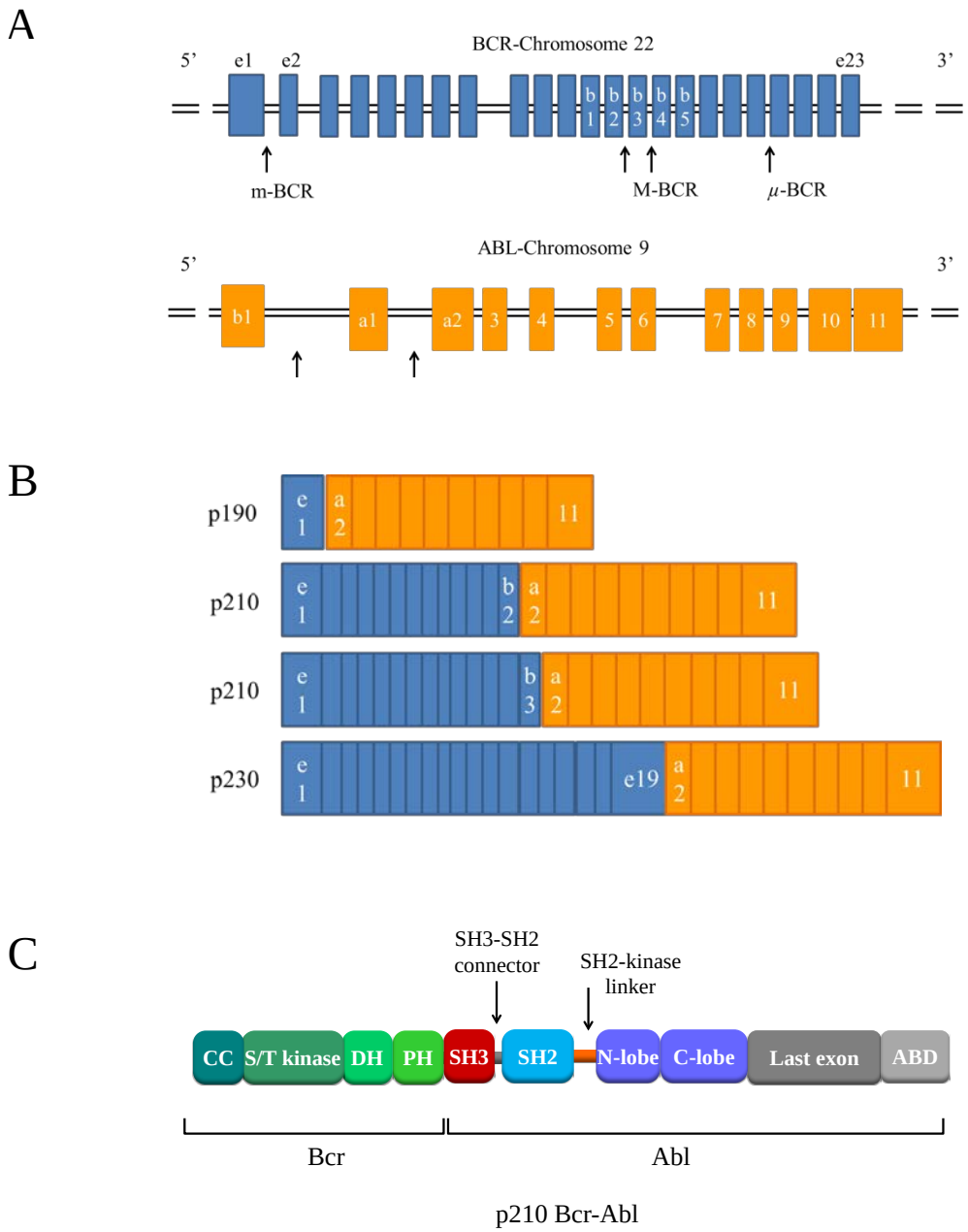

Figure 1: BCR-ABL variants. A) *BCR* and *ABL* genes and the site of the breakpoints in each are marked by the arrows. B) Chimeric *BCR-ABL* mRNA transcripts. C) Functional domain organizations of the chimeric p210 BCR-ABL protein. The BCR portion is composed of the following regions: CC: coiled-coil motif, S/T kinase: serine-threonine kinase, DH: Dbl homology domain, PH: pleckstrin homology domain. The ABL portion consists of SH3: Src homology domain 3, SH3-SH2 connector, SH2: Src homology domain 2, SH2-kinase linker, Tyrosine kinase

domain composed of an N-lobe and C-lobe, Last exon region composed of nuclear localization and export signals, proline rich regions (PxxP) capable of binding to SH3 domains, DNA binding domains, and ABD: actin binding domain. Adapted from (Inokuchi, 2006; Pendergast, 2002; Ren, 2005).

1.2 CML: CLINICAL COURSE, DISEASE INCIDENCE, MORTALITY AND SURVIVAL

CML is a clonal disorder that results from neoplastic transformation of hematopoietic stem cells. The presence of the Ph chromosome is the cytogenetic hallmark of this disease. The Ph chromosome encodes a constitutively active protein-tyrosine kinase known as BCR-ABL (p210 form) that drives CML pathogenesis through downstream signaling pathways promoting cell growth and survival (Sawyers, 1999; Wong and Witte, 2004; Nowell, 1962; Shtivelman et al., 1985; Groffen et al., 1984). The causal relationship between the expression of BCR-ABL and CML is well established by several experimental models. For example, retroviral transduction of murine bone marrow with p210 *BCR-ABL* oncogene was shown to induce myeloproliferative disease (MPD) in mice that resembled CML (Daley et al., 1990; Kelliher et al., 1990). Furthermore, the efficiency of MPD induction was increased when the p210 *BCR-ABL* oncogene was specifically expressed in hematopoietic stem or progenitor cells (Pear et al., 1998). In addition, studies using inducible expression of BCR-ABL in transgenic mice showed that mice developed a chronic phase CML like disease (Koschmieder et al., 2005).

CML is a rare disease and accounts for about 20% of all leukemias. It occurs at a similar frequency in different countries around the world. The annual incidence rate is 1.6 cases per 100,000 adults. The estimated number of new cases in the United States in 2012 is 5,430 and the

estimated deaths around 610. The median age at diagnosis is about 55 years (American Cancer Society, 2012).

Clinically, CML has a triphasic course and is usually diagnosed during the early chronic phase of the disease. The chronic phase is characterized by expansion of cells of the granulocytic lineage that retain their ability to differentiate. Most patients are diagnosed at this stage as a result of an increased number of mature granulocytes in the peripheral blood, weight loss and splenomegaly. This phase lasts approximately 5 years on average and then the disease progresses to the accelerated phase and the blast crisis phase. These later phases are characterized by the accumulation of immature blasts in the bone marrow and the peripheral blood and loss of hematopoietic cell differentiation. Phenotypically, the majority of the patients (~80%) enter a myeloid blast stage resembling acute myeloid leukemia (AML) and about 20% of the patients enter a stage similar to the acute lymphoid leukemia (B-ALL) (Kurzrock et al., 1988; Advani and Pendergast, 2002; Sawyers, 1999; Ren, 2005).

Allogeneic transplantation of bone marrow cells is the only curative treatment for CML. However, as discussed later in section 1.8, there are limitations to transplantation in terms of available compatible donors, age as well as large variability in 5 year survival rate. However, since BCR-ABL is required for the onset and maintenance of CML, it has become an ideal therapeutic target for long-term disease management. Imatinib mesylate (Signal Transduction Inhibitor-STI571; Gleevec) is a derivative of 2-phenylaminopyrimidine and was discovered in a screen for inhibitors of the platelet-derived growth factor receptor tyrosine kinase (PDGF-R). In 1996, Druker and colleagues showed that imatinib selectively inhibits the proliferation of BCR-ABL positive cells in vitro and in vivo (Druker et al., 1996). In 2001, FDA approved imatinib as the frontline therapy for CML (Schwetz, 2001). Imatinib is well-tolerated and most chronic

phase CML patients attain significant hematologic and cytogenetic responses. The relatively low toxicity of imatinib may be attributed to its selectivity for BCR-ABL, which is derived in part from its remarkable preference for the inactive conformation of the ABL kinase domain as discussed in the next section.

1.3 OVERVIEW OF C-ABL

The Abelson family of non-receptor protein-tyrosine kinases consists of two members, c-ABL and the ABL-related gene (ARG) (Hanks, 2003). c-ABL interacts with multitude of cellular proteins including transcription factors, the DNA repair machinery, cell cycle regulators, phosphatases and other kinases, signaling adaptors and the cytoskeleton. By the virtue of these interactions, c-ABL functions in many cellular processes including F-actin remodeling, cell adhesion and motility, DNA damage responses, cell proliferation and survival (Colicelli, 2010; Pendergast, 2002). There are two splice variants of c-ABL that differ in their amino termini; c-ABL 1b is myristoylated at the N-terminus while the splice variant c-ABL 1a is 19 amino acids shorter and not myristoylated (Shtivelman et al., 1986). Both forms of c-ABL have nuclear localization sequences, nuclear export signals, C-terminal actin binding domains and shuttle between nuclear and cytoplasmic compartments in a cell (Van Etten, 1999; Pendergast, 2002).

1.4 STRUCTURAL OVERVIEW OF THE C-ABL KINASE CORE

The kinase core of the c-ABL protein has a domain organization similar to that of the Src-family kinases (SFKs), and is comprised of an SH3 domain, an SH2 domain, an SH2-kinase linker and a tyrosine kinase domain that spans about 300 amino acids and structurally is composed of two lobes: the smaller amino-terminal lobe (N-lobe) and a larger c-terminal lobe (C-lobe) (Hubbard et al., 1994; Knighton et al., 1991; Superti-Furga and Courtneidge, 1995). However regions N-terminal to the SH3 domain and C-terminal to the kinase domain are different in c-ABL vs. c-SRC. At the N-terminus, c-ABL has an extended unique domain called the N-terminal "cap" (referred to hereafter as the NCap) while at the C-terminal end of the kinase domain there is a long cytoplasmic region called the last-exon region, which is important in subcellular localization and interaction of the protein with DNA, other SH3 containing proteins, and the actin cytoskeleton (Hantschel and Superti-Furga, 2004; Pendergast, 2002; Van Etten, 1999). Each of these key structural and regulatory elements is discussed in detail below.

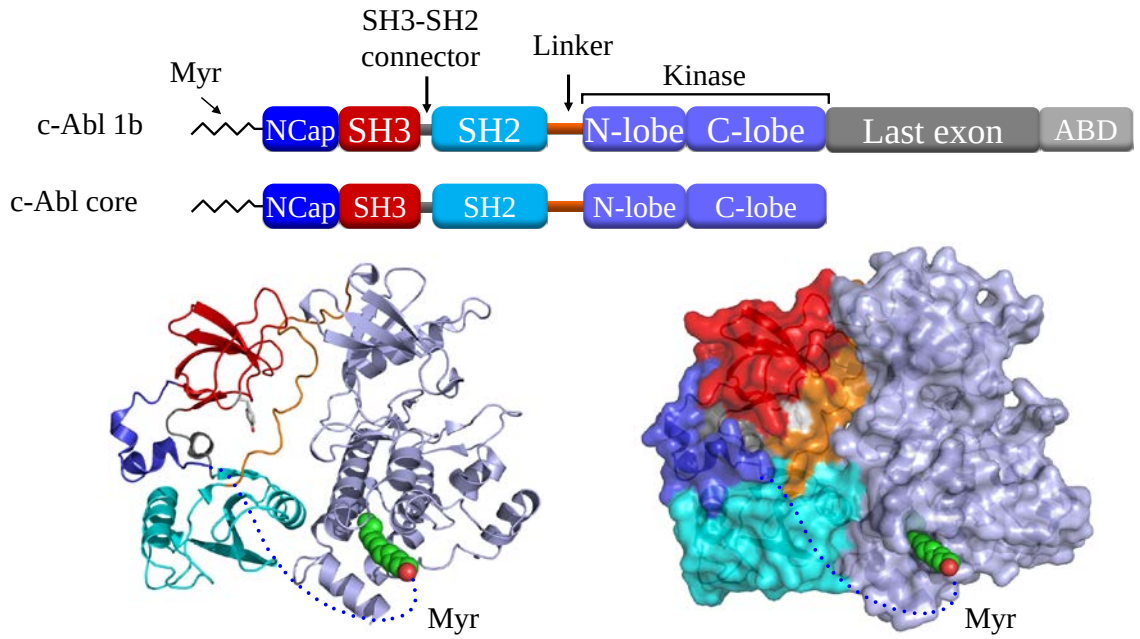

Figure 2: Domain Organization of ABL kinase. *Top*: Schematic domain organization of c-ABL 1b and c-ABL 1b core proteins: Ncap: N-terminal region, SH3: Src homology domain 3, SH2: Src homology domain 2, SH2-kinase linker (Linker), N-and C-lobe of tyrosine kinase domain, Last exon or c-terminal region, ABD: actin binding domain. *Bottom* X-ray crystal structure of c-ABL 1b core protein in the downregulated state (PDB 2FO0) is rendered as a ribbon on the lower left and with surface added on the right. The unstructured section of the myristoylated NCap (Myr) that engages the C-lobe of the kinase domain is shown as dotted line. Domains in the structure are color coded and correspond to the schematic in the top.

1.4.1 N-Terminal Cap (NCap)

The first exon and part of second exon of the human *ABL1* gene encodes an 80-residue region called the “NCap”. The NCap is located N-terminal to the SH3 domain and is myristoylated at its N-terminus in ABL-1b (Pluk et al., 2002). Prior to the first crystal structure of the c-ABL-1b core protein, mutational studies suggested that the NCap region has a role in inhibiting the kinase activity because its loss leads to activation of the c-ABL kinase. When the first crystal structure

of the core of ABL (residues 1-531) was solved, it became evident that the N-terminal myristic acid group penetrates into a deep hydrophobic pocket of the C-lobe of the kinase domain (Nagar et al., 2003) (Figure 2). Binding of the myristoyl group into this pocket induces a bend in helix αI which is also important for docking of the SH2 domain onto C-lobe of the kinase. Myristoylation is critical to maintaining autoinhibited state of the kinase as a non-myristoylated mutant of ABL-1b with a glycine to alanine mutation at position 2 (G2A) is highly active. Furthermore, when amino acids in the C-lobe pocket are replaced with bulkier or polar residues, the kinase is activated (Hantschel et al., 2003). Presumably, the myristoylated NCap is unable to interact with these C-lobe mutants. In addition, these changes may allosterically influence the active site as described in more detail below.

Besides the myristoyl moiety, the NCap has important contact points along the SH3-SH2 surface that also maintain the autoinhibited state of the kinase. NCap residues Leu73 and Lys70 are proximal to the first β strand of SH3 domain and when they are individually mutated to alanines, induce kinase activity (Hantschel et al., 2003; Pluk et al., 2002). In the first crystal structure of c-ABL core (Nagar et al., 2003), the entire NCap region connecting the myristoyl group to the SH3 domain was disordered. Subsequently a higher resolution crystal structure was solved with an ABL core protein that spanned residues 1-531 with an internal deletion of residues 15-56 (Nagar et al., 2006). This deletion was shown to be dispensable for maintaining effective regulation of kinase activity (Hantschel et al., 2003). In this newer structure, Ser69 in the NCap was observed to be phosphorylated and to make contact with the SH3-SH2 connector. ABL activity was increased when Ser69 was mutated to alanine but more so if mutated to glutamate (Nagar et al., 2006). In summary, the N-terminal myristoyl group of the NCap makes a key regulatory contact with the C-lobe of the kinase, while the C-terminal region of the NCap

spanning residues 65-80 contacts the SH2 surface and the SH3-SH2 connector. Thus, the NCap helps in clamping the SH3 and SH2 domains to the back of the kinase domain, favoring the auto-inhibited state.

1.4.2 SH3 domain

Src homology 3 (SH3) domains are small protein modules of about 60 amino acids. The first structure of an SH3 domain was reported in 1992 for c-SRC (Yu et al., 1992). Subsequently, a high resolution x-ray crystal structure of ABL SH3 domain was solved (Musacchio et al., 1994). Like other SH3 domains, the ABL SH3 is comprised of two small anti-parallel β-sheets packed against each other forming a barrel-shaped structure. SH3 domains bind to proline-rich peptides or stretches in partner proteins that adopt polyproline type II (PP-II) helical conformations (Kuriyan and Cowburn, 1997; Pawson and Gish, 1992; Pawson and Schlessingert, 1993) and often exhibit repeats of proline residues to form the sequence PxxP (where x is often a hydrophobic amino acid). Though SH3 domains were primarily considered as binding domains, it is now evident that they play an essential role in regulating kinase activity. The ABL SH3 domain plays a major role in keeping the kinase in its autoinhibited state by interacting with the amino-terminal lobe of the kinase domain as well the SH2-kinase linker through an atypical PxxP motif ($P_{242}TVY_{245}$) (Nagar et al., 2003). This interaction persists even in the absence of the kinase domain (Hochrein et al., 2006). Deletion or mutations of the SH3 domain enhance the transforming activity of c-ABL supporting a negative regulatory role for SH3 in kinase regulation (Franz et al., 1989; Mayer and Baltimore, 1994). Moreover phosphorylation of Tyr245 in the SH2-kinase linker or mutation of Pro242 can increase kinase activity (Barila and Superti-Furga, 1998; Brasher and Van Etten, 2000). Work from our laboratory also showed that

phosphorylation of ABL SH3 Tyr89 disturbs SH3:linker engagement and leads to enhanced ABL kinase activity and downstream signalling in the context of BCR-ABL (Chen et al., 2008b).

1.4.3 SH2 domain

Src homology 2 (SH2) domains are about 100 amino acids in length and participate in protein-protein interactions through sequence-specific recognition of phosphotyrosine-containing sequences. Structurally, SH2 domains are composed of a central anti-parallel β-sheet flanked by α-helices on each side. This central β-sheet divides the domain into two functionally distinct pockets, one which binds the P-Tyr side chain and another for binding of the side chain of the third amino acid C-terminal to the P-Tyr residue (Ladbury et al., 1995; Smithgall, 1995; Kuriyan and Cowburn, 1997). In SFKs, the SH2 domain engages a conserved phosphotyrosine residue in the C-terminal tail and this intramolecular interaction is critical to downregulation of kinase activity (Huse and Kuriyan, 2002). In contrast to c-SRC, however, c-ABL lacks a C-terminal phosphotyrosine residue, and the SH2 domain is coupled directly to the C-lobe of the kinase domain through network of hydrogen bonding interactions. Binding of the myristoylated NCap to the C-lobe reorients kinase domain helix αI which helps in docking to the SH2 domain (Hantschel et al., 2003; Nagar et al., 2003; Nagar et al., 2006). Several mutations at the SH2-C-lobe kinase interface, particularly of Tyr158, showed an increase in kinase activity demonstrating the importance of this interface in proper positioning of the SH2 domain and its contribution to downregulation of kinase activity (Hantschel et al., 2003). Furthermore, Small-angle X-ray Scattering (SAXS) analysis of a form of active ABL that is missing the NCap, myristoylation site and is mutated at two proline residues in the linker region (P242E, P249E), demonstrated that the

SH2 domain reorients itself to the N-lobe of the kinase and that this interaction may contribute to one active state of the protein (Nagar et al., 2006).

1.4.4 SH2-Kinase Linker

In c-ABL as well as SFKs the SH2-kinase linker forms a polyproline type II helix that serves as an internal ligand for the SH3 domain. This interaction is important in keeping the kinase in its downregulated form as describe above. Mutations disrupting SH3:linker interaction lead to kinase activation and enhance the transforming capability of both c-ABL and SFKs (Barila and Superti-Furga, 1998; Hantschel et al., 2003; Meyn, III et al., 2006; Briggs and Smithgall, 1999). Despite the overall structural similarities between SFKs and the c-ABL core, there are important differences in the SH2-kinase linker. The c-ABL SH2-kinase linker has a unique conformation created in part by the insertion of two residues (W254, E255) near the N-lobe of the kinase relative to SFKs. Biophysical evidence supports the persistence of SH3:linker interaction in the absence of the kinase domain and shows that W254 and E255 are important in stabilizing the linker and promoting SH3:linker interaction. This is in contrast to the SFK HCK, where SH3:linker interaction does not occur in the absence of the kinase domain. These results suggest that SH3:linker interaction may have a more prominent role in regulating the c-ABL kinase activity relative to the SFKs (Chen et al., 2007; Hochrein et al., 2006; Lerner et al., 2005).

1.4.5 Kinase domain

Overall protein kinase domain structure is highly conserved among Ser/Thr and Tyr kinases (Hubbard et al., 1994; Knighton et al., 1991). The kinase domain functions in the catalytic

transfer of γ-phosphate from ATP onto serine, threonine or tyrosine residues in substrate proteins and peptides (Hanks et al., 1988). The relative orientation of the two lobes and conserved residues in the active site play a major role in the catalytic reaction and in the dynamic interconversion of the active and inactive conformations of the kinase. Structural studies of kinases solved to date show that while the active conformations of most protein kinases are quite similar, the conformations of the inactive states are more varied and distinct, which provide opportunities for selective inhibitor discovery (Nagar et al., 2002; Zhang et al., 2009).

Structural analyses of the c-ABL kinase domain as well as the larger core protein described above revealed the structural basis of its regulation (Schindler et al., 2000; Nagar et al., 2002). The N-lobe of c-ABL is composed of a 5-stranded antiparallel β-sheet and a single α-helix called the αC helix. On the other hand, the C-lobe is mainly helical and contains the peptide substrate binding site and the catalytic loop (Cox et al., 1994). The two lobes contribute to the active site with important conserved residues. The loop connecting strands β1 and β2 in the N-lobe forms the phosphate binding loop or P-loop. A conserved glutamate (Glu286) from helix αC forms an ion pair with Lys271 of the N-lobe. This pairing is important in coordinating the phosphate group of ATP and is conserved in virtually all protein kinase structures. The orientation of helix αC also plays a major role in determining the active vs. inactive conformations of the kinase domain. In the inactive c-SRC and cyclin-dependent kinase structures, the αC helix is rotated out of the active site such that the Glu-Lys ion pair is disrupted. However, the orientation of the αC helix is unchanged and this ion pair is maintained in inactive ABL. The C-lobe contributes to the active site through the activation loop, another structural feature common to most kinases, with a single tyrosine site (Tyr412) that undergoes autophosphorylation. Phosphorylation of Tyr412 in the ABL activation loop allows electrostatic

interaction with a neighboring arginine residue, stabilizing an 'open' conformation of the active site and allowing the access to the peptide substrate. In the inactive conformation, Tyr412 is not phosphorylated and forms a hydrogen bond with the critical catalytic aspartate (Asp363) instead. This interaction orients the activation loop into the active site and mimics the binding mode of substrates. N-terminal to the activation loop is a highly conserved aspartate-phenylalanine-glycine ($D_{381}FG_{383}$) motif. In active kinases including ABL, the aspartate of the DFG motif is oriented towards the active site to coordinate a catalytically important magnesium ion. In inactive ABL, unlike in inactive c-SRC, this aspartate residue is flipped away from the active site, removing the side chain of Asp381 from the site of Mg^{++} coordination (so called 'DFG Out' conformation). This DFG-out conformation accounts in part for the specificity of imatinib binding to ABL (Schindler et al., 2000; Nagar et al., 2002; Levinson et al., 2006a; Nagar, 2007). (This point is explained in more detail in Section 1.9.1, below).

1.4.6 Last-exon region

Despite the structural similarities with SFKs noted above, c-ABL has a unique C-terminal extension beyond the kinase domain. This region contains proline-rich motifs that serve as binding sites for SH3 containing adaptor proteins. It also contains binding sites for tumor suppressor proteins, RNA polymerase II, DNA and F-actin. It also contains three nuclear localization signals and one nuclear export signal which are important in the subcellular localization of the protein (Feller et al., 1994; Smith et al., 1999; Goga et al., 1995a; Baskaran et al., 1996; Van Etten et al., 1989; Van Etten et al., 1994).

1.5 REGULATION OF C-ABL BY PHOSPHORYLATION AND PROTEIN PARTNER BINDING

The c-ABL protein is ubiquitously expressed and its activity is tightly regulated in cells. In the absence of activating stimuli, neither endogenous nor overexpressed c-ABL are phosphorylated (Brasher and Van Etten, 2000; Dorey et al., 2001). The crystal structures of the downregulated c-ABL core protein as well as biochemical studies revealed the key intramolecular interactions that are involved in regulating kinase activity. When these inhibitory intramolecular interactions are disrupted, phosphotyrosine content is increased which is positively correlated with activity (Barila and Superti-Furga, 1998). Thus phosphorylation at several tyrosine residues is crucial for regulation of ABL activity. Phosphorylation of Tyr412 in the activation loop is necessary to stabilize the active kinase activation as described in the previous section. This residue can undergo both autophosphorylation as well as *trans*-phosphorylation by other tyrosine kinases such as members of the SRC family. Mutation of this residue to phenylalanine impairs kinase activation (Brasher and Van Etten, 2000). Along with Tyr412, Tyr245 in the SH2-kinase linker contributes to the full activation of the kinase and mutation of this site inhibits maximal activation of c-ABL by about 50% in vitro (Brasher and Van Etten, 2000). Other phosphorylation sites implicated in c-ABL regulation include Tyr134 in the SH3 domain which is involved in binding to SH2-kinase linker. Phosphorylation of this residue is predicted to interfere with the proper interaction of the SH3 domain with the linker. Tyr238 in the N-lobe and Ser94 in the SH3 domain are two other residues that come into close proximity. Phosphorylation of these residues may interfere with the packing of the SH3 against the N-lobe of the kinase domain and disturb the inhibitory intramolecular interactions (Brasher et al., 2001). Furthermore,

phosphorylation of SH3 Tyr89 interferes with linker binding, thereby disrupting negative regulatory interaction and leading to kinase activation (Chen et al., 2008b).

Besides regulation by phosphorylation, c-ABL is also regulated through tyrosine phosphatases. Upon stress stimuli, SH3 domain of c-ABL interacts with SH3 binding motif in the catalytic domain of PTPN6 (also known as SHP-1). Overexpression of PTPN6 has also been implicated in reduction of the transforming potential of K562 cells, which were derived from a blast crisis CML patient and are p210 BCR-ABL-positive. PTPN12 and PTPN18 also dephosphorylate ABL and suppress its function (Kharbanda et al., 1996; Bruecher-Encke et al., 2001; Cong et al., 2000).

ABL is also regulated by interacting partners (Colicelli, 2010), and the interaction mechanisms are often complex. ABL may interact with other proteins through its SH2 or SH3 domains via phosphotyrosine sites or PxxP motifs within the interacting partner, respectively. Conversely, SH2 or SH3 domains on partner proteins may associate with their respective phosphotyrosine sites and PxxP motifs on ABL. Interactions may also occur through other binding motifs in the C-terminal region of the protein. One class of ABL-binding proteins include the ABL interactor proteins ABI1 and ABI2, which bind to the C-terminal region of ABL through their SH3 domains and also interact with ABL SH3 domain through their PxxP motifs. ABI1 binding enhances phosphorylation of ABL substrates and facilitates ABL oligomerization and autophosphorylation (Dai and Pendergast, 1995; Shi et al., 1995; Xiong et al., 2008). In the context of BCR-ABL expressing cells, ABI2 undergoes ubiquitin-dependent degradation while ABI1 does not (Li et al., 2007). ABI1 is phosphorylated and is a downstream substrate of BCR-ABL in hematopoietic cells. There is increasing evidence to support the role of ABI1 in BCR-ABL induced cytoskeletal remodeling, altered adhesion and migration of leukemic

cells (Li et al., 2007; Zhuang et al., 2011; Sato et al., 2011; Sun et al., 2008). The Ras effector protein RIN1 is another ABL interacting protein that binds to the ABL SH3 domain through its PxxP motif and to the ABL SH2 domain via a phosphotyrosine residue (Cao et al., 2008). Interaction of RIN1 with ABL removes the autoinhibitory contribution of both SH3 and SH2 domains and stabilizes the active conformation of ABL. Other interacting partners that are implicated in negative regulation of ABL kinase activity include but are not limited to PRDX1 (PAG) and TUSC2 (FUS1) (Wen and Van Etten, 1997; Lin et al., 2007).

1.6 CONFORMATIONAL DYNAMICS OF C-ABL PROTEIN

In collaboration with Professor John Engen at Northeastern University, our laboratory has previously studied the conformational dynamics of the ABL regulatory region (Ncap-SH3-SH2-linker) as well as the intact c-ABL core using Hydrogen Exchange (HX) coupled with Mass Spectrometry (MS). This section gives an overview of the principles of the HX MS technique and summarizes the findings of these previous studies which form the foundation for my thesis project.

1.6.1 Hydrogen exchange mass spectrometry (HX MS)

Proteins are dynamic macromolecules in solution that respond to different stimuli and their function and regulation cannot be fully understood based solely on a static structural view such as that provided by X-Ray crystallography. In this regard, HX MS is used to understand how conformational changes and dynamic properties of proteins correlate with structure and function.

Hence, HX MS reveals the dynamic aspects of a protein that complement available crystal structures (Engen, 2009).

The fundamental principle of HX MS is the exchange of hydrogen atoms (1.0078 Da) in proteins with deuterium atoms (2.0141 Da) upon exposure to D_2O solvent followed by detection and analysis of this exchange process by MS. The hydrogens that are detected by the exchange process are the backbone or amide hydrogens. These amide hydrogens are present in all amino acids except for proline and are hydrogen bonded either to other parts of the protein or to water. Thus the relative rate of exchange at the backbone is useful in studying conformational changes. The hydrogens in the side chains of amino acids are also deuterated during the exchange reaction. However, deuterium is back-exchanged during sample processing and does not contribute to the observed increase in mass. In contrast, hydrogens bonded directly to carbon do not undergo exchange (Figure 3 A).

During HX MS experiments, when temperature and pH are held constant, solvent accessibility and hydrogen bonding are the primary factors that affect the rate and location of deuterium incorporation. In folded proteins, hydrogens in highly dynamic regions exposed to solvent display fast deuteration while regions less exposed to solvent or involved in hydrogen bonding display slower exchange kinetics. Hence, when there is a conformational change that exposes certain regions of the protein to the solvent or changes local hydrogen bonding, the location and extent of deuterium exchange reflecting these changes can be monitored and detected over time.

In general, continuous deuterium labeling is commonly used to label proteins which are initially equilibrated in H_2O buffer at room temperature and physiological pH. Deuteration is initiated by diluting the protein in the same buffer except that D_2O is the solvent instead of H_2O.

The labeling reaction is then quenched at various time points (seconds to minutes to hours) by lowering the pH to 2.5 and the temperature to 0°C. Under these conditions, the rate of the exchange reaction is reduced by a factor of ~10^5, which is critical to limit back-exchange (Sebastien Brier and John R.Engen, 2008). Intact proteins are then sprayed into the mass spectrometer and monitored for increases in mass due to deuterium incorporation. Studying the change in mass of an intact protein over time reveals global changes but does not indicate the location of deuterium incorporation. Intact protein exchange may also reveal the presence of different populations of molecules that acquire deuterium at different rates. Such a difference may reflect the rate of interconversion between folded and unfolded protein states (more below). To have spatial resolution for the deuterium incorporation, proteins can be digested by pepsin under quench conditions, separated by chromatography and injected into MS. Subsequent detection and analysis of the peptic peptides can reveal the location of the deuterium incorporation (Wu and Engen, 2004; Wales and Engen, 2006; Sebastien Brier and John R.Engen, 2008; Marcsisin and Engen, 2010).

As discussed above, HX MS is capable of detecting populations of molecules and their interconversion between folded and unfolded states over time (Figure 3 B). When the refolding rate of a protein is much greater than the deuterium exchange rate, then the protein exhibits EX2 kinetics. EX2 kinetics is common in proteins and can be detected in the mass spectra as a single peak that increases in mass over the course of the labeling time. On the other hand, a rarer event in protein dynamics is termed EX1 kinetics. EX1 kinetics is observed when the rate of unfolding and refolding is much slower than the deuterium exchange rate. Proteins undergoing EX1 exchange exhibit a unique bimodal isotopic distribution in the mass spectra. The bimodal pattern is contributed by unfolded species that have higher mass due to more deuterium incorporation

than the folded species. Using HX MS, the Engen group discovered EX1 kinetics in the SH3 domain of Src-family kinase, HCK. The HCK SH3 domain undergoes a slow cooperative unfolding-refolding event under physiological conditions with a half-life of ~20 min. Using the HCK SH3 unfolding as a reference point, many other SH3 domains were studied and compared including the ABL SH3. Interestingly the ABL SH3 domain also exhibited slow cooperative unfolding with a half-life of ~10 min. This observation was crucial in establishing a biophysical approach to measuring the modification of the SH3 unfolding rate in the presence of SH3-binding ligands, SH3:linker interaction and in the cases of mutations or modifications in the linker or the SH3 domain itself.

A

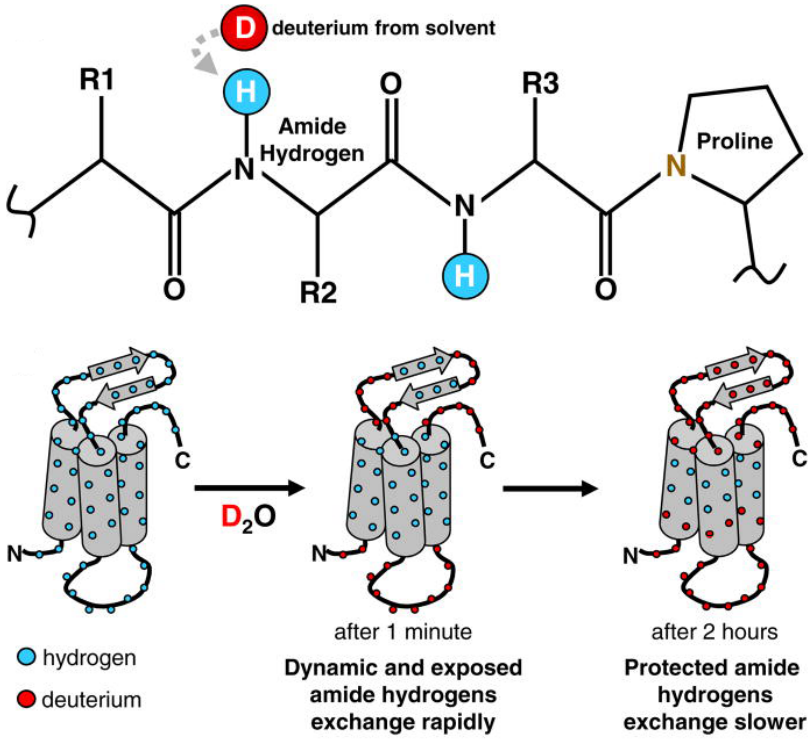

B

$$F_H \underset{k_{-1}}{\overset{k_1}{\rightleftharpoons}} U_H \xrightarrow[D_2O]{k_2} U_D \underset{k_1}{\overset{k_{-1}}{\rightleftharpoons}} F_D$$

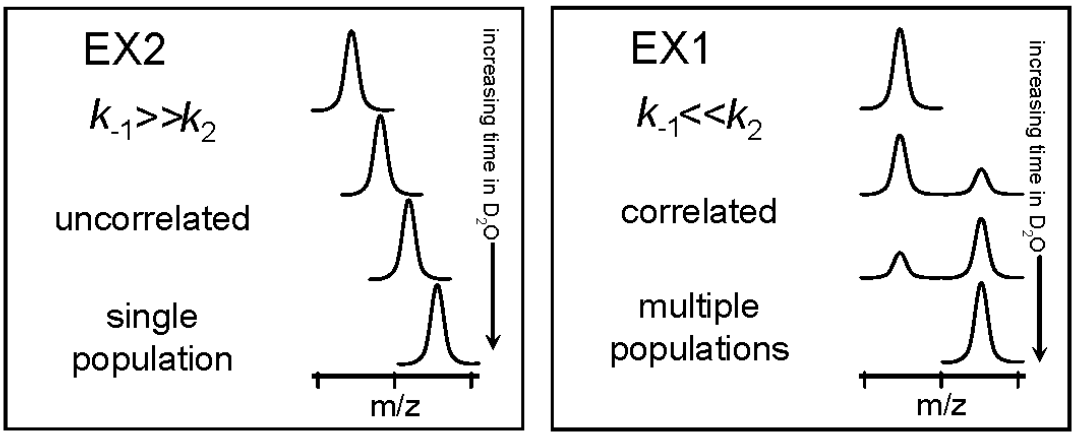

Figure 3: Overview of amide hydrogen exchange in proteins. A) Amino acid sequence showing amide hydrogens (blue). Backbone nitrogen (brown) in proline has no amide hydrogen. Amide hydrogens exchange with solvent hydrogens when exposed and become deuterated (red) when placed in a solution of D_2O. The exposed and dynamic regions of proteins will exchange more rapidly than protected regions as shown in the lower part of figure A. **B**) The equation showing the rate constants for unfolding (K_1) and refolding (K_{-1}) of proteins in solution. The lower panel shows EX1 and EX2 kinetics with their respective mass spectra. EX1 exchange occurs when the unfolding rate is faster than the refolding rate, resulting in two populations of molecules, one deuterated (higher mass peak) and the other not deuterated (lower mass peak). EX2 occurs when refolding rate is much faster than unfolding rate resulting in single population of molecules that increase in mass upon deuteration over time. Adapted from (Marcsisin and Engen, 2010; Weis et al., 2006).

The dynamic association between the ABL SH3 domain and the SH2-kinase linker was studied by monitoring the changes in cooperative unfolding of ABL SH3 domain. In this study, the unfolding of the SH3 domain upon association with the linker was determined in a series of recombinant ABL SH3-SH2-linker proteins that lacked the kinase domain. To define the linker residues necessary for the association, the constructs included different lengths of the linker. Comparison of the rate of SH3 domain unfolding in SH3-SH2 proteins with and without the linker showed that the presence of the linker slowed down the unfolding rate, providing direct evidence for SH3:linker interaction. However, a shortened version of the linker that lacked the last two residues (Trp254 and Glu255) restored the SH3 unfolding rate to that observed in the absence of the linker. This experiment defined the minimum length of the linker required for SH3 engagement (Chen et al., 2007).

Furthermore, studies using HX MS investigated the contribution of the NCap in stabilizing the intramolecular interactions with different constructs of ABL (SH3/3, SH3-SH2/32, SH3-SH2-Linker/32L) (Chen et al., 2008a). In this study, changes in the partial

unfolding half-life of SH3 domain in the presence or absence of the other domains were measured. The results showed that the NCap stabilizes SH3 unfolding in the presence of the SH2 domain but not in its absence. Also, the SH3 unfolding half-life was doubled in NCap32L relative to the 32L protein. This study clearly shows that NCap contributes to SH3 stabilization, and that this influence requires the SH2 domain. In doing so, the NCap may compensate to some extent to the absence of the negative regulatory C-terminal tail, which engages the SH2 domain in the downregulated conformation of c-SRC and other SFKs. This study also suggests that fusion of BCR to ABL, which removes the stabilizing effect of NCap, contributes to kinase activation (Chen et al., 2008a).

Prior work from our laboratory showed that Src family kinases phosphorylate the ABL SH3 domain at Tyr89. Phosphorylation at this site enhances kinase activity and is required for the full transforming activity of BCR-ABL protein. In the crystal structure of the downregulated c-ABL core, Tyr89 is at the interface between the SH3 domain and the SH2-kinase linker. HX MS studies demonstrated that phosphorylation of Tyr89 by the SFK HCK disengages SH3 from the linker, disrupting its negative regulatory interaction with the linker. This result is consistent with the biological data, in which phosphorylation of this site is required for full kinase activity. Phosphorylation at this residue also interferes with the binding of the ABL interacting protein ABI1 to the SH3 domain (Chen et al., 2008b; Meyn, III et al., 2006).

HX MS was also used to investigate conformational changes in the complete c-ABL kinase core (NCap-SH3-SH2-kinase). These studies addressed conformational changes resulting from imatinib resistance mutations as well as binding of allosteric inhibitors to the myristic acid binding site either alone or in combination with ATP competitive inhibitors. The most recalcitrant imatinib resistant mutation is the T315I mutation also known as the ‘gatekeeper’

mutation. This substitution not only results in the loss of hydrogen bonding with the drug and a steric clash in the drug binding pocket, but it also activates the kinase (discussed in more detail in Section 1.9.3.2) (Shah et al., 2002; Azam et al., 2008). Remarkably, the ABL T315I protein showed increased deuterium incorporation not only at the site of the mutation reflecting local conformational changes but also at a distant site in the SH3 domain (Iacob et al., 2011). Subsequent studies showed that binding of allosteric inhibitor GNF-5 to the myristic acid binding pocket induces both local dynamic changes as well as allosteric changes in the ATP-binding site. These observations have important implications for the mechanisms of drug resistance (addressed in Section 1.11, below). Indeed, simultaneous binding of GNF-5 and the ATP-competitive inhibitor to ABL T315I induced similar conformational changes to those observed when dasatinib was bound to wild-type ABL (Iacob et al., 2011; Zhang et al., 2010). This observation supports the idea that binding of small molecule antagonists to the myristate binding pocket helps to stabilize the downregulated conformation of the active site, thus promoting synergy with dasatinib.

1.7 BCR-ABL

The causal relationship between expression of BCR-ABL and CML pathogenesis is well established. Fusion of BCR to ABL and consequent activation of the ABL kinase is essential for BCR-ABL oncogenicity. Expression of BCR-ABL in mouse fibroblasts, human CD34+ myeloid progenitor cells, and primary bone marrow cells all lead to increased cell proliferation, factor-independent growth and survival, as well as reduced adhesion to fibronectin (Ren, 2005; Ramaraj et al., 2004; Zhao et al., 2001; Ren, 2002). These properties mimic those of transformed

hematopoietic progenitor cells isolated from CML patients. Besides transformation of cells in culture, retroviral transduction of mouse bone marrow cells with BCR-ABL induces myeloproliferative disease (MPD) that resembles CML following transplantation into irradiated mice (Daley et al., 1990). Furthermore, expression of kinase-dead forms of BCR-ABL in the bone marrow transplantation mouse model of CML does not induce leukemogenesis, providing direct evidence that kinase activity is critical to the evolution of the disease in vivo (Ren, 2005).

As described in Sections 1.0 and 1.1, BCR-ABL is the chimeric oncoprotein that drives CML pathogenesis. BCR fusion removes most of the NCap from the N-terminus of c-ABL removing important negative regulatory elements from the tyrosine kinase portion of the protein. In addition, fusion of BCR adds structural features crucial to the activation of downstream signaling pathways and oncogenic activities of BCR-ABL. BCR has a coiled-coil oligomerization domain at the N-terminus (McWhirter et al., 1993; Zhao et al., 2002), and fusion of BCR to ABL induces clustering and juxtaposition of kinase domains that leads to intermolecular *trans*-phosphorylation and activation of the kinase. The coiled-coil domain is followed by serine/threonine kinase domain, a Dbl/CDC24 guanine-nucleotide exchange factor homology domain (DH), a pleckstrin homology domain (PH), calcium-dependent lipid binding site (CaLB), a RAC guanosine triphosphatase-activating protein (RAC-GAP) domain, a growth factor receptor-bound protein 2 (GRB2) docking site as well as binding sites for GRB10, 14-3-3 and an ABL SH2 binding domain (Advani and Pendergast, 2002; Quintas-Cardama and Cortes, 2009).

BCR-ABL drives CML through its interaction with many signaling proteins and induction of downstream signaling pathways. These pathways can be mechanistically grouped as follows: 1) altered adhesion to stroma cells and extracellular matrix, 2) mitogenic signaling

pathways, 3) reduced apoptosis, and 4) increased proteasomal degradation of negative regulators (Deininger et al., 2000). Examples of these pathways are provided in the following sections.

1.7.1 RAS and MAP kinase pathways

The mitogen-activated protein kinase pathway (RAS/RAF/MEK/ERK) plays important mitogenic and antiapoptotic signaling roles for BCR-ABL via downstream transcription factors (Steelman et al., 2008; Steelman et al., 2004). Tyr177 in the BCR portion of BCR-ABL is an important residue for interaction with adaptor proteins and activation of downstream signaling pathways including the MAPK pathway. Upon phosphorylation of this residue, the GRB2 adaptor protein is recruited and docks onto BCR-ABL. GRB2 in turn recruits the guanine nucleotide exchange factor, SOS (named for the orthologous *Drosophila* protein, Son of Sevenless) which activates Ras. Binding of GRB2 also promotes docking of GAB2 which in turn activates the PI3K/AKT pathway as discussed in Section 1.7.3. Mutation of Tyr177 to phenylalanine abolishes binding of GRB2 and activation of Ras. As a consequence, the transformation of primary bone marrow cultures by this mutant is also impaired and the induction of MPD in vivo is reduced (Pendergast et al., 1993; Ren, 2005). On the other hand, BCR-ABL-mediated Ras activation has also been shown to occur through two other adaptor proteins, SHC and CRKL (Oda et al., 1994; Puil et al., 1994). Independent studies showed that docking of SHC requires BCR-ABL SH2 domain as well as its kinase activity. Following its tyrosine phosphorylation, SHC can recruit GRB2 and activate RAS. CRKL is highly expressed in hematopoietic cells and binds to BCR-ABL through its N-terminal SH3 domain (de et al., 1995; ten et al., 1994). CRKL was also shown to bind to C3G, another guanine nucleotide exchange factor (Feller et al., 1998). Hence, BCR-ABL can also activate the Ras pathway by

binding and phosphorylating the CRKL-C3G complex (Goga et al., 1995b; Cortez et al., 1995; Cortez et al., 1996).

1.7.2 JAK/STAT pathway

The Janus (JAK) family of non-receptor tyrosine kinases is composed of four members (JAK1, JAK2, JAK3 and Tyk2). Jaks are rapidly activated by many cytokines and growth factors and couple receptor activation to effector recruitment downstream. Important effectors in this pathway include the signal transducer and activator of transcription (STAT) factors, which are recruited to the receptor via their SH2 domains followed by JAK-mediated phosphorylation. Following phosphorylation and dimerization, STATs are transported into the nucleus, bind to DNA and transcribe genes responsible for cell growth, survival and differentiation. Several STAT transcription factors are constitutively activated by BCR-ABL in CML cells, including STAT1, STAT3 and STAT5, with STAT5 being the most prominent. STAT5 plays a major role in leukemia initiation, maintenance, progression as well as imatinib resistance. STAT5 activation leads to increased expression of the anti-apoptotic proteins Mcl-1 and Bcl-X_L as well as Cyclin D1 which is essential to the progression from G1 to S phase of the cell cycle (Ilaria, Jr. and Van Etten, 1996; Carlesso et al., 1996; Frank and Varticovski, 1996; Gesbert and Griffin, 2000; Sillaber et al., 2000; de Groot et al., 2000). The mechanism of STAT activation by BCR-ABL is complex, involving both direct phosphorylation as well as intermediate kinases of the SRC and JAK families as described in the following sections.

JAK2 is an important non-receptor kinase that is activated by point mutations in many myeloproliferative diseases. JAK2 has also been associated with BCR-ABL mediated leukemogenesis, as pharmacological inhibition of JAK2 decreases the viability of both imatinib-

sensitive and resistant CML cells. However a more recent report shows that inhibition of JAK2 was correlated with “off-target” effects of JAK2 inhibitors such as TG101348, TG101209 and AG490 on BCR-ABL directly (Hantschel et al., 2012). Samanta et al. showed that activation of JAK2 by BCR-ABL induces phosphorylation of GAB2, thus linking JAK2 to the phosphatidylinositol-3-kinase (PI3K) and Ras pathways (Samanta et al., 2006; Samanta et al., 2011). Although BCR-ABL phosphorylates JAK2 on Tyr1007, cells expressing kinase-inactive JAK2 do not exhibit reduced levels of active STAT5 (Xie et al., 2001). More recently, Hantschel et al showed that STAT5 activation is uncoupled from JAK2 activation in BCR-ABL expressing cells and that STAT5 is directly phosphorylated by BCR-ABL (Hantschel et al., 2012).

1.7.3 Phosphatidylinositol 3-kinase (PI3K) Pathway

PI3Ks are a family of kinases that phosphorylate membrane phosphatidylinositols on the 3’-hydroxyl inositol head group. PI3K lipid products create docking sites for proteins with pleckstrin homology domains such as the kinases Akt and phosphoinositide-dependent kinase-1 (PDK-1). PI3Ks of class I_A are activated downstream of tyrosine kinases and are composed of regulatory and catalytic subunits. Class I_A PI3Ks are heterodimers consisting of a catalytic subunit of 110kDa (p110α, p110β and p110δ) and a regulatory subunit (p85α, p85β and p55γ).

Phosphatidylinositol-3,4,5-triphosphate (PIP_3) accumulates in BCR-ABL transformed cells, and pharmacological inhibition of PI3K blocks myeloid and lymphoid transformation indicating functional relevance and activation of PI3K downstream of this oncogene (Skorski et al., 1997; Kharas et al., 2004). The mechanism of PI3K activation downstream of BCR-ABL has been controversial. Jain’s et al. showed that mutation of the ABL domain that interacts with p85

subunit of PI3K did not abrogate PI3K activity (Jain et al., 1996). This study suggested that pI3K can be activated by other proteins that are tyrosine phosphorylated by BCR-ABL.

One crucial pathway for activation of PI3K involves BCR-ABL Tyr177. As described in the preceding section, phosphorylation of this BCR residue recruits GRB2 and hence GAB2 adaptor proteins. GAB2 is then tyrosine-phosphorylated and the p85 regulatory subunit docks onto GAB2 by virtue of its SH2 domain, followed by activation of the PI3K catalytic subunit (Sattler et al., 2002). Mutation of Tyr177 to phenylalanine abolishes GAB2 association, decreases GAB2 phosphorylation and PI3K activation. Furthermore, murine myeloid cells from GAB2-null mice could not be transformed by BCR-ABL. These experiments suggest that Tyr177 and GAB2 are required for BCR-ABL-mediated activation of PI3K. PI3K is also activated by BCR-ABL through a GAB2-independent mechanism that involves the adaptor proteins CRKL, c-CBL and c-CRK. CRKL or c-CRK associate with ABL through their respective SH3 domains and to c-CBL through their SH2 domains. PI3K is then recruited to phospho-CBL through its p85 regulatory subunit and is activated (Sattler et al., 1996).

One major downstream effector of PI3K is the Ser/Thr kinase, AKT, which plays an important role in regulating growth and survival associated with BCR-ABL-mediated transformation. There are several AKT substrates that provide a survival advantage to BCR-ABL-transformed cells and contribute to transformation, including the Forkhead Box Subgroup O (FOXO) transcription factors. AKT-mediated phosphorylation of FOXO transcription factors sequesters them in the cytoplasm through their association with 14-3-3 chaperones. As a result, transcription of proapoptotic proteins are reduced (Obsilova et al., 2005). Proapoptotic BAD is also phosphorylated by AKT and sequestered by 14-3-3. Unphosphorylated BAD associates with the anti-apoptotic BCL-2 protein, displacing BAX which is then available for mitochondrial

permeabilization and apoptosis via cytochrome C release. However, AKT-dependent phosphorylation of BAD and 14-3-3 binding prevents its association with BCL-2 which sequesters BAX, thus inhibiting BAX associated apoptosis (Zha et al., 1996). Another target of AKT is glycogen synthase kinase-β (GSK3β) which is inactivated by phosphorylation. When it is inactivated, GSK3β cannot phosphorylate its downstream targets such as β-Catenin and Cyclin D1 that otherwise would be targeted for proteasomal degradation. As a result β-Catenin accumulates in the nucleus and drives the transcription of target genes such as c-MYC and c-JUN which contribute to cell survival (Pap and Cooper, 1998; Diehl et al., 1998). β-Catenin also interacts with BCR-ABL directly leading to its stability in a GSK3β- independent way (Coluccia et al., 2007).

1.7.4 BCR-ABL signaling through Src-Family Kinases

Src-family kinases (SFKs) play a central role in BCR-ABL signaling in CML and there is accumulating evidence for their role in imatinib resistance as well. These observations have led to the development of drugs that target the kinase activities of both BCR-ABL and SFKs, such as dasatinib (Martinelli et al., 2005; Kantarjian et al., 2011).

Initial evidence for SFK activation came from studies in murine 32D cells transformed with BCR-ABL and in the human K562 CML cell line (Danhauser-Riedl et al., 1996). In these cells, BCR-ABL associates with and activates the myeloid SFKs, HCK and LYN. The association of HCK and BCR-ABL involves the SH3, SH2, kinase and C-terminal regions of BCR-ABL and the SH3 and SH2 domains of HCK. Interestingly, this association did not require the kinase activity of ABL (Stanglmaier et al., 2003a; Lionberger et al., 2000; Warmuth et al., 1997).

SFKs also act as mediators of signaling pathways downstream of BCR-ABL. For example, Stat5 activation is mediated by HCK in myeloid cells as expression of kinase-dead HCK attenuates phosphorylation of Stat5 at Tyr699 and abolishes BCR-ABL induced transformation of myeloid cells (Klejman et al., 2002). Further evidence to support a role for SFKs in BCR-ABL mediated signaling comes from pharmacological inhibition of these kinases. Previous work from our laboratory showed that selective inhibition of SFKs in CML cell lines by the pyrrolopyrimidine A-419259, an SFK-selective inhibitor, blocks cell proliferation and induces apoptosis only in BCR-ABL expressing cells. Indeed, the specific inhibition of SFK activity with this compound correlated with downregulation of STAT5 and ERK activity (Lionberger et al., 2000; Wilson et al., 2002). More recently, our group has shown that A-419259 also induces apoptosis in primary CD34+ cells from CML patients with similar potency to imatinib (Pene-Dumitrescu et al., 2008).

SFKs have also been implicated in the regulation of both c-ABL and BCR-ABL through direct phosphorylation of key tyrosine residues involved in kinase regulation and signaling. Both LYN and HCK have been implicated in phosphorylation of Tyr177 in the BCR-derived portion of BCR-ABL (Warmuth et al., 1997; Meyn, III et al., 2006; Wu et al., 2008). The phosphorylation of this residue is important as a docking site for GRB2 and other adaptor proteins and activation of downstream signaling pathways as discussed earlier. Phosphorylation of Tyr412 in the c-ABL activation loop is mediated by SFKs in response to growth factor stimulation. Tyr245 in the SH2-kinase linker is also phosphorylated by SFKs, which results in upregulation of c-ABL activity. In addition, work from our laboratory has shown that FYN, LYN and HCK strongly phosphorylate multiple tyrosine residues in BCR-ABL SH3-SH2 region. These phosphorylation sites were identified by mass spectrometry and include: Tyr89 and

Tyr134 (SH3 domain), Tyr147 (SH3-SH2 connector), Tyr158, Tyr191, Tyr204 and Tyr234 (SH2 domain). Substitution of these residues with phenylalanine reduced the transforming potential of BCR-ABL in the human myeloid leukemia cell line, TF-1. Based on their positions in the downregulated conformation of the c-ABL core, phosphorylation of these sites may have an important role in regulating the intramolecular interactions, kinase activity and might interfere with drug binding and sensitivity (Meyn, III et al., 2006). As discussed in Section 1.6.1, phosphorylation of SH3 Tyr89 causes displacement of SH3 from the linker, providing direct biophysical evidence for this idea.

1.8 CML THERAPY BEFORE IMATINIB

CML therapy in the early 1900s was purely palliative and included splenic irradiation and the use of cytostatic agents such as busulfan and hydroxyurea. Over time, the goal of CML treatment became curative with the introduction of allogeneic stem cell transplantation. The requirements for successful transplant are many and include patient tolerance of the aggressive chemotherapy and irradiation used to kill the leukemic cells prior to transplantation, age of the patient (older patients have more complications), the stage of the disease and most importantly availability of a compatible donor (Hehlmann et al., 2007; Hehlmann et al., 2005).

In cases where allogeneic stem cell transplantation is not possible, or in cases of relapse following transplantation, interferon alpha (IFN-α) in combination with hydroxyurea or cytosine arabinoside (Ara-C) was a standard treatment. IFN-α leads to hematologic and cytogenetic responses in the chronic phase of CML. However, over time the majority of patients have

reduced quality of life due to the adverse effects of IFN-α and also develop resistance (Hehlmann et al., 2007).

1.9 IMATINIB: TARGETED FRONT LINE THERAPY FOR CML

The first evidence that a tyrosine kinase could be targeted by pharmacological inhibitors came in 1988 when Yaish's group described compounds called tyrphostins that inhibit the epidermal growth factor receptor (EGFR) (Yaish et al., 1988). At the same time, screening of compound libraries at Novartis (Ciba-Geigy at the time) identified 2-phenylaminopyrimidine compounds as promising tyrosine kinase inhibitors, although the original compounds had low specificity and potency (Buchdunger et al., 1995). Imatinib was later developed as an inhibitor of this chemical class with specificity for the PDGFR, and was subsequently shown to inhibit ABL tyrosine kinases and stem-cell factor receptor c-KIT. A landmark 1996 paper from the Druker laboratory reported that imatinib inhibited myeloid cells expressing BCR-ABL but not cells that are BCR-ABL negative (Druker et al., 1996). In addition, imatinib inhibited colony formation of cells from CML patients (Druker et al., 1996; Savage and Antman, 2002a). Following these in vitro studies, oral administration of imatinib to mice bearing human-derived CML cells inhibited tumor growth with minimal side effects (Buchdunger et al., 1996; le et al., 1999). Based on these promising preclinical data, clinical trials with imatinib began in 1998. In phase I clinical trials, the efficacy and safety of imatinib was investigated in chronic phase CML patients. In this study, imatinib showed remarkable success whereby 98% of patients displayed a complete hematologic response (CHR) and this response was maintained over a year. Fifty-five percent of the patients in the accelerated or blast crisis phase achieved partial hematological responses. In phase II

clinical trials, despite great responses of patients in the chronic phase, patients in the accelerated and blast crisis phases achieved 69% and 29% CHR rate respectively. The Phase III study was the International Randomized Study of Interferon and STI571 (IRIS). This study compared imatinib at 400 mg/dl with the standard treatment at the time (IFN-α plus Ara-C) in over 1000 patients. Compared to patients on INFα and Ara-C, the imatinib treatment group showed a significantly higher complete cytogenetic response rate (CCyR) and event-free survival after 60 months. However, after 8 year follow up from the study 17% of patients did not achieve complete cytogenetic response, 15% lost their response and 5% could not tolerate imatinib. Given the overall efficacy and survival rate, imatinib was approved by the FDA in 2001 for the treatment of CML disease (Savage and Antman, 2002b; Fava et al., 2012) and is now the first-line therapy for CML.

1.9.1 Imatinib: Mechanism of action

Imatinib is 2-phenylaminopyrimidine ATP-competitive inhibitor that has high affinity and specificity for ABL tyrosine kinases. Structural studies of the ABL kinase domain by the Kuriyan group showed that imatinib binds between the N- and C-lobes of the kinase domain near the activation loop and the helix αC. Interestingly, imatinib preferentially binds to the downregulated structure of the kinase. In the downregulated state the salt bridge between Glu286 of helix αC and Lys271 of the N-lobe is maintained but the highly conserved DFG motif is flipped out, inhibiting ligation of a critical magnesium ion by the conserved aspartate residue (discussed earlier in Section 1.4.5). The outward rotation of the DFG motif also results in the movement of the flexible activation loop such that the tyrosine autophosphorylation site forms a hydrogen bond with the catalytic aspartate, mimicking the effect of bound substrate. The binding

of imatinib is stabilized by 21 interactions, of which 6 are hydrogen bonds with Met318, Thr315 (the gatekeeper residue mentioned earlier), Glu286, His361, Ile360 and Asp381 (Schindler et al., 2000). The specificity of imatinib binding to ABL is achieved by the conformational structure of ABL in its inactive form which is unique even when compared to the highly similar structures of SFKs. Thus, although these kinases have similar structures in their active states, differences in the inactive states can be exploited to achieve differential inhibition by imatinib (Levinson et al., 2006b; Nagar, 2007; Nagar et al., 2002).

1.9.2 Imatinib Resistance

Despite the unprecedented hematologic and cytogenetic response rates with imatinib, resistance to imatinib treatment is a growing concern. It is estimated that about 20-30% of CML patients will eventually develop resistance to imatinib (Quintas-Cardama and Cortes, 2009). Resistance to imatinib can be divided into two categories: primary resistance and acquired resistance. Acquired resistance can be further subdivided into BCR-ABL dependent or independent mechanisms. Each of these types of resistance is discussed in more detail below.

Primary resistance is a rare event. Patients who fail to achieve complete hematologic response after 3 months from the start of imatinib therapy, cytogenetic response by 6 months, partial cytogenetic response by 12 months or complete cytogenetic response by 18 months are considered to be insensitive to imatinib. The mechanisms driving primary resistance are not very well understood. However, one possible explanation for primary resistance is the presence and refractoriness of CML stem cells (Graham et al., 2002; Holtz et al., 2005; Holtz et al., 2002). These quiescent cells are intrinsically resistant to imatinib therapy. The insensitivity of these quiescent cells may include alterations in drug uptake, efflux, expression level of *BCR-ABL*

transcript, increased activity level and kinase domain mutations that occur even prior to imatinib therapy (Ernst et al., 2008; Copland et al., 2006) .

In acquired resistance, patients initially respond to imatinib for various periods of time but eventually become drug resistant. This type of drug resistance is characterized at three levels: hematologic, cytogenetic and molecular. Thus in acquired resistance, patients lose their hematologic response and hence cannot normalize their peripheral blood counts, Ph chromosome positive cells persist, and at the molecular level *BCR-ABL* transcripts are still present (Quintas-Cardama et al., 2009; Roychowdhury and Talpaz, 2011).

1.9.3 BCR-ABL-dependent mechanisms of acquired imatinib resistance

1.9.3.1 BCR-ABL overexpression

BCR-ABL gene amplification results in overexpression of the protein. *BCR-ABL* gene amplification was first observed in studies using BCR-ABL-transformed Ba/F3 cells (Mahon et al., 2000). Clinically, the first studies on the 11 patients who presented with imatinib resistance, 3 patients showed gene amplification when studied by fluorescent in situ hybridization (FISH) in the absence of kinase domain mutations (Gorre et al., 2001). However, when a larger group of patients were tested for *BCR-ABL* gene amplification, 2 of 66 patients were positive for the amplification (Gorre et al., 2001; Hochhaus et al., 2002). Interestingly, a correlation has been reported between high levels of BCR-ABL protein and a faster rate of imatinib resistance mutations (Barnes et al., 2005).

1.9.3.2 Kinase Domain Point mutations

The first report of ABL kinase domain mutations associated with imatinib resistance was reported by Gorre and coworkers. This study reported a single nucleotide change that resulted in threonine to isoleucine substitution at position 315 of the kinase domain (Gorre et al., 2001). This mutation is the most recalcitrant mutation known to date and is unresponsive to all clinically available drugs. When this mutation was identified, the crystal structure of ABL kinase domain bound with a variant of imatinib had just been solved (Schindler et al., 2000). Modeling the T315I mutation on this structure (Nagar et al., 2002), it was evident that isoleucine could not form a critical hydrogen bond with the secondary amino group of imatinib and also the bulkier isoleucine side chain would sterically hinder the binding of imatinib to the drug-binding pocket. Furthermore, Daley's group showed that mutations at the gatekeeper residue in the c-ABL, c-SRC, PDGFR and EGFR activate the kinases (Azam et al., 2008). In the same study, structural analysis, mutagenesis and cell based assays showed that in ABL the gatekeeper mutation stabilizes the hydrophobic spine which was first defined by Kornev's group (Kornev et al., 2006). The four residues that make up the hydrophobic spine, Leu320, Met309, Phe401 and His380, are ordered in the active state of the kinase and threonine to isoleucine substitution that would occur at the tip of the spine that stabilizes the active conformation of the kinase. In addition, work from our group showed that T315I induces dynamic conformational changes locally at the site of the mutation as well as in the SH3 domain of myristoylated ABL core protein (Iacob et al., 2009). Taken together, these studies show that T315I substitution has important implications not only for imatinib resistance for loss of kinase regulation as well.

Following the first report of T315I mutation in a small group of patients (Gorre et al., 2001), studies of BCR-ABL kinase domain mutations in a larger cohort group of patients with

imatinib resistance revealed that 29 of the 32 patients had kinase domain mutations (Shah et al., 2002). The mutations involved 15 amino acid substitutions at 13 distinct kinase domain positions, involving the P-loop, the catalytic loop as well as the activation loop. While some of these residues are directly involved in imatinib binding, others do not contact imatinib directly but instead have an effect on the conformation of the kinase that prevents its interaction with imatinib. A comprehensive study using random mutagenesis of BCR-ABL to study the different amino acid substitutions conferring resistance to imatinib was reported by Azam et al (Azam et al., 2003). This approach identified all of the mutations previously observed in clinical samples and numerous others. Clinically relevant mutations were distributed along the whole kinase domain, and include the P-loop, the activation loop, helix αC, the SH2 and SH3 domains, the SH3-SH2 connector as well as the SH2-kinase linker (the positions of these residues are mapped to the structure of the ABL core in Figure 4). The numerous mutations recovered that did not directly interfere with imatinib binding defined a new class of mutations that can confer resistance by allosteric modification of the downregulated structure of the kinase. Despite the large number of resistance mutations that have been reported so far, most of these are rare in terms of clinical experience, with changes at ABL residues Gly250, Tyr253, Glu255, Thr315, Met351 and Phe359 accounting for about 60-70% of kinase domain point mutations (Quintas-Cardama et al., 2009).

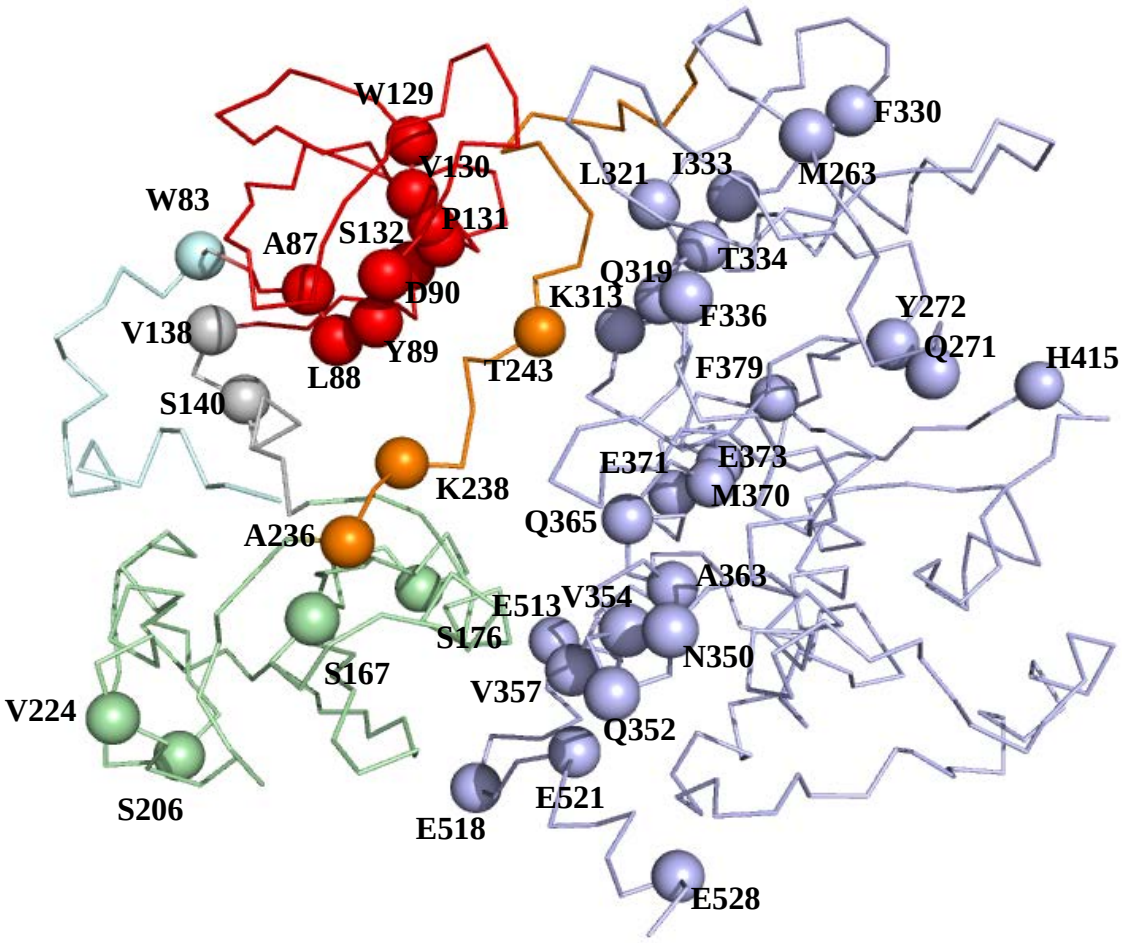

Figure 4: Point mutations leading to imatinib resistance in BCR-ABL. Residues that render BCR-ABL resistant to imatinib are mapped on the downregulated structure of ABL core (PDB:F2O0). These mutations have been identified in an unbiased *in vitro* screen (Azam et al., 2003). The NCap region is rendered in pale cyan; SH3 domain in red; SH3-SH2 connector in grey; SH2 domain in green; SH2-kinase linker in orange; kinase domain in light blue. These residues are numbered as per the crystal structure (ABL1b residues 1-531, 15-56 deleted), and are offset relative to the numbering convention used for BCR-ABL residues. Thus the gatekeeper residue is numbered as T334 rather than T315 in this scheme.

1.9.4 BCR-ABL-independent mechanisms of resistance

Kinase domain mutations and gene amplification account for about 50% of resistant cases in CML(Roychowdhury and Talpaz, 2011). Thus, BCR-ABL-independent mechanisms also contribute to clinical imatinib resistance in CML and include α-1 acid glycoprotein levels, drug transport, metabolism by cytochrome p450, BCR-ABL downstream signaling and minimal residual disease.

Plasma levels of imatinib have been correlated with α-1 acid glycoprotein levels (AGP), which increase in the advanced stages of CML. Binding of imatinib to AGP has been shown to increase the clearance of imatinib in patients with gastrointestinal stromal tumors treated with imatinib (le et al., 2002; Gambacorti-Passerini et al., 2002; Delbaldo et al., 2006).

Intracellular levels of imatinib are a function of influx and efflux of the drug. Imatinib is a substrate of the ATP-binding cassette transporter ABCB1 that has been shown to be overexpressed in patient samples in the advanced stages of CML and many other cancers (Dai et al., 2003; Thomas et al., 2004). The overexpression of this transporter increases the efflux of imatinib and potentially contributes to drug resistance. However, the role of ABCB1 transporter in inducing imatinib resistance remains controversial as the activity of this transporter on imatinib relative to other cytotoxic agents is very small and the overexpression of ABCB1 in the K562 CML cell line does not lead to imatinib resistance in vitro (Ferrao et al., 2003). On the other hand, imatinib is transported into the cell through the human organic cation transporter (hOCT1). Low levels of hOCT1 have been associated with suboptimal responses in patients while higher activity levels have been associated with an improved response rate (Crossman et al., 2005). Along with drug transport and association with AGP, levels of the cytochrome p450

isoenzymes CYP3A4 and CYP3A5 that metabolize imatinib are important contributors to plasma levels and thus its effectiveness (Quintas-Cardama et al., 2009).

Alterations of signaling pathways downstream of BCR-ABL can also contribute to imatinib resistance. Signaling through SFKs has attracted major attention in the context of imatinib resistance and hence drug development. Early experiments showed that K562 CML cells made resistant to imatinib by culturing in increasing concentrations of the drug displayed upregulation of LYN kinase activity. LYN is a member of the Src-kinase family that is strongly expressed in cells of myeloid and B-lymphoid lineage. Inhibition of LYN kinase by siRNA reduced proliferation of these resistant cells in response to imatinib (Ptasznik et al., 2004). Furthermore, in samples from patients with advanced CML, imatinib resistance was associated with upregualtion of HCK or LYN and reduction of LYN by siRNA reduced cell survival. In addition, Chandra's group showed that FYN levels are upregulated in blast phase of the disease compared to the chronic phase (Ban et al., 2008). Also, knockdown of FYN by shRNA slowed cell survival and resensitized cells to the effects of imatinib (Gao et al., 2009). The Auberger group investigated gene expression profiles of imatinib-resistant as well as pan-Src kinase inhibitor-resistant cell lines. In this study they showed increased expression of FYN and its inhibition resensitized cells to imatinib (Grosso et al., 2009).

As discussed earlier, work from our laboratory has shown that FYN, LYN and HCK strongly phosphorylate multiple tyrosine residues in BCR-ABL SH3-SH2 region. Substitution of these residues with phenylalanine reduced BCR-ABL oncogenicity. Also, the position of these residues may have an important role in regulating the intramolecular interactions, kinase activity and therefore might interfere with imatinib binding and sensitivity (Meyn, III et al., 2006). In support of this notion, it was shown that there are some mutations that occur at the SH3, SH2 and

the linker regions in CML patients with different responses to imatinib that may explain clinical resistance without kinase domain mutations (Sherbenou et al., 2010).

Recently, work from our laboratory showed that overexpression of the SFK HCK, as well as a gatekeeper mutant of this kinase (HCK T338A) that is specifically inhibited by the pyrazolopyrimidine NaPP1, induced imatinib resistance in K562 CML cell lines. The imatinib resistance due to overexpression of either form of HCK correlated with sustained BCR-ABL tyrosine phosphorylation. Remarkably, NaPP1 treatment reversed the imatinib resistance only in cells that expressed HCK T338A but not the control cells expressing wild-type HCK. Importantly, HCK-mediated imatinib resistance correlated with specific phosphorylation of BCR-ABL on its SH3 domain (Tyr89) and activation loop (Tyr412), and these phosphorylation events were reversed by NaPP1 treatment in cells expressing HCK-T338A. These results support the idea that HCK kinase activity is sufficient to cause imatinib resistance in the absence of BCR-ABL mutations. Resistance may result from HCK-mediated phosphorylation of regulatory regions of BCR-ABL that promote active kinase conformations incompatible with imatinib binding. This study also provides a mechanistic basis for SFKs in imatinib resistance and provides a rationale for using dual ABL/SRC inhibitors in some cases of imatinib-resistant CML (Pene-Dumitrescu et al., 2008; Pene-Dumitrescu and Smithgall, 2010).

1.10 SECOND GENERATION TYROSINE KINASE INHIBITORS

Despite the clinical success of imatinib in CML therapy, relapse due to drug resistance is inevitable. The emergence of resistance to imatinib through BCR-ABL-dependent mechanisms

such as kinase domain mutations, spurred the development of more potent, second generation tyrosine kinase inhibitors (TKIs).

One such second generation TKI is nilotinib (Tasigna, AMN107; Novartis). Nilotinib, like imatinib, recognizes and binds the inactive (DFG out) conformation of the kinase. Nilotinib is about 30-fold more potent than imatinib as an ABL inhibitor and inhibits c-Kit and the PDGFR with similar potency as imatinib (Weisberg et al., 2005). Most importantly, nilotinib inhibits 32 of the 33 imatinib-resistant mutants of BCR-ABL both in vitro and in vivo (Weisberg et al., 2006; O'Hare et al., 2005). The sole mutant that is unresponsive to nilotinib is the T315I 'gatekeeper' mutation described above. In 2007, the FDA approved nilotinib for the treatment of patients resistant to imatinib in the chronic and accelerated phases of the disease (Weisberg et al., 2007).

Another second generation tyrosine kinase inhibitor is dasatinib (Sprycel; Bristol-Meyers Squibb). Unlike imatinib and nilotinib, dasatinib inhibits both the active and inactive conformations of the kinase domain and has a much broader specificity profile, with activity against SFKs, c-KIT, PDGFR, ABL and many others (Melnick et al., 2006). Dasatinib is 300 times more active than imatinib against BCR-ABL and overcomes most imatinib resistant mutations with the exception of T315I. In 2006, FDA approved dasatinib for the treatment of all phases of CML with resistance to imatinib (Lombardo et al., 2004; Shah et al., 2004; Quintas-Cardama et al., 2007).

Bosutinib (SKI-606; Wyeth) is an orally available TKI that has dual SFK and ABL tyrosine kinase inhibitory activity. Unlike the other TKIs, bosutinib has no significant activity against c-KIT and PDGFR. This compound also decreases the phosphorylation of many downstream cellular proteins including MAPKs, STAT5 and others and inhibits proliferation of

CML cells. Bosutinib like the other TKI cannot override the T315I mutation. The results of the phase III Bosutinib Efficacy and Safety in newly diagnosed, chronic-phase myeloid LeukemiA (BELA) clinical trial was recently published (Cortes et al., 2012). The primary objective was to achieve CCyR rate after one year of treatment. However, the CCyR rate at 12 months for bosutinib (70%) was not significantly different than that of imatinib (68%). Though the primary objective was not met, patients on bosutinib showed higher major molecular response rate (MMR), achieved CCyR and MMR at a faster rate, and had fewer transformations to blast phase.

Interestingly, recent work from Nathanael Gray's group at Harvard used a "hybrid-design" approach to develop inhibitors that are selective for the DFG-out kinase conformation (Choi et al., 2012). This new approach combined functionality from dasatinib with moieties from imatinib, nilotinib and sorafenib. More specifically, this new class of inhibitors were designed by hybridizing the thiazole functionality of dasatinib that interacts with the hinge region with 3-trifluoromethylbenzamide of imatinib, nilotinib or sorafenib that occupy a region adjacent to the ATP-binding site in DFG-out conformations. The new compounds inhibit wild-type and T315I BCR-ABL activity.

Other TKIs are in different stages of clinical trials for CML and include the ABL/LYN kinase inhibitor INNO-406 (Bafetinib, CytRx), the ABL/SRC inhibitor AP24534 (Ponatinib, Ariad Pharmaceuticals). Another class of inhibitors, known as switch pocket inhibitors (DCC-2036, DCC-2157; Deciphera Pharmaceuticals), bind to the residues Arg386/Glu282 that are involved in switching ABL kinase between active and inactive conformations. DCC-2036 also has activity against SFKs.

In addition to TKIs, Aurora kinase inhibitors such PHA-739358 (dansertib), XL-228, KW-2449 among others are in clinical trials for CML. Aurora kinases are serine/threonine

kinases involved in different stages of mitosis and have increased expression in myeloid tumors and other forms of cancer. These inhibitors that target the kinase's ATP binding site have shown activity against wild-type and T315I ABL (Agrawal et al., 2010).

1.11 ALLOSTERIC INHIBITORS

An alternative strategy to overcome imatinib resistance is to target BCR-ABL kinase activity through an allosteric site at a distance from the active site. In general, allosteric kinase inhibitors are anticipated to target regulatory mechanisms unique to a given kinase and therefore may exhibit improved selectivity and reduced off-target effects compared to active inhibitors.

Using a high-throughput cytotoxicity assay, Gray and coworkers discovered GNF2, the first allosteric inhibitor of BCR-ABL (Adrian et al., 2006). Biochemical and structural studies showed that GNF2 binds the myristic acid binding pocket of ABL and stabilizes the inactive conformation of the kinase. Surprisingly, GNF2 alone was not active against the imatinib-resistant mutant T315I or several other prominent imatinib-resistant mutants. However, the combination of GNF2 with nilotinib was effective at inhibiting the T315I mutant. In vivo studies using a murine bone marrow transplantation model of CML showed that the combination of GNF5 (an analog of GNF2 with improved pharmacokinetics) and nilotinib reduced spleen size, white blood cell counts and STAT5 phosphorylation while increasing overall survival. In addition, HX MS studies revealed conformational changes in the ATP binding site upon GNF5 binding that directly support allosteric communication between the myristic acid binding pocket and the active site, which are separated by more than 30 Å in the crystal structure. Hence, this

new class of drug defines and potentiates the development of allosteric inhibitors that could be clinically tested (Iacob et al., 2011; Zhang et al., 2010).

Besides allosteric inhibition by GNF2, peptides that target the BCR-derived region of the protein and induced modification of the kinase activity expanded the understanding of allosteric inhibitors. Specifically these peptides target the N-terminal coiled-coil region of BCR-ABL and inhibit oligomerization, reduce kinase activity and increases sensitivity to both imatinib and GNF2 (Beissert et al., 2008). In a more recent study Feng et al. showed that adenoviral transduction of SH2-DED (dead effector domain) in CML cells, resulted in its binding to pTyr177 through the SH2 domain and activation of Caspase 8 through the DED domain. As a result, BCR-ABL positive leukemia cells exhibited reduction in cell proliferation and enhancement of apoptosis (Peng et al., 2012). Whether or not peptide-based approaches such as these will ever be translated to the clinic remains unclear.

1.12 HYPOTHESIS

Despite the constitutive activation of ABL that results from Bcr fusion, mounting evidence suggests that the SH3 and SH2 domains are not necessarily displaced from their regulatory positions on the back of the kinase domain. Mutations in the BCR-ABL SH3 and SH2 domains as well as the linker promote imatinib resistance, consistent with the kinase domain adopting the active conformation incompatible with drug binding. Similarly, phosphorylation of the BCR-ABL linker and SH3 domain by the Src-family kinase HCK also results in imatinib resistance, most likely by perturbing SH3:linker interaction (Meyn, III et al., 2006; Azam et al., 2003; Pene-Dumitrescu and Smithgall, 2010). A logical conclusion from these findings is that the SH3 and

SH2 domains maintain their regulatory influence on the kinase domain even in the context of BCR-ABL. Given the regulatory influence of SH3 on the kinase domain, I propose the hypothesis that strengthening the regulatory SH3:linker interaction present in BCR-ABL stabilizes a downregulated kinase domain conformation, and sensitizes the kinase domain to both imatinib and allosteric inhibitor action.

An alternate approach to inhibit BCR-ABL mediated signal transduction and oncogenesis in imatinib-resistant CML involves small-molecule targeting of Src family kinases (SFKs). BCR-ABL binds to and activates multiple SFKs in CML cells, including HCK and LYN. In turn, active SFKs directly phosphorylate regulatory tyrosine residues in the ABL SH3 domain, the SH2-kinase linker, and the BCR-derived portion of BCR-ABL (Meyn, III et al., 2006). Previous work from our group showed that global inhibition of SFK activity with the ATP-competitive pyrrolo-pyrimidine A-419259 leads to growth arrest and apoptosis in CML cell lines and in primary CD34+ CML cells. In addition, expression of an HCK mutant with engineered resistance to A-419259 protects CML cells against the antiproliferative and apoptotic effects of this compound (Wilson et al., 2002; Pene-Dumitrescu et al., 2008). Other studies also correlate CML progression and drug resistance with overexpression and activation of HCK and LYN (Wu et al., 2008). In the latter case, clinical drug resistance was reported in the absence of ABL kinase domain mutations. Based on these associations, I propose the hypothesis that imatinib resistant ABL mutants may induce cross-resistance to Src-selective inhibitors as a result of cross-phosphorylation.

1.12.1 Specific Aims

1.12.1.1 Aim 1: Investigate the role of SH3:linker interaction in the regulation of c-ABL dynamics, signaling, and inhibitor sensitivity.

In the c-ABL core, the SH2-kinase linker forms a PPII helix that serves as an internal docking site for the SH3 domain. This interaction is essential for downregulation of the kinase. However, the linker is a suboptimal ligand for the SH3 domain, with two charged lysine residues facing the hydrophobic binding surface of SH3. In this aim, I tested the hypothesis that the SH3:linker interaction is a key regulator of c-ABL kinase activity and that activating mutations can be overcome by enhancing the SH3:linker interaction. To test this hypothesis, it was necessary to strengthen the SH3:linker interaction experimentally. In order to achieve tight SH3:linker interaction we created a series of ten modified linkers with increasing proline content and termed these engineered sequences as "High Affinity Linkers" or HALs for short. Using hydrogen exchange mass spectrometry (HX MS), we show that the HAL9 modification enhances SH3:linker interaction dramatically. Next, I also determined whether SH3:linker interaction allosterically influences the effects of activating mutations in c-ABL core. To do this, I combined HAL9 with activating mutations in the myristate-binding pocket (A356N), the gatekeeper at the active site (T315I) and in the non-myristoylated (G2A) c-ABL core and expressed the proteins in 293T cells. Remarkably, the HAL substitution completely reversed ABL core activation by the A356N mutation, and partially reversed the effect of T315I and G2A. Next, I investigated whether HAL9 resensitizes imatinib resistant BCR-ABL mutants to inhibition by compounds that target the kinase domain active site and the allosteric binding pocket using transformed human myeloid cells as a model system. Surprisingly, enhanced SH3:linker interaction also dramatically sensitized the BCR-ABL tyrosine kinase associated with CML to small molecule

inhibitors. Using HX MS we also show that there is allosteric network linking the SH3 domain, the myristic acid binding pocket, and the active site of the c-ABL core, providing a structural basis for the biological observations.

1.12.1.2 Aim 2: Determine the mechanism of cross-resistance of SFKs to the Src-selective inhibitor A-419259 in cells transformed with the BCR-ABL imatinib-resistant mutant, T315I.

Given the important role of SFKs in BCR-ABL-mediated signaling and drug resistance, I studied the effect of the SFK inhibitor A-419259 on human TF-1 myeloid cells transformed with clinically relevant imatinib-resistant mutants of BCR-ABL (E255V, Y253H and T315I). The anti-proliferative effects of the inhibitor correlated with suppression of overall SFK activity. However, TF-1 cells transformed with the gatekeeper mutant T315I were completely cross-resistant to A-419259 and endogenous SFK activity was not inhibited. These data suggest a new mechanism of BCR-ABL T315I-induced resistance to drugs that target SFKs in CML. In this aim, I explored the possibility that BCR-ABL T315I-induced resistance to drugs that target SFKs in CML is due to an acquired ability of BCR-ABL T315I to phosphorylate SFKs at novel sites that interfere with drug action.

2.0 ENHANCED SH3:LINKER INTERACTION ALLOSTERICALLY SENSITIZES ABL KINASES TO SMALL MOLECULE INHIBITORS

2.1 ABSTRACT

Multi-domain kinases such as c-SRC and c-ABL are regulated by complex allosteric interactions involving their non-catalytic SH3 and SH2 domains. In this study we show that enhancing natural allosteric control of kinase activity by SH3:linker engagement has long-range suppressive effects on the kinase activity of the c-ABL core. Surprisingly, enhanced SH3:linker interaction also dramatically sensitized the BCR-ABL tyrosine kinase associated with CML to small molecule inhibitors that target either the active site or the myristic acid binding pocket in the kinase domain C-lobe. Dynamics analyses using hydrogen exchange mass spectrometry revealed a remarkable allosteric network linking the SH3 domain, the myristic acid binding pocket, and the active site of the c-ABL core, providing a structural basis for the biological observations. These results suggest a rational strategy for enhanced drug targeting of BCR-ABL and other multi-domain kinase systems that uses small molecules to exploit natural mechanisms of kinase control.

2.2 INTRODUCTION

Chronic myelogenous leukemia (CML) is characterized by the Philadelphia chromosome translocation, which fuses the *BCR* (*break point cluster*) region locus on chromosome 22 with the c-*ABL* (*Abelson tyrosine kinase*) proto-oncogene on chromosome 9. This translocation results in the expression of BCR-ABL, a constitutively active protein-tyrosine kinase that drives CML pathogenesis through downstream pathways that promote cell growth and survival. Expression of BCR-ABL in bone marrow cells induces a CML-like syndrome in mouse models, demonstrating BCR-ABL kinase activity alone is sufficient to cause the disease (Wong and Witte, 2004; Hantschel and Superti-Furga, 2004).

Clinical management of CML has been revolutionized by imatinib mesylate, a selective ATP-competitive inhibitor of BCR-ABL kinase activity (Druker, 2004). Despite this clinical success, imatinib is less effective in advanced CML due to selection of drug resistant mutants of BCR-ABL (Nardi et al., 2004). Resistance mutations often arise in the drug binding site, and include the T315I gatekeeper mutation that also enhances BCR-ABL kinase and transforming activities (Griswold et al., 2006). Other mutations occur outside of the active site and allosterically reduce drug binding by promoting an active kinase domain conformation incompatible with imatinib binding. Second generation ATP-competitive inhibitors, including nilotinib and dasatinib; have been approved for the clinical management of imatinib-resistant CML (Rix et al., 2007). While these newer inhibitors are more potent, they do not inhibit the BCR-ABL T315I mutant.

In contrast to BCR-ABL, c-ABL kinase activity is tightly regulated in cells. Structural and functional studies attribute intramolecular interactions to downregulation of the c-ABL

kinase core, which consists of a myristoylated N-terminal region (NCap), followed by regulatory SH3 and SH2 domains, the SH2-kinase linker and the kinase domain (Nagar et al., 2006). The kinase domain is comprised of a smaller N-lobe connected to a larger C-lobe through a flexible hinge, allowing for articulation of the two lobes during kinase activation. The NCap, SH3 and SH2 domains work in concert to keep the kinase in the autoinhibited state (Nagar et al., 2003; Nagar et al., 2006; Hantschel et al., 2003). By binding to the SH2-kinase linker through an atypical PxxP motif ($P_{242}TVY_{245}$), the SH3 domain stabilizes the N-lobe of the kinase domain in the inactive state. Mutations within the SH3 domain, as well as the linker, switch on the kinase and transforming activities of c-ABL (Barila and Superti-Furga, 1998). Moreover, phosphorylation of residues in the linker (Tyr245) or in the SH3 domain (Tyr89) disrupt SH3:linker engagement and also enhance ABL kinase activity (Chen et al., 2008b; Meyn, III et al., 2006). The SH2 domain docks onto the back of the kinase domain C-lobe through a network of hydrogen bonds to further stabilize the downregulated conformation of the core. Mutation of SH2 Tyr158 disturbs this interaction and leads to kinase activation (Hantschel et al., 2003). Finally, the N-terminal myristate group penetrates into a deep pocket in the C-lobe, inducing a kink in helix αI that is critical for SH2:C-lobe interaction. Mutations in the hydrophobic pocket of the C-lobe that prevent myristic acid insertion (e.g. A356N) activate the kinase. Recently, a new class of allosteric BCR-ABL inhibitors has been described that target the C-lobe myristic acid binding site (Adrian et al., 2006; Zhang et al., 2010). These compounds, of which GNF-2 is the prototype, stabilize the inactive conformation of the ABL core and work in concert with ATP-competitive inhibitors to overcome imatinib-resistant mutants of BCR-ABL, including T315I (Zhang et al., 2010; Iacob et al., 2011).

In the context of BCR-ABL, BCR fusion prevents N-terminal myristoylation of c-ABL, thereby removing one important element of kinase downregulation. In addition, BCR adds an N-terminal coiled-coil oligomerization domain that induces clustering of BCR-ABL and promotes kinase activation through *trans*-phosphorylation of the activation loop (McWhirter et al., 1993). Unlike the c-ABL core, the contribution of the SH3 and SH2 domains to kinase domain control within BCR-ABL is less clear. Despite the constitutive activation of ABL that results from BCR fusion, mounting evidence suggests that the SH3 and SH2 domains are not necessarily displaced from their regulatory position on the back of the kinase domain. Experimental and clinical mutations in the BCR-ABL SH3 and SH2 domains as well as the linker promote imatinib resistance, consistent with the kinase domain adopting the active conformation incompatible with drug binding (Azam et al., 2003). Similarly, phosphorylation of the BCR-ABL linker and SH3 domain by the Src-family kinase HCK also results in imatinib resistance, most likely by perturbing SH3:linker interaction (Pene-Dumitrescu and Smithgall, 2010). A logical conclusion from these findings is that the SH3 and SH2 domains maintain their regulatory influence on the kinase domain even in the context of BCR-ABL. This raises the exciting possibility that strengthening the regulatory SH3:linker interaction present in BCR-ABL may stabilize a single downregulated kinase domain conformation, thus sensitizing the kinase domain to both imatinib and allosteric inhibitor action.

In this study, we explored this possibility by creating a series of modified c-ABL and BCR-ABL proteins with enhanced SH3:linker interactions. By systematically increasing the proline content of the linker, we identified high-affinity linkers that stabilized intramolecular SH3:linker binding without disturbing the overall regulation of the kinase core. Enhanced SH3:linker interaction completely reversed c-ABL core activation by a C-lobe myristate binding

pocket mutation, and substantially reduced activation by mutations in the ATP binding site (T315I) as well as the SH2:C-lobe interface (Y158D). Remarkably, enhanced SH3:linker interaction dramatically sensitized BCR-ABL not only to imatinib but also to the allosteric inhibitor, GNF-2. These effects were observed in the context of both wild-type and imatinib-resistant forms of BCR-ABL. Hydrogen exchange mass spectrometry of recombinant ABL core proteins with high-affinity linkers revealed a previously unrecognized dynamic coupling between the SH3:linker interface and the GNF-2 binding site in the C-lobe myristate binding pocket. Taken together, these studies provide strong evidence that regulatory SH3:linker interaction is retained in the context of BCR-ABL, and that overall kinase regulation is controlled by an 'allosteric triangle' linking the SH3 domain, the C-lobe, and the active site. Small molecules enhancing natural regulatory interaction at the SH3:linker interface may have clinical utility as chemical sensitizers of existing BCR-ABL drug action.

2.3 RESULTS

2.3.1 Design and characterization of High Affinity Linker (HAL) variants of ABL

In the context of the c-ABL core, the SH2-kinase linker forms a polyproline type II (PPII) helix that serves as an internal docking site for the SH3 domain. This interaction is essential to downregulation of c-ABL activity. Compared with high affinity peptide ligands for the ABL

SH3 domain (Pisabarro et al., 1998), however, the linker represents a suboptimal SH3 docking site, with a charged residue (lysine) facing the hydrophobic binding surface of SH3 (Figure 5). In order to strengthen internal SH3:linker interaction, we systematically substituted linker residues in close proximity with the SH3 surface with prolines, resulting in a set of 10 modified linkers (see Figure 6A for sequences). These engineered sequences are referred to hereafter as high affinity linkers (HALs).

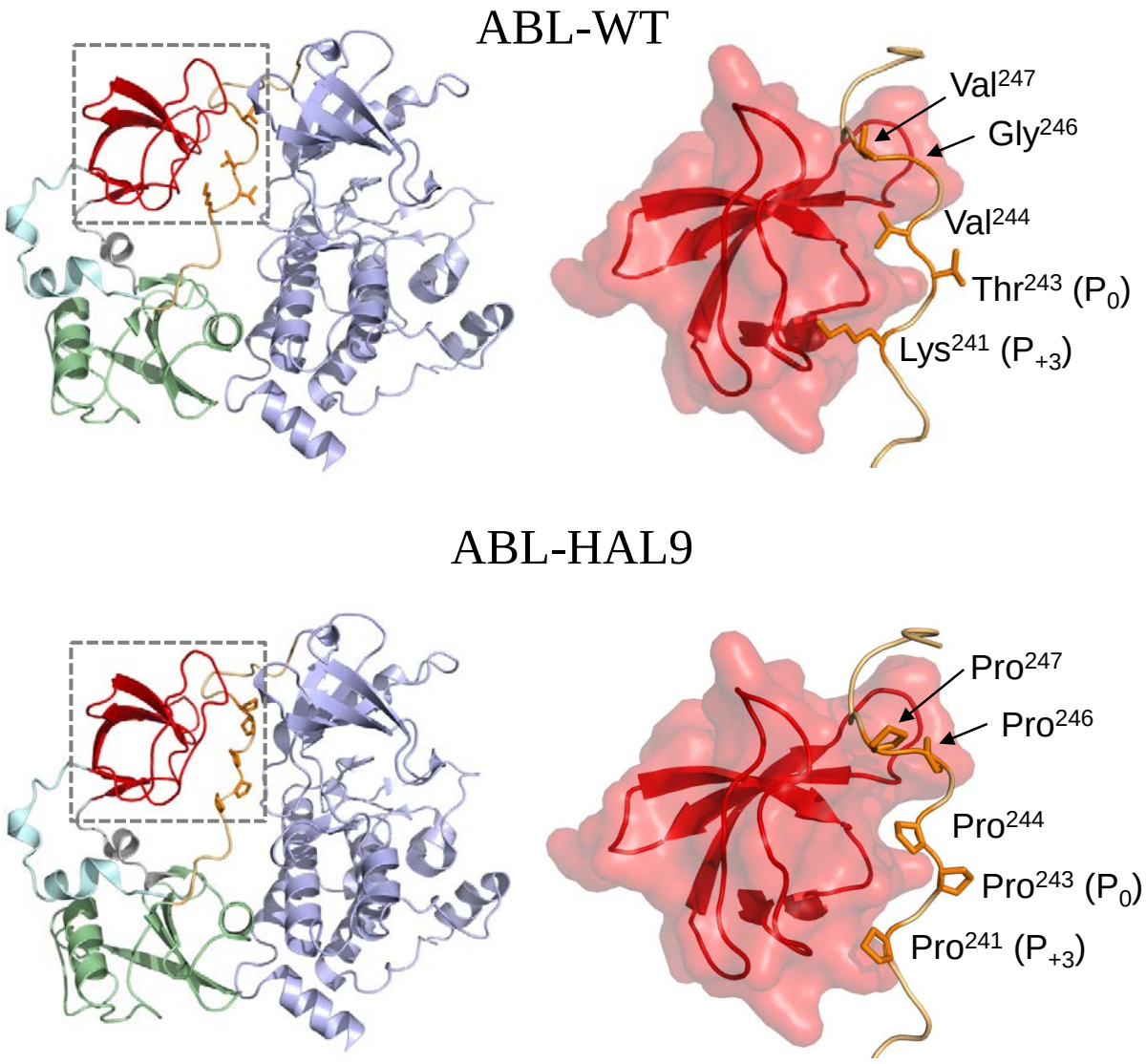

Figure 5: Model of c-ABL core with enhanced SH3:linker interface. Model of the downregulated wild-type c-ABL core is shown at the top left, and includes the NCap (light blue), SH3 domain (red), SH2 domain (green), SH2-kinase linker (orange), and kinase domain (purple). The SH3:linker interface (boxed) is enlarged on the right to highlight the side chains of the linker residues that were modified in the HAL9 mutant. Models of the c-ABL HAL9 core protein and SH3:linker interface are shown in the lower panels, in which proline residues were substituted for five wild-type residues shown at the top. Models and residue numbering is based on the X-ray crystal structure of the myristoylated c-ABL core (PDB: 2FO0) and PyMol.

To determine whether increased proline content stabilized intramolecular SH3 binding, the modified linkers were first incorporated into bacterial expression vectors for the Abl SH3-SH2-linker region. The resulting proteins were expressed, purified and examined for enhanced SH3:linker interaction using hydrogen exchange mass spectrometry (HX MS), a method previously developed to explore the impact of linker engagement on ABL SH3 dynamics (Chen et al., 2008b; Chen et al., 2008a). With HX MS, protein dynamics are determined by measuring the rate of backbone amide hydrogen exchange following transfer to a deuterated solvent (Wales and Engen, 2006). Under physiological conditions, HX MS has shown that the c-ABL SH3 domain undergoes a cooperative partial unfolding event which is stabilized by ligand binding either in *cis* (linker) or in *trans* (high affinity peptide). The extent of SH3 unfolding is directly proportional to the affinity of the ligand, and complete inhibition of SH3 unfolding can be achieved by binding to the BP1 peptide, a sequence with relatively high affinity towards the ABL SH3 domain (Chen et al., 2008b; Chen et al., 2008a). HX MS measurements provide a direct assay for the impact of the HAL substitutions on intramolecular SH3 engagement.

HX MS was performed on the wild-type ABL SH3-SH2-linker protein as well as all ten recombinant HAL mutants, and the results are summarized in Figure 6B. Introduction of single proline residues in the so-called P_0 or P_{+3} (HAL1; HAL2) positions alone, which directly oppose the SH3 domain in the downregulated structure of the c-ABL core (Figure 5), did not alter SH3 unfolding relative to the wild-type protein. However, double proline substitution at both of these positions (HAL3) showed a moderate increase in the SH3 unfolding half-life compared to the wild type and singly substituted linkers, although this effect was subtle (about 2-fold; Figure 6B). Substitution of prolines at the P_{+1} (HAL4) and P_{-2} (HAL5) positions, either individually or in combination (HAL6), did not increase SH3:linker engagement, nor did addition of the P_{+1}

proline to the HAL3 protein (HAL7). However, sequential addition of prolines to HAL7 at the P_{-2} (HAL8) and P_{-3} (HAL9) positions resulted in dramatic increases to the unfolding half-life of about 5-fold and 7-fold for HAL8 and HAL9, respectively. Addition of one final proline to HAL9 at position P_{-4} (HAL10) completely suppressed cooperative unfolding, suggesting that the SH3 domain is essentially locked to this modified linker.

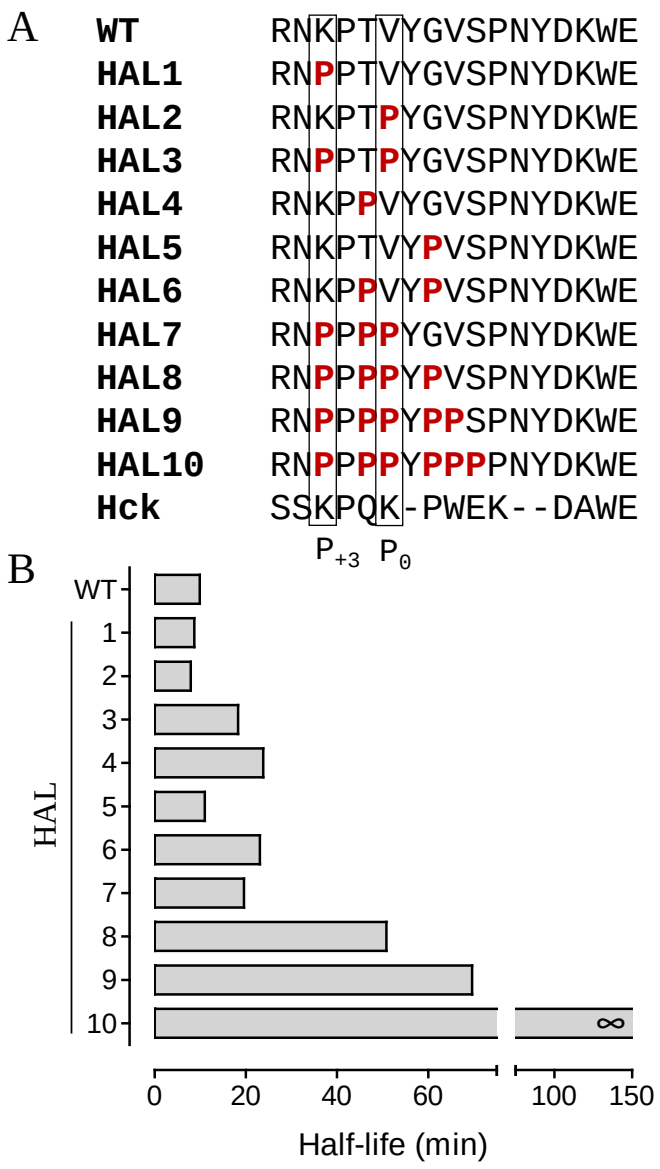

Figure 6: Linker proline substitutions enhance SH3 engagement. A) The sequence of the wild-type c-ABL linker is aligned with each of the ten HAL sequences as well as the linker of the Src-family kinase, HCK. Proline substitutions introduced into each of the HAL sequences are highlighted in red. **B)** Analysis of intramolecular SH3:linker interaction by HXMS. Recombinant c-ABL proteins consisting of the NCap, SH3 and SH2 domains plus each of the linkers shown were expressed in bacteria, purified, and subjected to HX MS analysis as described in the text. Data are expressed as the unfolding half-life of the SH3 domain which is directly proportional to the strength of the internal SH3-linker interaction.

We next introduced all ten HAL sequences into a c-ABL kinase core protein composed of the NCap, the SH3 and SH2 domains, the SH2-kinase linker and the kinase domain. The X-ray crystal structure of this core protein has been determined previously and it contains all of the structural elements necessary for downregulation (Nagar et al., 2006). To determine the impact of the HAL sequences on ABL kinase activity, the wild-type and HAL core proteins were expressed in 293T cells, immunoprecipitated and immunoblotted with antibodies against key phosphotyrosine residues in the activation loop (pTyr412), the SH2-kinase linker (pTyr245) and in the SH3 domain (pTyr89). As shown in Figure 7A, ABL core proteins with HAL sequences 1, 4, 6, 8 and 9 were phosphorylated at each of these sites to the same or reduced levels relative to wild-type ABL, suggesting that these modified linkers adopt a PPII helical conformation compatible with downregulation of the wild-type ABL kinase core (Figure 5). As an independent measure of kinase activity, we also assessed levels of tyrosine phosphoproteins in lysates from the transfected cells. As shown in Figure 7B, the extent of protein-tyrosine phosphorylation in the cell lysates parallels the level of phosphorylation at each of the regulatory tyrosines in each c-ABL core protein. A quantitative analysis of regulatory site phosphorylation is presented in Figure 7C.

In contrast, ABL core proteins with HAL substitutions 2, 3, 5, and 7 showed much higher phosphorylation of autoregulatory tyrosine sites and a concomitant increase in cellular phosphotyrosine content (Figure 7). The HAL10 core protein also appeared to be upregulated, albeit to a lesser extent. While the HXMS studies show that the HAL10 substitutions strongly enhances SH3 domain interaction, it must also produce additional changes to the linker structure that interfere with its ability to contact the kinase domain to effectively downregulate kinase activity.

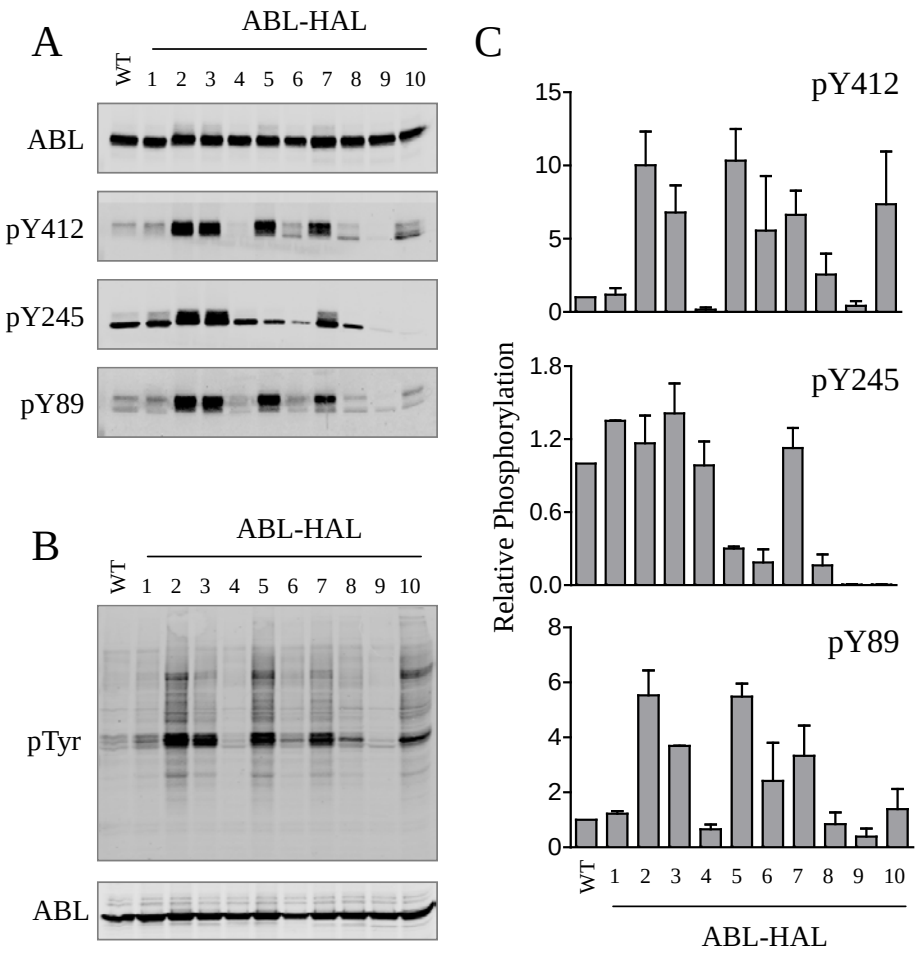

Figure 7: ABL-HAL core protein expression and relative kinase activity. A) Each of the HAL sequences shown in Figure 6A were introduced into the c-ABL kinase core, consisting of the NCap, the SH3 and SH2 domains, the SH2-kinase linker, and the kinase domain. Each ABL core proteins was expressed in 293T cells, immunoprecipitated, and immunoblotted with phosphospecific antibodies against phosphotyrosine residues in the activation loop (pY412), the SH2-kinase linker (pY245) and the SH3 domain (pY89) as well as for ABL protein recovery. **B)** Overall protein-tyrosine phosphorylation was assessed in the cell lysates by immunoblotting; ABL blots were also performed as a control. **C)** The phosphotyrosine signal intensities from two independent experiments were normalized to the levels obtained with wild-type ABL, and the results are presented as fold change ± S.D.

2.3.2 Enhanced SH3:linker interaction overcomes ABL core activation by gatekeeper and myr-binding pocket mutations

Previous studies have shown that the ABL "gatekeeper" mutant associated with imatinib resistance (T315I) is much more active in vitro than the corresponding wild-type kinase. Furthermore, mutations of the N-terminal c-ABL myristoylation site or the complementary myristate binding pocket in the kinase domain C-lobe (e.g., A356N) strongly upregulate ABL kinase activity (Hantschel et al., 2003). These observations led us to explore whether enhanced SH3:linker interaction could reverse these activating influences through an allosteric mechanism. To test this possibility, we first confirmed the activating effects of these ABL mutations using the 293T cell expression system. Three ABL core protein mutants were expressed: the T315I gatekeeper mutant, a myristoylation-defective mutant in which the essential N-terminal glycine is replaced with alanine (G2A), and the myristic acid binding pocket mutant (A356N) described above. As shown in Figure 8, all three mutations strongly enhanced the phosphorylation of the activation loop (pY412), linker (pY245) and SH3 domain (pY89) regulatory sites and resulted in a parallel increase in overall protein-tyrosine phosphorylation in cell lysates.

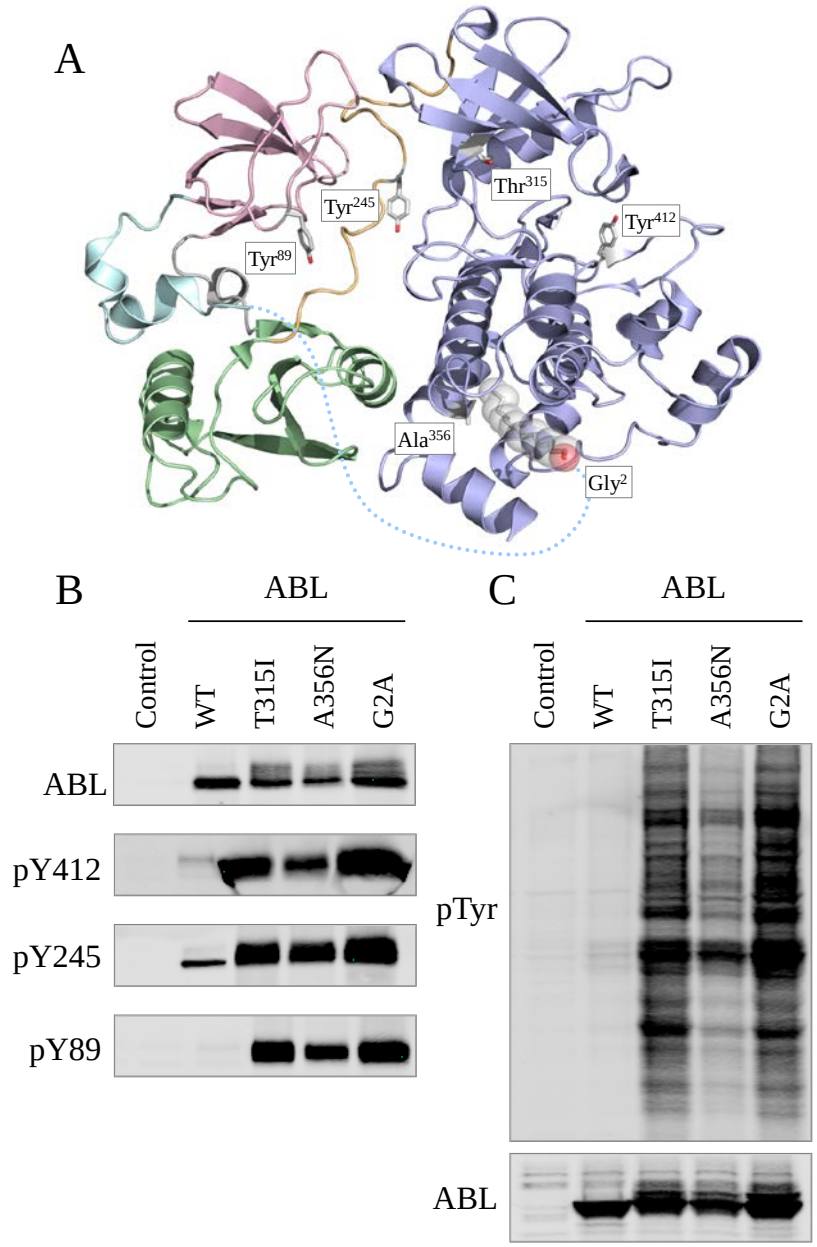

Figure 8: Activating mutations of the ABL-core protein. A) Model of the downregulated, myristoylated c-ABL core showing the positions of key tyrosine autophosphorylation sites in the SH3 domain (Tyr89), SH2-kinase linker (Tyr245) and kinase domain activation loop (Tyr412). The positions of three activating mutations are also shown, which involve Ile substitution for the gatekeeper residue (Thr315), Asn substitution for Ala356 in the myristate binding pocket, and substitution of Gly2 with Ala, which prevents myristoylation. (Numbering is based on the crystal structure of the c-ABL core (PDB: 2FO0) with the exception of the gatekeeper residue, which is numbered as Thr315 by convention; this position corresponds to Thr334 in structure 2FO0. **B)** The wild-type (WT) c-ABL core

and active mutants described in part A (T315I, A356N, and G2A) were expressed in 293T cells, immunoprecipitated, and immunoblotted with phosphospecific antibodies against pY412, pY245 and pY89 as well as for ABL protein recovery. Untransfected cells served as the negative control. **C)** Overall protein-tyrosine phosphorylation was assessed in the cell lysates by immunoblotting; ABL blots were also performed as a control.

To determine whether enhanced SH3:linker interaction influences the effect of activating mutations in the ABL core, we combined all ten HAL sequences with the myristate-binding pocket mutation (A356N). We then expressed these proteins in 293T cells and looked for changes in autophosphorylation of the three regulatory tyrosines. As shown in Figure 9, HAL9 completely reversed the potent activating effects of the A356N mutation as judged by the reduced phosphorylation of all three tyrosine sites. In addition, the overall phosphotyrosine content of lysates from cells expressing ABL-HAL9-A356N is dramatically reduced. These data support the idea that SH3:linker interaction allosterically overrides the activating effect of the myristic acid binding pocket mutation.

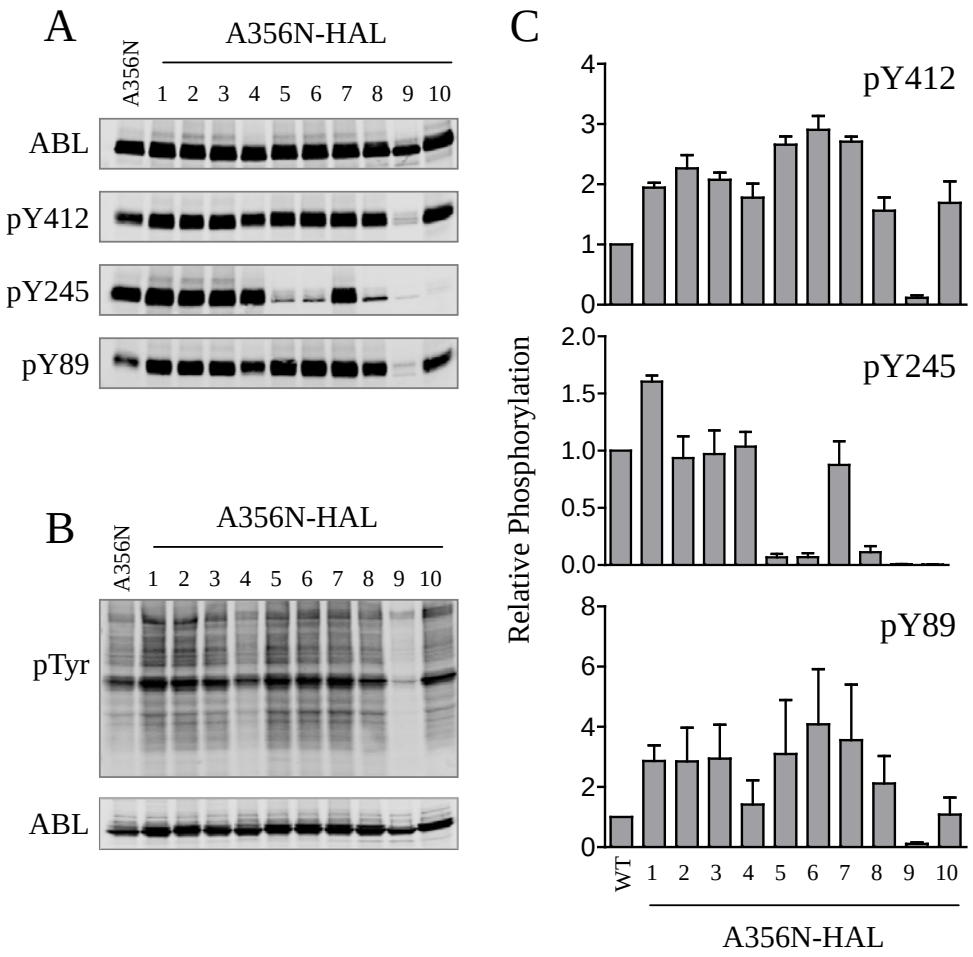

Figure 9: HAL9 completely suppresses c-ABL activation caused by myristic acid binding pocket mutation (A356N). A) Each of the ten HAL sequences was combined with the A356N mutation in the c-ABL core and the resulting compound mutants were expressed in 293T cells. ABL proteins were immunoprecipitated and immunoblotted with phosphospecific antibodies against the activation loop (pY412), the SH2-kinase linker (pY245) and the SH3 domain (pY89) as well as for Abl protein recovery. **B)** Overall protein-tyrosine phosphorylation was assessed in the cell lysates by immunoblotting; ABL blots were also performed as a control. **C)** The phosphotyrosine signal intensities from three independent experiments were normalized to the levels obtained with the A356N ABL mutant with a wild-type linker, and the results are presented as fold change ± S.D.

We next combined each of HAL sequences with the myristoylation-defective ABL core mutant, G2A. Compared to ABL A356N, HAL9 substitution partially reversed the activating effects of this mutation both in terms of autophosphorylation and cell protein phosphorylation (Figure 10). This result suggests that disruption of myr-NCap interaction with the kinase domain C-lobe by mutating the myristoylation site results in a different active state of the ABL core compared to mutation of the myristic acid binding pocket.

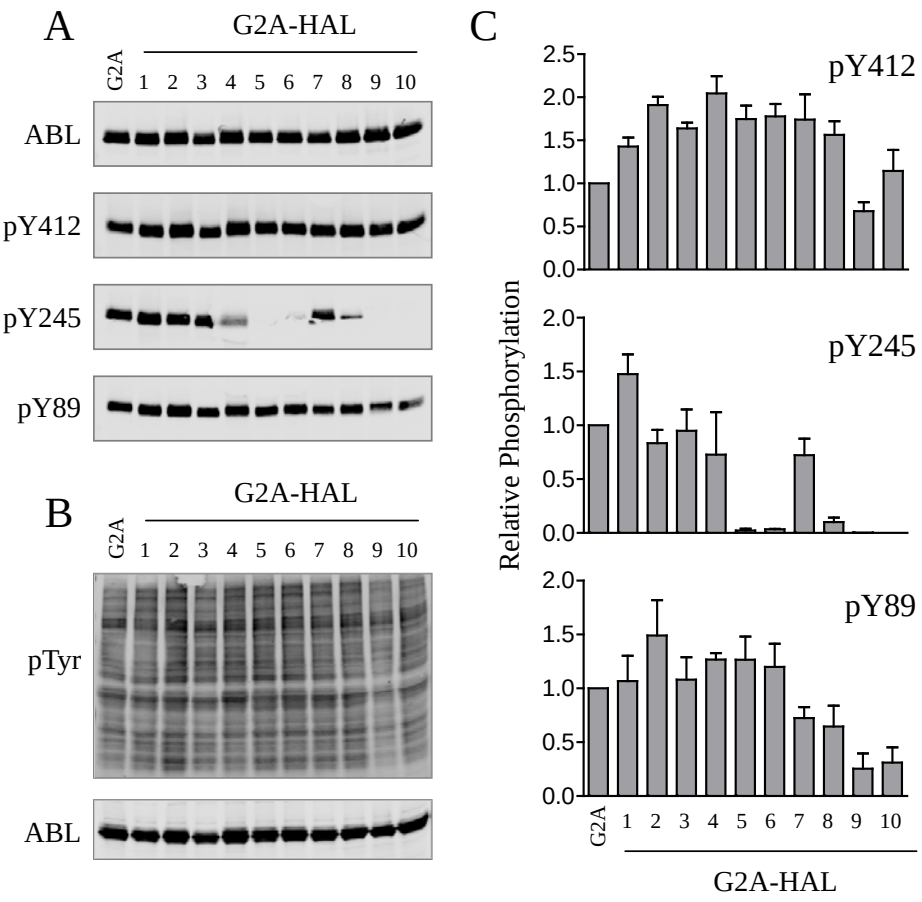

Figure 10: HAL9 partially reverses c-ABL activation caused by myristoylation signal sequence mutation (G2A). A) Each of the ten HAL sequences was combined with the G2A mutation in the myristoylation signal sequence of the c-ABL core, and the resulting compound mutants were expressed in 293T cells. ABL proteins were immunoprecipitated and immunoblotted with phosphospecific antibodies against the activation loop (pY412), the SH2-kinase linker (pY245) and the SH3 domain (pY89) as well as for ABL protein recovery. **B)** Overall protein-

tyrosine phosphorylation was assessed in the cell lysates by immunoblotting; ABL blots were also performed as a control. C) The phosphotyrosine signal intensities from two independent experiments were normalized to the levels obtained with the G2A ABL mutant with a wild-type linker, and the results are presented as fold change ± S.D.

We have previously observed that the activating gatekeeper mutation in the c-ABL core (T315I) causes local conformational changes in the kinase domain and at a distance in the SH3 domain. To investigate whether enhanced SH3:linker interaction impacted the activating effect of the gatekeeper mutation, we combined all ten HAL sequences with T315I and determined their relative activity in 293T cells. As shown in Figure 11, HAL9 reversed ABL core T315I activation loop tyrosine phosphorylation (pTyr412) by more than 60%, while phosphorylation of the linker (pTyr245) and SH3 domain (pTyr89) was completely suppressed. Consistent with these observations, HAL9 substitution also substantially reduced cellular phosphotyrosine content. These results show that the destabilizing impact of ABL gatekeeper mutation on the ABL kinase domain remains under the allosteric control of SH3:linker interaction.

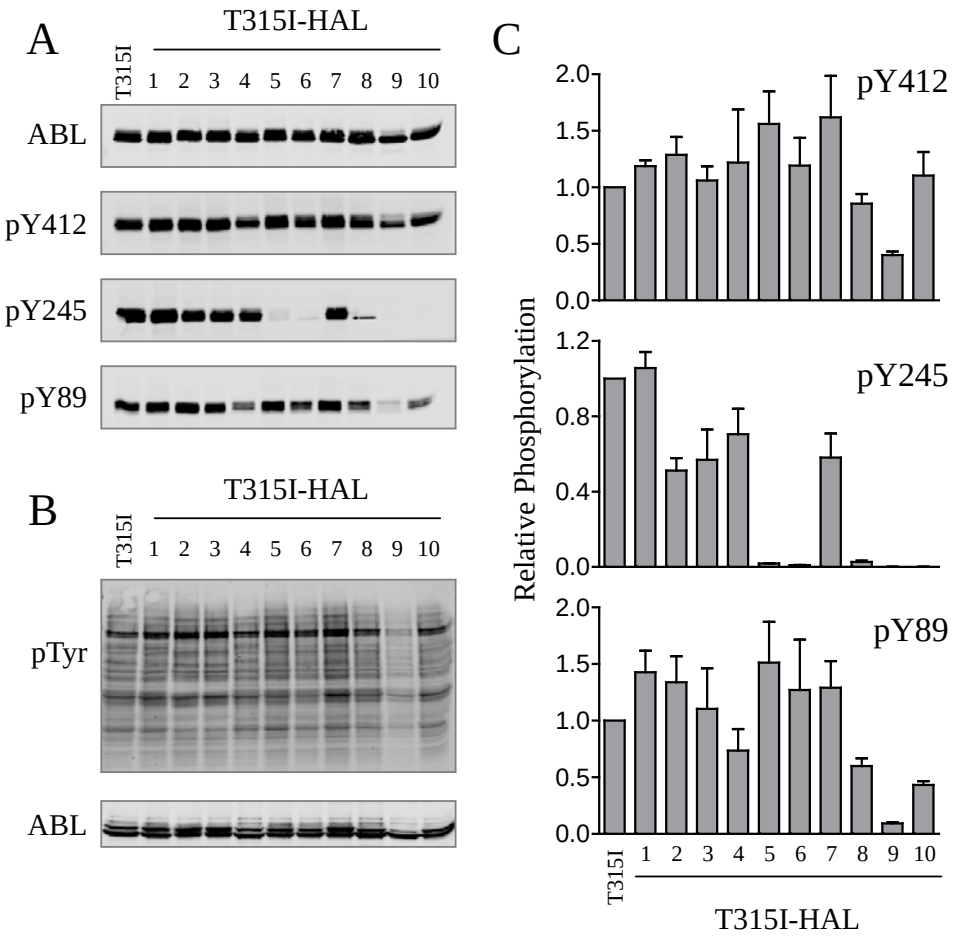

Figure 11: HAL9 suppresses c-ABL activation caused by gatekeeper mutation (T315I). A) Each of the ten HAL sequences was combined with the T315I gatekeeper mutation in the c-ABL kinase domain, and the resulting compound mutants were expressed in 293T cells. ABL proteins were immunoprecipitated and immunoblotted with phosphospecific antibodies against the activation loop (pY412), the SH2-kinase linker (pY245) and the SH3 domain (pY89) as well as for ABL protein recovery. **B)** Overall protein-tyrosine phosphorylation was assessed in the cell lysates by immunoblotting; ABL blots were also performed as a control. **C)** The phosphotyrosine signal intensities from two independent experiments were normalized to the levels obtained with the T315I ABL mutant with a wild-type linker, and the results are presented as fold change ± S.D.

2.3.3 Enhanced SH3:linker interaction overcomes ABL kinase activation by SH2-kinase interface mutation

The interface of the SH2 and kinase domain C-lobe is also important for auto-inhibition of the c-ABL kinase. In the X-ray crystal structure of the downregulated core, Tyr158 in the SH2 domain makes a pi-stacking interaction with Tyr361 of kinase domain helix αE and is also hydrogen bonded to Asn393 (Nagar et al., 2003; Nagar et al., 2006). Substitution of SH2 Tyr158 with aspartate (Y158D) has been shown to increase ABL kinase activity, presumably by disturbing this interaction. To determine whether enhanced SH3:linker interaction influences the activating effects of the Y158D mutation, the HAL9 sequence was combined with this SH2 mutation in the c-ABL core. As shown in Figure 12, the Y158D mutation alone strongly enhanced autophosphorylation of regulatory tyrosines 412, 89 and 245, and enhanced the phosphorylation of cellular proteins. Remarkably, introduction of the HAL9 sequence almost completely reversed the activation resulting from this SH2 domain mutation. Activation loop phosphorylation was suppressed by 80%, while phosphorylation of the regulatory SH3 and linker tyrosines was almost completely suppressed. The presence of HAL9 also significantly reduced overall protein-tyrosine phosphorylation in lysates from cells expressing this mutant. These data show that enhanced SH3-linker interaction overcomes the activating effect of disturbing the SH2:kinase domain interaction, and reveal an allosteric connection between the SH3:linker and SH2:C-lobe.

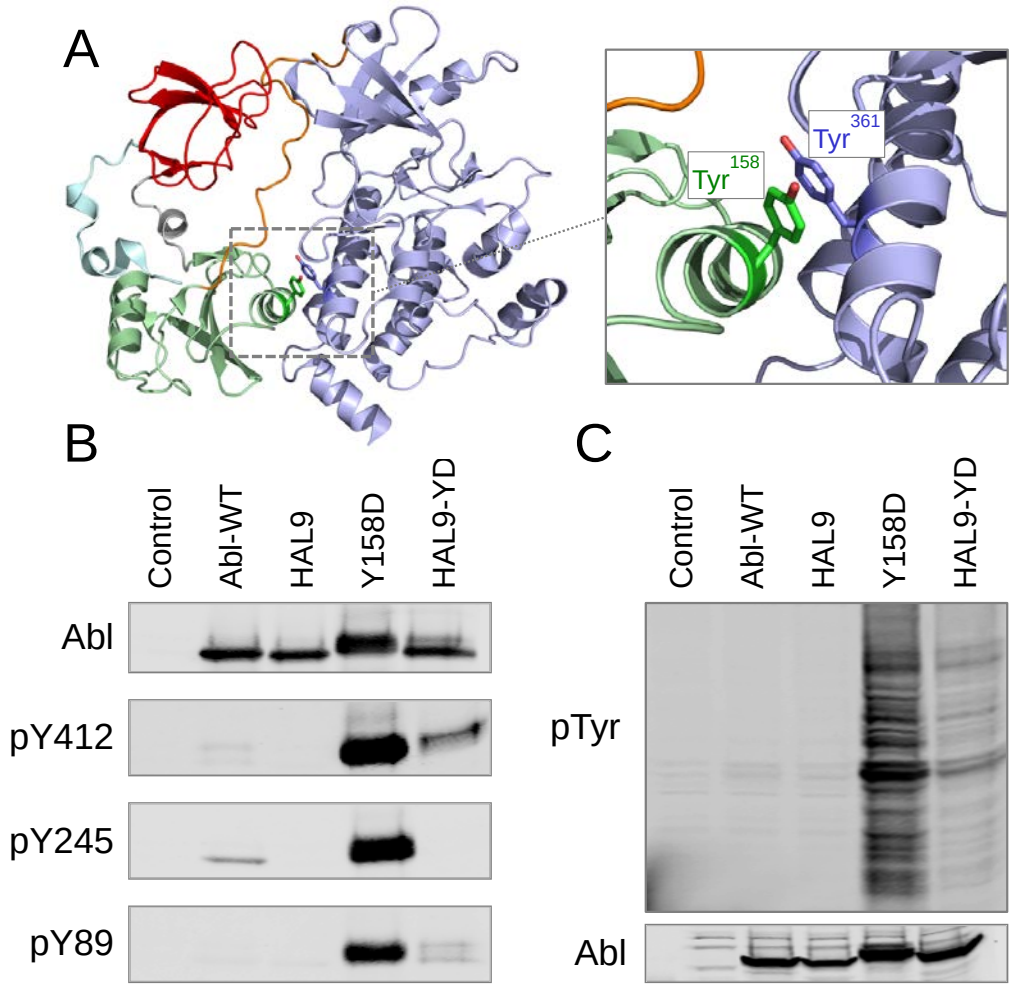

Figure 12: HAL9 substitution suppresses c-ABL core activation by SH2-kinase interface mutation (Y158D). **A)** Model of the c-ABL core highlighting tyrosine residues in the SH2 domain (Tyr158) and kinase domain C-lobe (Tyr361) that interact as part of the downregulated conformation. **B)** The wild-type c-ABL core protein (WT), HAL9, the SH2 Tyr158 to aspartate mutant (Y158D), as well as the compound mutant (HAL9-YD) were expressed in 293T cells. Untransfected cells were included as a negative control. ABL proteins were immunoprecipitated and immunoblotted with phosphospecific antibodies against the activation loop (pY412), the SH2-kinase linker (pY245) and the SH3 domain (pY89) as well as for ABL protein recovery. **C)** Overall protein-tyrosine phosphorylation was assessed in the cell lysates by immunoblotting; ABL blots were also performed as a control. This experiment was repeated twice and produced comparable results; a representative example is shown.

2.3.4 High affinity linkers sensitize BCR-ABL-transformed cells to imatinib-induced apoptosis

Structural and biochemical data have established that imatinib inhibits BCR-ABL by stabilizing the inactive conformation of the kinase domain, which provides the basis for some of its kinase selectivity. Results presented so far show that enhanced SH3:linker interaction suppresses ABL kinase activity, suggesting that the HAL sequence may stabilize the inactive ABL kinase domain conformation and enhance imatinib sensitivity. To test this idea, we transformed human TF-1 myeloid cells with the wild-type and HAL9 forms of BCR-ABL. Each transformed cell population was then treated with imatinib at concentrations ranging from 0.03 to 1 μM for 48 hours, followed by assays for effector caspase activation and cell viability. As shown in Figure 13A, TF-1 cells transformed with wild-type BCR-ABL showed a dose-dependent increase in apoptosis following imatinib treatment. When this experiment was repeated with cells expressing BCR-ABL-HAL, the apparent potency of imatinib was increased, supporting the idea that enhanced SH3-linker interaction stabilizes the "DFG-out" kinase domain conformation required for imatinib binding. Immunoblots for BCR-ABL activity were consistent with the apoptosis data, showing enhanced sensitivity to imatinib at the activation loop (pY412), the SH3 domain (pY89) and in overall tyrosine phosphorylation of proteins in cell lysates (Figure 13B). In contrast, HAL9 substitution did not sensitize TF-1 cells transformed with BCR-ABL T315I responded to imatinib, even at concentrations as high as 10 μM (Figure 14). This is consistent with the steric clash and loss of the T315 H-bond to imatinib that results from the T315I mutation (Gorre et al., 2001).

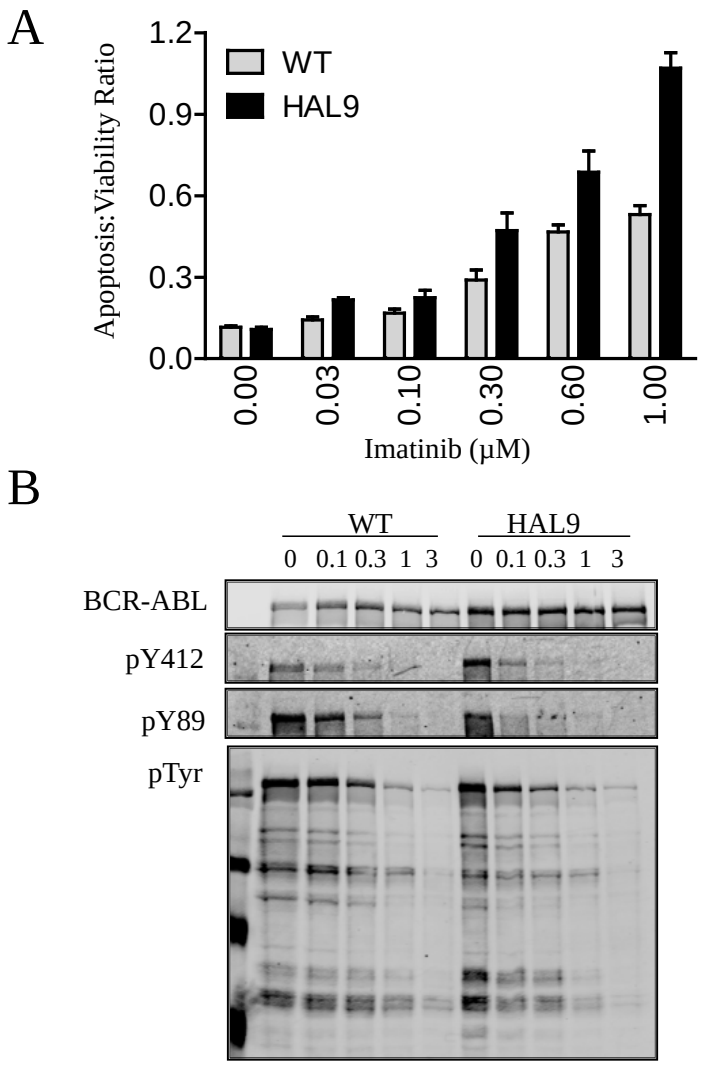

Figure 13: HAL9 sensitizes BCR-ABL-transformed cells to imatinib-induced apoptosis. A) Human TF-1 myeloid cells were transduced with BCR-ABL retroviruses with either wild-type (WT) or high-affinity (HAL9) SH2-kinase linkers. Transformed cells were plated in triplicate wells in the presence of the indicated concentrations of imatinib for 48 h. Apoptosis (assayed as Caspase3/7 activity) and cell viability were measured simultaneously as described under Materials and Methods. Apoptosis data were normalized to viable cell number and are presented in the bar graph as the average of three independent experiments performed in each of two independently transformed cell lines. **B)** TF-1 cells transformed with wild-type (WT) or HAL9 BCR-ABL were treated with the indicated concentrations of imatinib for 16 h. Cell lysates were immunoblotted with antibodies to the BCR-ABL protein, phosphospecific antibodies for the BCR-ABL activation loop (pY412) and SH3 domain (pY89), and for overall levels of protein tyrosine phosphorylation (pTyr).

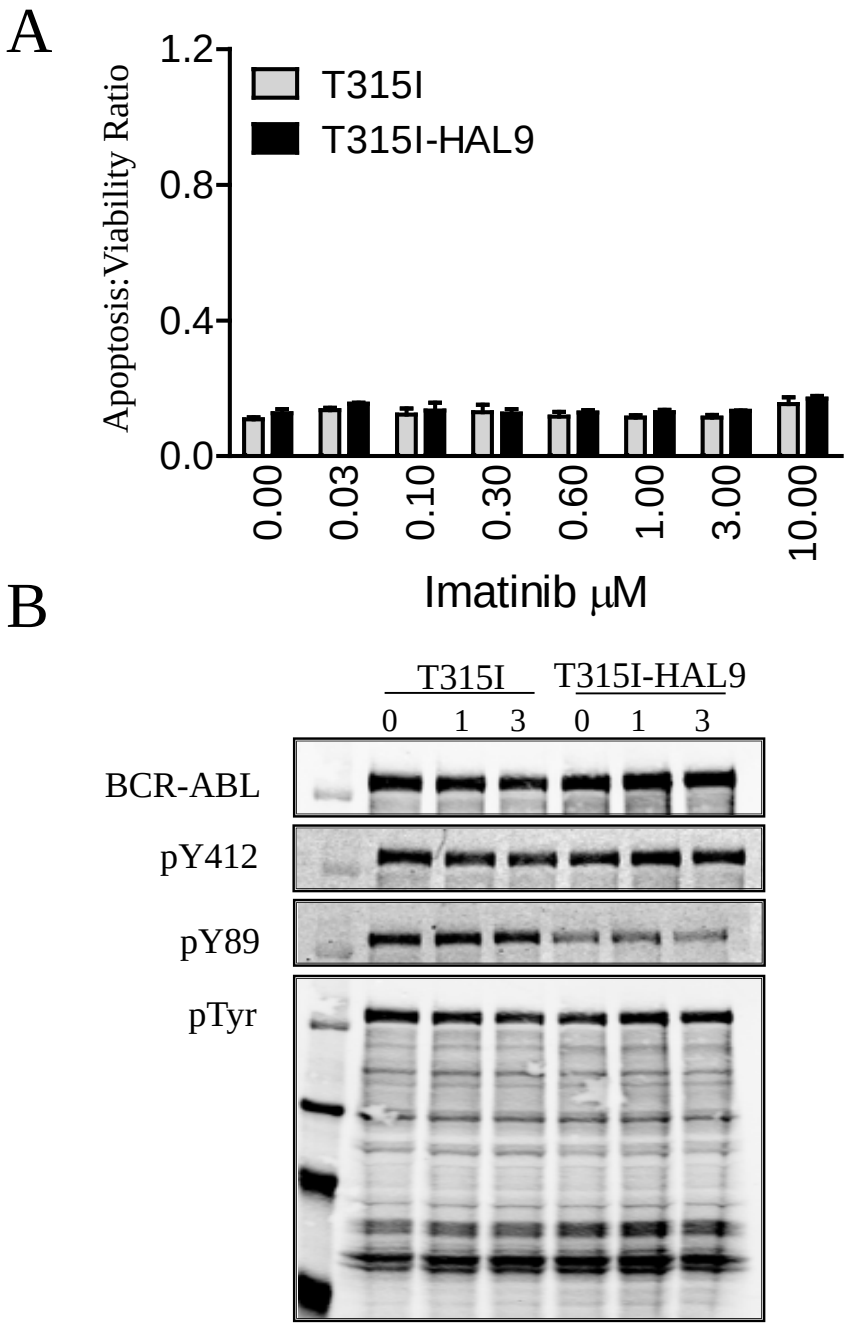

Figure 14: HAL9 does not affect imatinib-induced apoptosis in myeloid cells transformed with BCR-ABL T315I. A) Human TF-1 myeloid cells were transduced with BCR-ABL T315I retroviruses with either wild-type (T315I) or high-affinity (T315I-HAL9) SH2-kinase linkers. Transformed cells were plated in triplicate wells in the presence of the indicated concentrations of imatinib for 48 h. Apoptosis (assayed as Caspase3/7 activity) and cell viability were measured simultaneously as described under Materials and Methods. Apoptosis data were normalized to viable cell number and are presented in the bar graph as the average of three independent experiments performed

in each of two independently transformed cell lines. **B)** TF-1 cells transformed with the T315I or T315I-HAL9 forms of BCR-ABL were treated with the indicated concentrations of imatinib for 16 h. Cell lysates were immunoblotted with antibodies to the BCR-ABL protein, phosphospecific antibodies for the BCR-ABL activation loop (pY412) and SH3 domain (pY89), and for overall levels of protein tyrosine phosphorylation (pTyr).

2.3.5 High affinity linkers sensitize BCR-ABL-transformed cells to the allosteric kinase inhibitors

Recent studies have identified a novel class of BCR-ABL inhibitors that interact with the myristic acid binding pocket in the C-lobe of the kinase domain (Adrian et al., 2006; Zhang et al., 2010). Structural and dynamics studies show that these inhibitors, of which the phenylaminopyrimidine compound GNF-2 is the prototype, stabilize the active site of the kinase through an allosteric mechanism (Zhang et al., 2010; Iacob et al., 2011). These observations led us to investigate whether HAL substitution also enhances the sensitivity of BCR-ABL-transformed TF-1 cells to allosteric inhibitors such as GNF-2. We first evaluated the sensitivity of TF-1 cells transformed with the wild-type and HAL9 forms of BCR-ABL to GNF-2 treatment (Figure 15A). In this case, the presence of the high affinity linker dramatically enhanced the apoptotic response to GNF-2, with half-maximal induction of apoptosis at 200 nM. In contrast, cells transformed with wild-type BCR-ABL were much less sensitive to GNF-2, with an IC_{50} value of at least 10 μM. Immunoblots for BCR-ABL kinase activity closely parallel the apoptosis results, with nearly complete inhibition of BCR-ABL-HAL9 kinase activity with as little as 100 nM GNF-2 (Figure 15B). These results support an allosteric connection between the SH3 domain and the myristic acid binding pocket, and show that inhibitors targeting this C-lobe binding site are sensitive to the overall conformation of the ABL kinase domain.

Although the binding site for GNF-2 is localized to the C-lobe of the kinase domain, the imatinib-resistant BCR-ABL mutant T315I is also insensitive to this allosteric inhibitor. Given the strong sensitizing effect of the HAL substitution on the apoptotic response to GNF-2 in wild-type BCR-ABL, we repeated these experiments using TF-1 cells transformed with BCR-ABL T315I bearing either a wild-type linker or the HAL9 substitution. As shown in Figure 16A, HAL9 substitution markedly enhanced the sensitivity of TF-1 cells transformed with BCR-ABL T315I to the apoptotic effects of GNF-2, although the impact was not as strong as that observed for wild-type BCR-ABL. Immunoblots for BCR-ABL T315I kinase activity also show the influence of the HAL9 substitution on GNF-2 sensitivity (Figure 16B). This result shows that enhanced SH3:linker interaction can influence the T315I kinase domain conformation in the context of BCR-ABL. Very similar results were obtained with the second-generation analog, GNF-5, for which in vivo efficacy has recently been demonstrated (Figure 17).

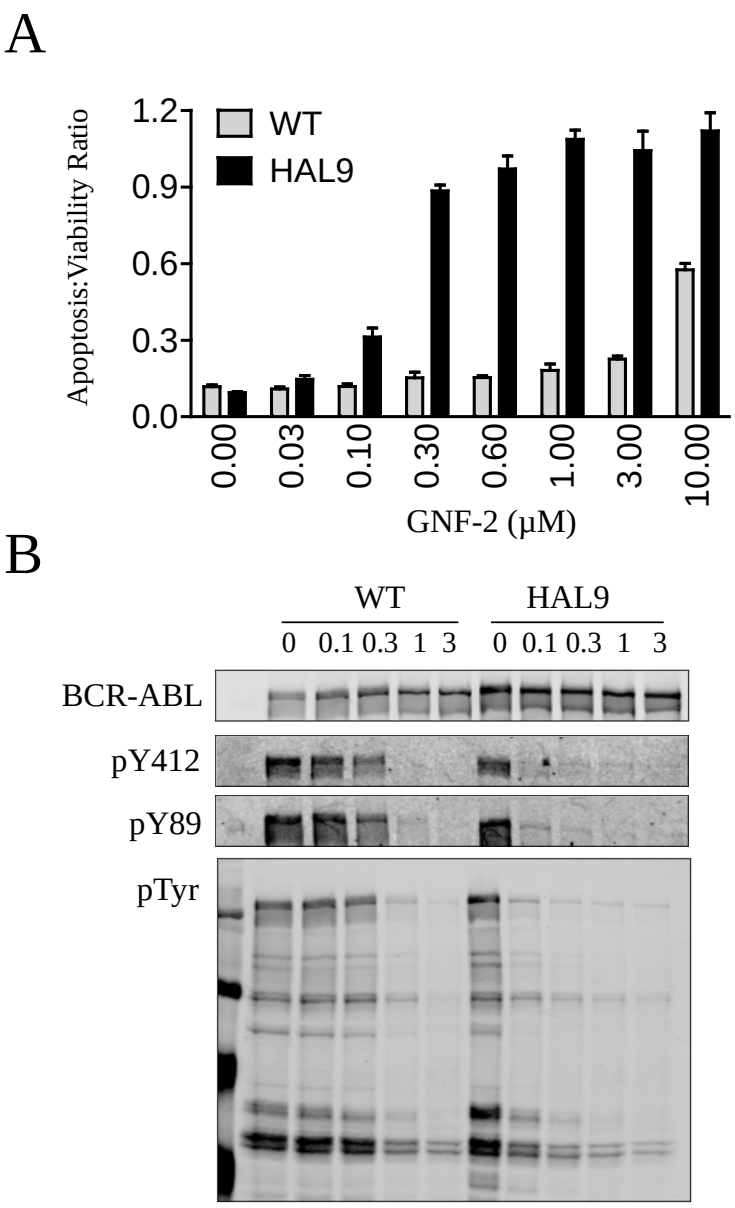

Figure 15: HAL9 sensitizes BCR-ABL-transformed cells to GNF-2-induced apoptosis. A) Human TF-1 myeloid cells were transduced with BCR-ABL retroviruses with either wild-type (WT) or high-affinity (HAL9) SH2-kinase linkers. Transformed cells were plated in triplicate wells in the presence of the indicated concentrations of GNF-2 for 48 h. Apoptosis (assayed as Caspase3/7 activity) and cell viability were measured simultaneously as described under Materials and Methods. Apoptosis data were normalized to viable cell number and are presented in the bar graph as the average of three independent experiments performed in each of two independently transformed cell lines. **B)** TF-1 cells transformed with wild-type (WT) or HAL9 BCR-ABL were treated with the indicated concentrations of GNF-2 for 16 h. Cell lysates were immunoblotted with antibodies to the BCR-ABL protein,

phosphospecific antibodies for the BCR-ABL activation loop (pY412) and SH3 domain (pY89), and for overall levels of protein tyrosine phosphorylation (pTyr).

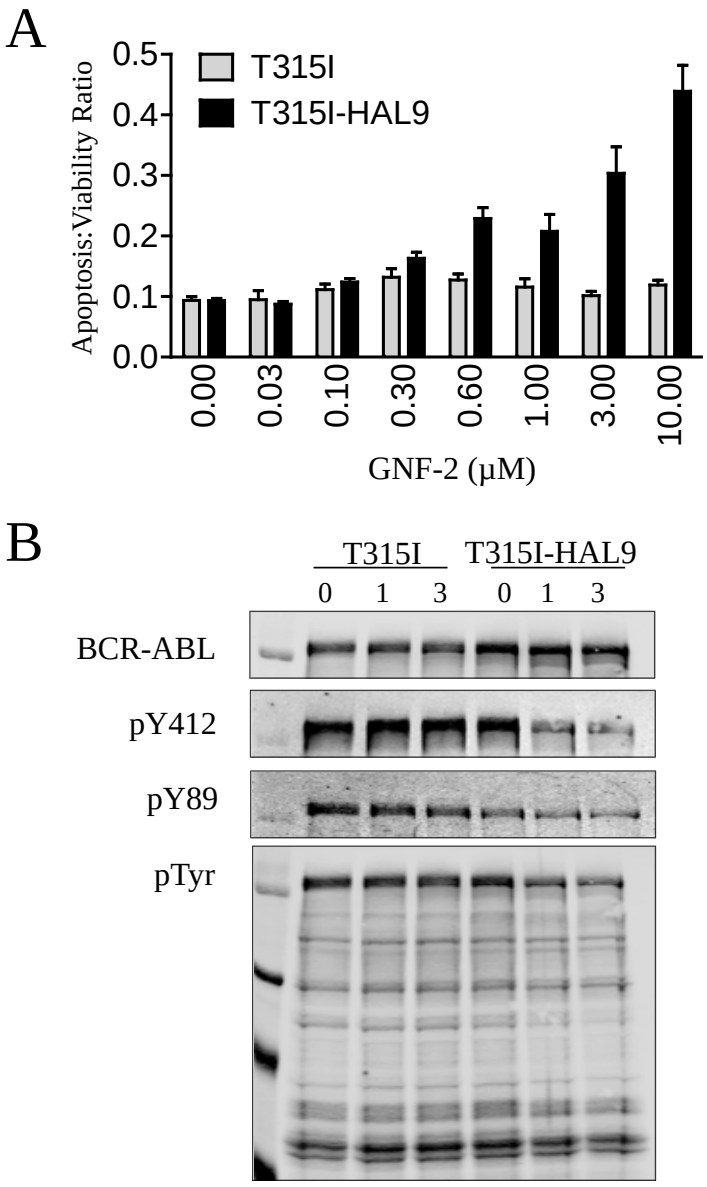

Figure 16: HAL9 sensitizes myeloid cells transformed with BCR-ABL T315I to GNF-2-mediated apoptosis. A) Human TF-1 myeloid cells were transduced with BCR-ABL T315I retroviruses with either wild-type (T315I) or high-affinity (T315I-HAL9) SH2-kinase linkers. Transformed cells were plated in triplicate wells in the presence of the indicated concentrations of GNF-2 for 48 h. Apoptosis (assayed as Caspase3/7 activity) and cell viability were measured simultaneously as described under Materials and Methods. Apoptosis data were normalized to viable cell number and are presented in the bar graph as the average of three independent experiments performed in each of two

independently transformed cell lines. **B)** TF-1 cells transformed with the T315I or T315I-HAL9 forms of BCR-ABL were treated with the indicated concentrations of GNF-2 for 16 h. Cell lysates were immunoblotted with antibodies to the BCR-ABL protein, phosphospecific antibodies for the BCR-ABL activation loop (pY412) and SH3 domain (pY89), and for overall levels of protein tyrosine phosphorylation (pTyr).

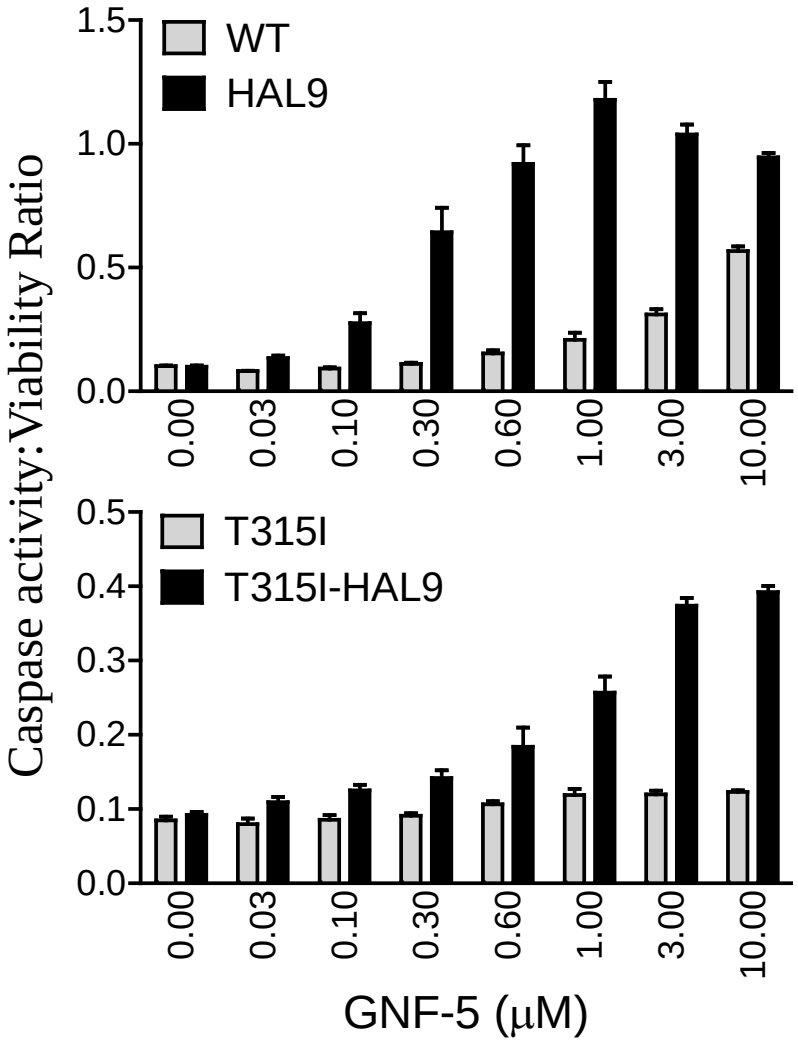

Figure 17: HAL9 sensitizes wild-type and T315I BCR-ABL-transformed cells to GNF-5-induced apoptosis. Human TF-1 myeloid cells were transduced with wild-type (WT; *top*) or T315I (*bottom*) *BCR-ABL* retroviruses with either wild-type or high-affinity (HAL9) SH2-kinase linkers as indicated. Transformed cells were plated in triplicate wells in the presence of the indicated concentrations of GNF-2 for 48 h. Apoptosis (assayed as Caspase3/7 activity) and cell viability were measured simultaneously as described under Materials and Methods. Apoptosis data were

normalized to viable cell number and are presented in the bar graph as the average of three independent experiments performed in each of two independently transformed cell lines.

2.3.6 Hydrogen exchange mass spectrometry (HXMS) supports allosteric interplay between the SH3 domain, the GNF-2 binding pocket and the active site of the c-Abl core

Results presented above demonstrate that enhanced SH3:linker interaction completely suppresses the activity of a c-ABL core domain myristate binding pocket mutant (A356N; Figure 9), and dramatically enhances the sensitivity of BCR-ABL to allosteric inhibitors (GNF-2, GNF-5) that bind to this C-lobe pocket (Figures 15-17). These findings suggest that the SH3:linker interface exerts remarkable allosteric control over the regulatory influence of the C-lobe on the active site. To test this possibility from a structural perspective, we investigated global conformational changes in recombinant c-ABL kinase core proteins that result from the A356N mutation and HAL9 substitution using hydrogen exchange mass spectrometry (HX MS).

The c-ABL core proteins chosen for comparison include wild-type (WT), the A356N mutant, HAL9, and the combined HAL9-A356N protein. All four proteins were expressed in their myristoylated forms using Sf9 cells as the host, and purified to homogeneity. The intact mass of each protein was determined, and showed that the WT and HAL9 proteins were largely unphosphorylated, while the A356N mutant was heavily phosphorylated, consistent with the activating effect of this mutation (Figure 18). Interestingly, HAL9 substitution nearly reversed autophosphorylation of A356N, supporting the dominant allosteric control of enhanced SH3:linker interaction on overall kinase activity.

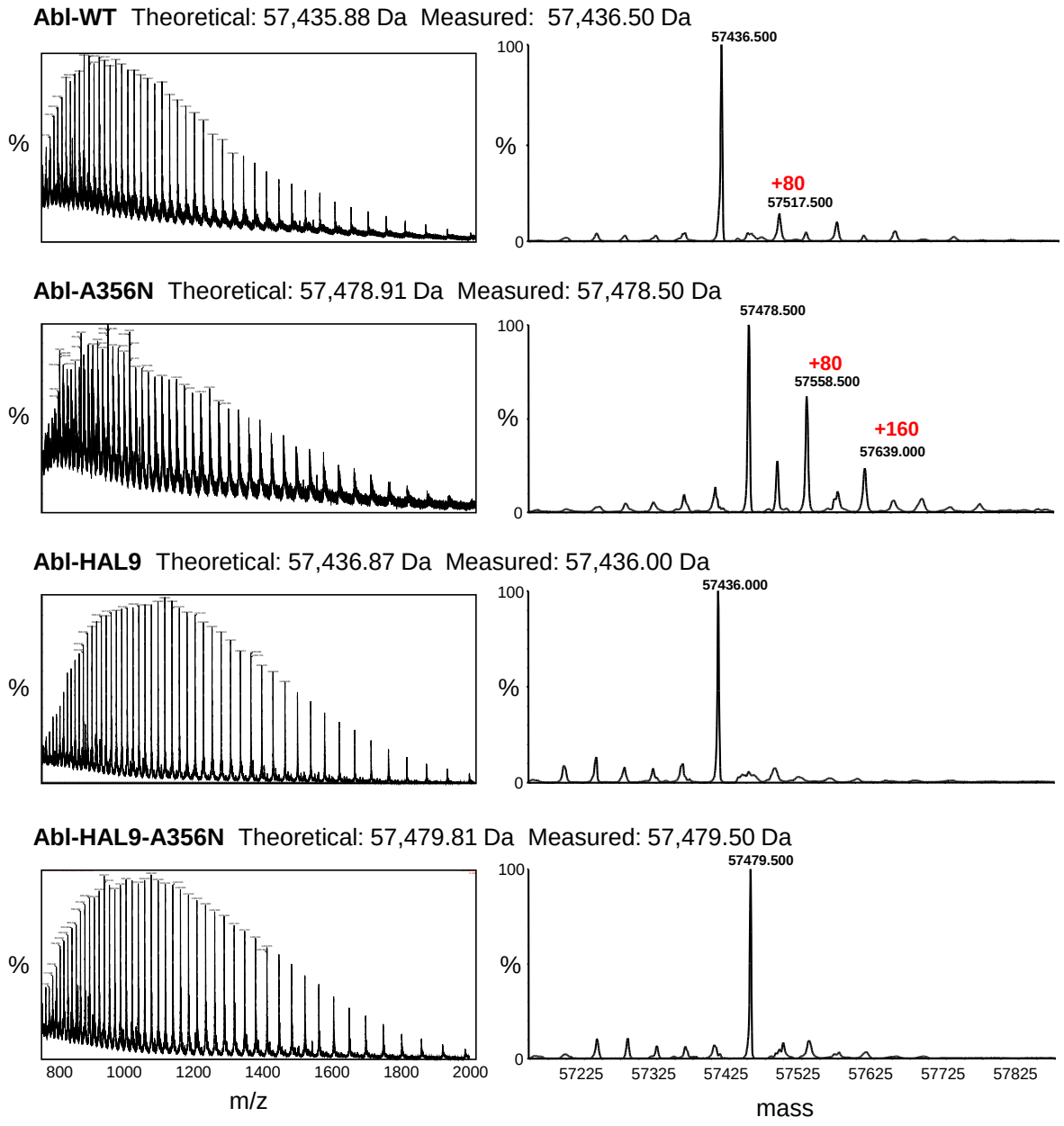

Figure 18: Mass analysis of recombinant c-ABL core proteins. Wild-type c-ABL core (WT), A356N, HAL9 and A356N-HAL9 proteins were overexpressed in Sf9 insect cells together with the Yersinia phosphatase, YopH, as described previously for the wild-type c-ABL core (Iacob et al., 2009). For intact protein mass spectral analysis, each protein was injected onto a POROS 20 R2 protein trap and desalted with 0.05% trifluroacetic acid (TFA) at a flow rate of 100 µL/min. The proteins were eluted into the mass spectrometer, using a linear 15-75% (vol/vol) acetonitrile gradient over 4 min at 50 µL/min and a Shimadzu HPLC system (LC-10ADvp). Intact protein analyses were performed on an LCT-Premier instrument (Waters) equipped with a standard electrospray source. The capillary

voltage was 3.2 kV and the cone voltage was 35 V. Nitrogen was used as desolvation gas. A source temperature of 175 °C and a desolvation temperature of 80 °C were applied. The instrument was calibrated by infusing a solution of 500 fmol/µL myoglobin and the mass accuracy was 10 ppm. The raw m/z data are shown on the left and the transformed, mass-only spectra are shown on the right. The measured and theoretical molecular masses are indicated, and the additional + 80 Da peaks correspond to tyrosine phosphorylated species. All masses are consistent with stoichiometrically myristoylated proteins.

For HX MS experiments, each recombinant ABL core protein was diluted into D_2O-based buffer, and aliquots were removed at various time points followed by rapid quenching. In order to refine to location of deuterium incorporation, each protein was digested with pepsin prior to mass spectrometry. The peptic peptide coverage maps are shown in Figure 19. Deuterium uptake curves were then generated for each peptic peptide, and are presented pairwise for the WT vs. A356N mutant (Figure 20A), WT vs. HAL9 (Figure 20B), and A356N vs. A356N-HAL9 (Figure 20C). Overall, the rate of deuterium incorporation, and therefore protein dynamics, was the same for most of the peptides across all three comparisons during the time frame of the experiment (4 hours). However, several important differences were observed that provide remarkable insight into the impact of the opposing effects of the A356N and HAL9 substitutions on overall dynamics.

Abl-WT

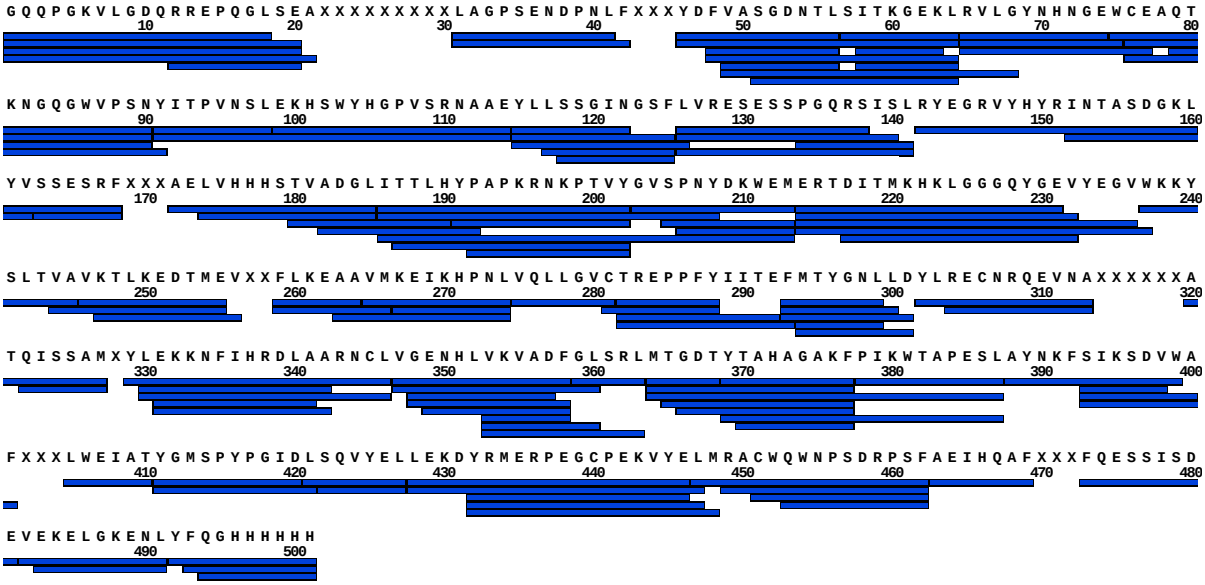

Abl-A356N

Abl-HAL9

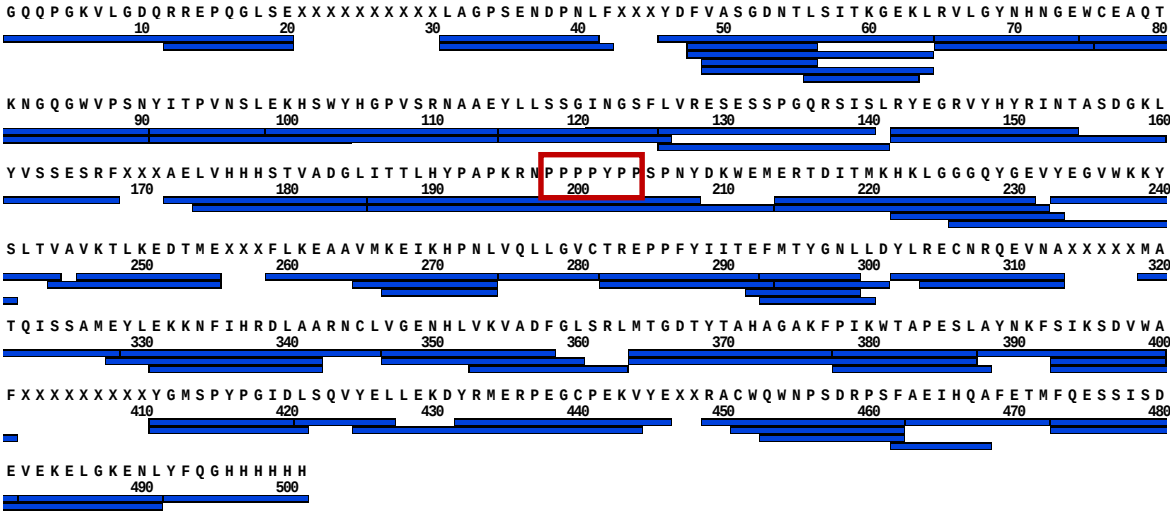

Abl-HAL9-A356N

Figure 19: Amino acid sequences and peptic peptide coverage of all four c-ABL core proteins studied by HX MS. The protein coverage maps were generated using the DynamX software package (Waters Corp.). Amino acids not covered by pepsin digestion are indicated by the letter 'X'. The location of the A356N myristic acid binding pocket mutation as well as the region encompassing the modified HAL9 linker are outlined in red.

Figure 20A

WT A356N

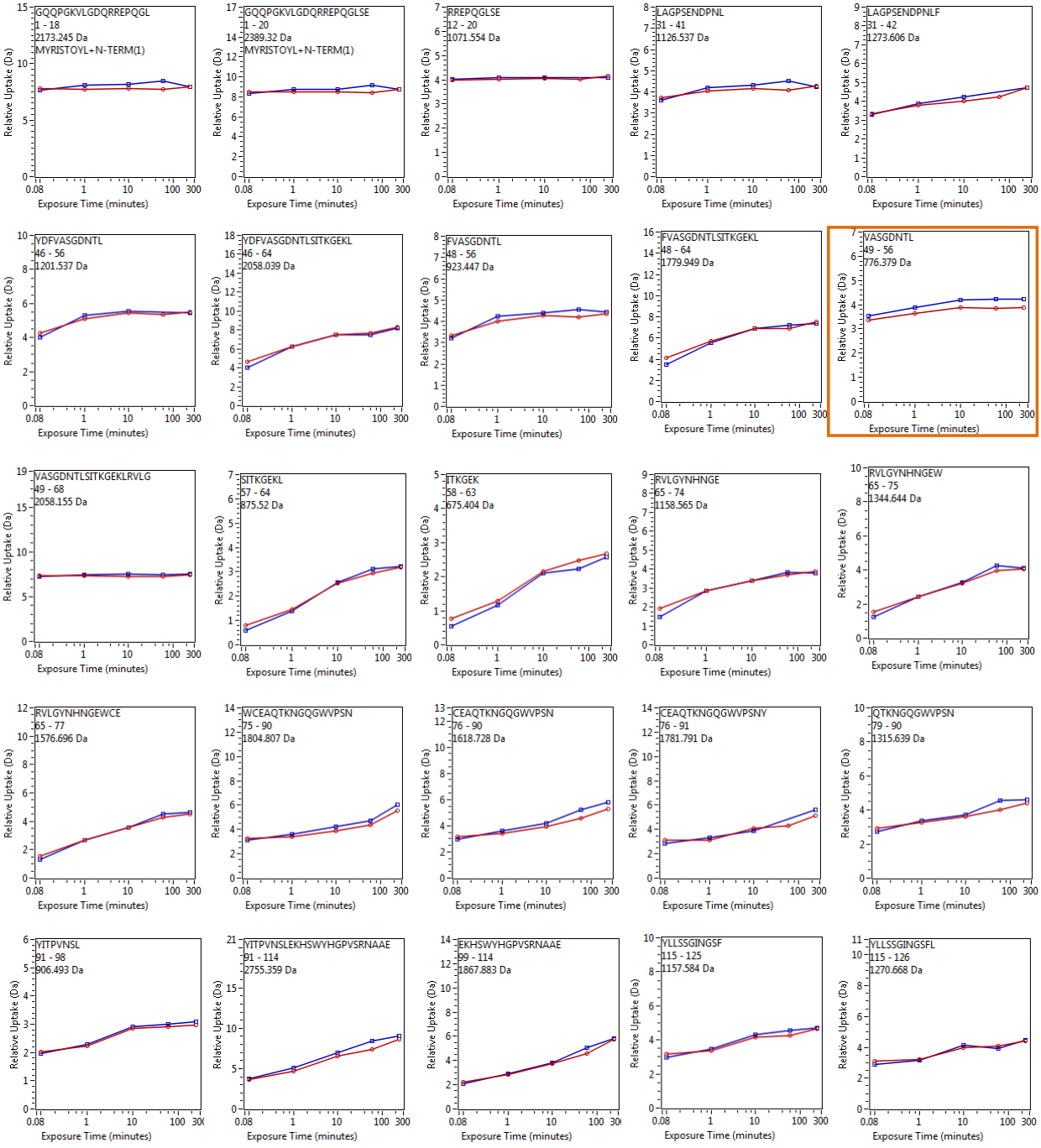

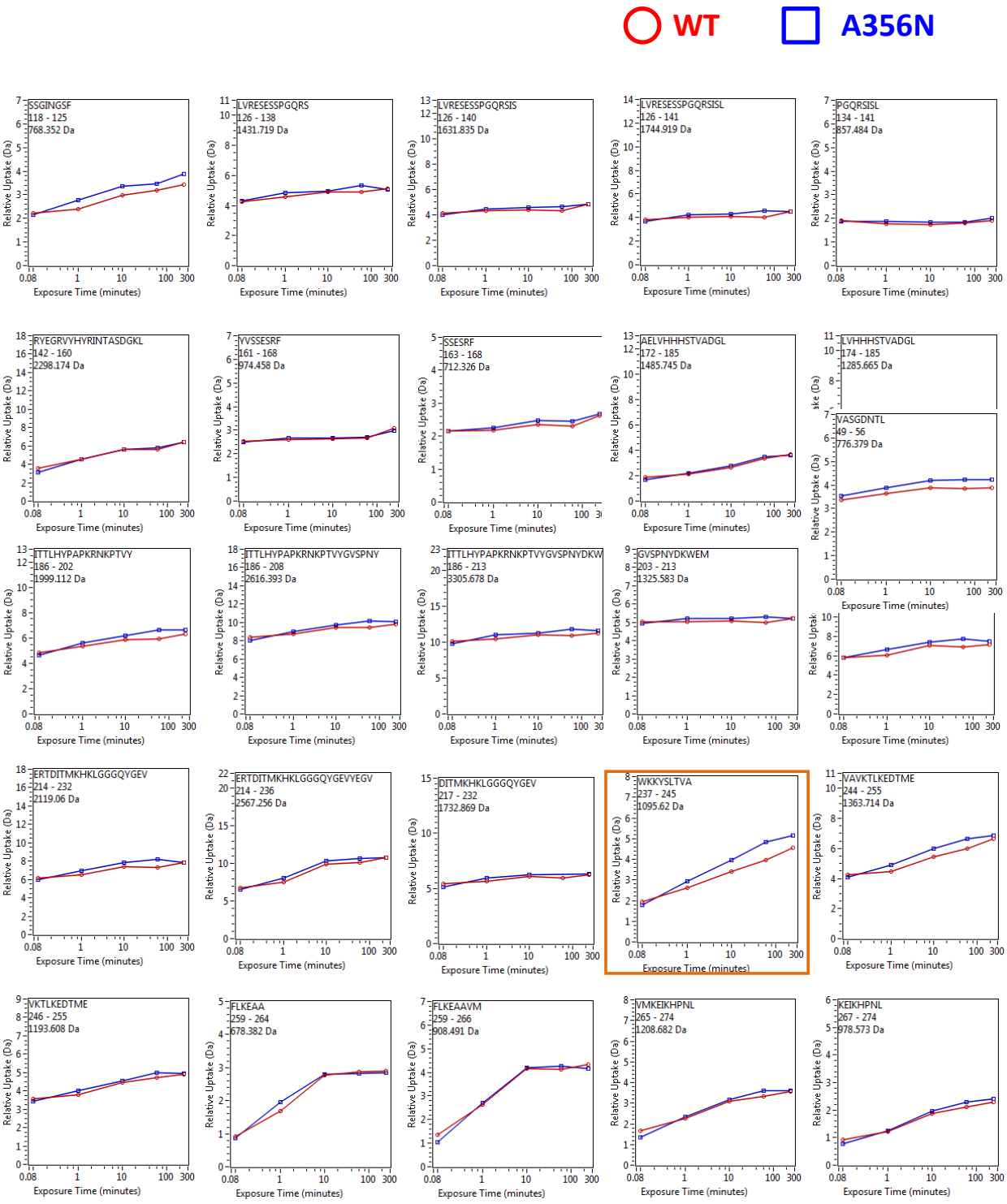
WT
A356N
SSGINGSF
118 - 125
768.352 Da
LVRESESSPGQRS
126 - 138
1431.719 Da
LVRESESSPGQRSIS
126 - 140
1631.835 Da
LVRESESSPGQRSISL
126 - 141
1744.919 Da
PGQRSISL
134 - 141
857.484 Da
RYEGRVYHYRINTASDGKL
142 - 160
2298.174 Da
YVSSESRF
161 - 168
974.458 Da
SSESRF
163 - 168
712.326 Da
AELVHHHSTVADGL
172 - 185
1485.745 Da
LVHHHSTVADGL
174 - 185
1285.665 Da
VASGDNTL
49 - 56
776.379 Da
ITTLHYPAPKRNKPTVY
186 - 202
1999.112 Da
ITTLHYPAPKRNKPTVYGVSPNY
186 - 208
2616.393 Da
ITTLHYPAPKRNKPTVYGVSPNYDKW
186 - 213
3305.678 Da
GVSPNYDKWEM
203 - 213
1325.583 Da
ERTDITMKHKLGGGQYGEV
214 - 232
2119.06 Da
ERTDITMKHKLGGGQYGEVYEGV
214 - 236
2567.256 Da
DITMKHKLGGGQYGEV
217 - 232
1732.869 Da
WKKYSLTVA
237 - 245
1095.62 Da
VAVKTLKEDTME
244 - 255
1363.714 Da
VKTLKEDTME
246 - 255
1193.608 Da
FLKEAA
259 - 264
678.382 Da
FLKEAAVM
259 - 266
908.491 Da
VMKEIKHPNL
265 - 274
1208.682 Da
KEIKHPNL
267 - 274
978.573 Da
Relative Uptake (Da)
Exposure Time (minutes)

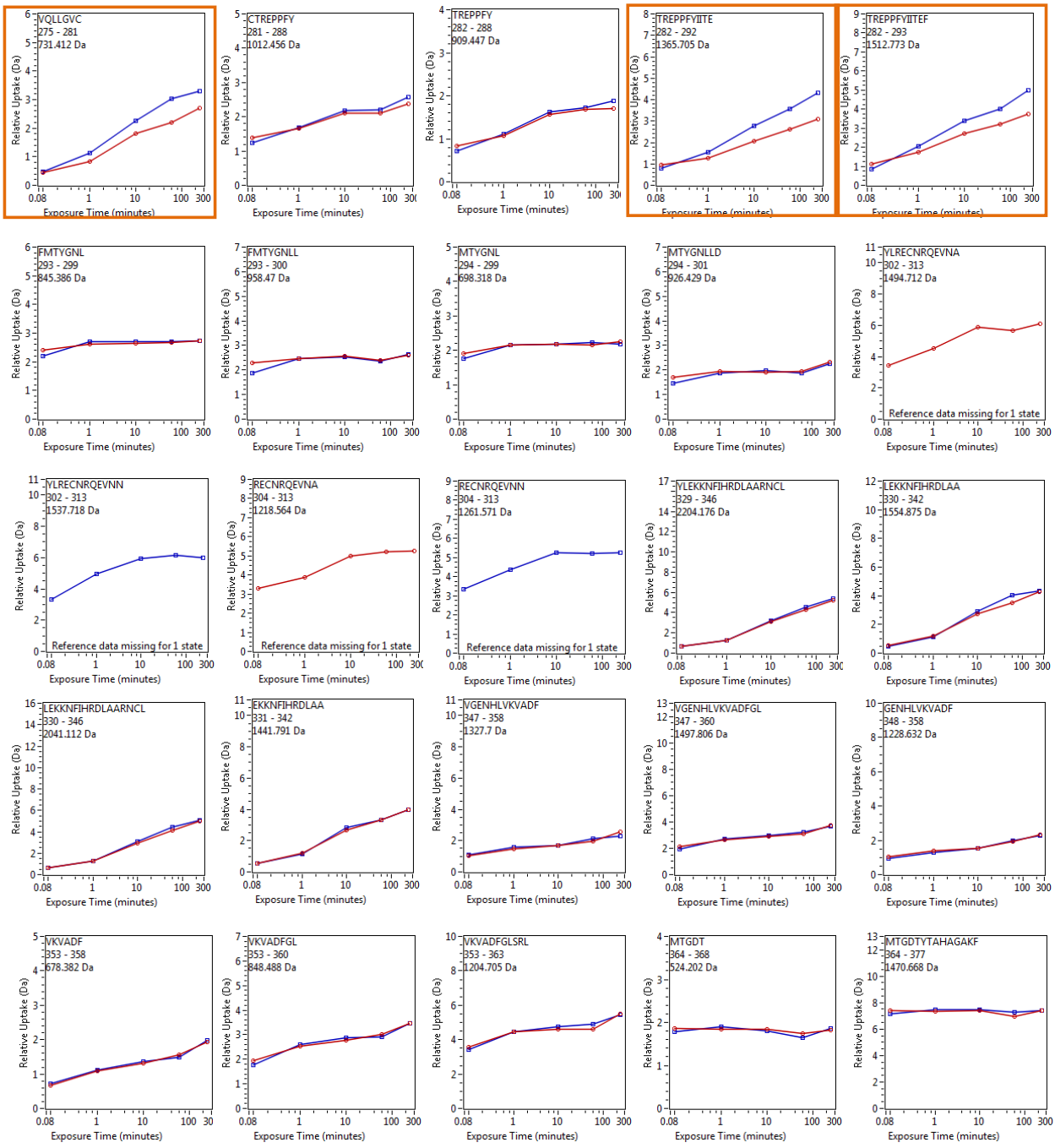
WT
A356N
VQLLGVC
275 - 281
731.412 Da
CTREPPFY
281 - 288
1012.456 Da
TREPPFY
282 - 288
909.447 Da
TREPPFYIITE
282 - 292
1365.705 Da
TREPPFYIITEF
282 - 293
1512.773 Da
FMTYGNL
293 - 299
845.386 Da
FMTYGNLL
293 - 300
958.47 Da
MTYGNL
294 - 299
698.318 Da
MTYGNLLD
294 - 301
926.429 Da
YLRECNRQEVNA
302 - 313
1494.712 Da
Reference data missing for 1 state
YLRECNRQEVNN
302 - 313
1537.718 Da
RECNRQEVNA
304 - 313
1218.564 Da
RECNRQEVNN
304 - 313
1261.571 Da
YLEKKNFIHRDLAARNCL
329 - 346
2204.176 Da
LEKKNFIHRDLAA
330 - 342
1554.875 Da
LEKKNFIHRDLAARNCL
330 - 346
2041.112 Da
EKKNFIHRDLAA
331 - 342
1441.791 Da
VGENHLVKVADF
347 - 358
1327.7 Da
VGENHLVKVADFGL
347 - 360
1497.806 Da
GENHLVKVADF
348 - 358
1228.632 Da
VKVADF
353 - 358
678.382 Da
VKVADFGL
353 - 360
848.488 Da
VKVADFGLSRL
353 - 363
1204.705 Da
MTGDT
364 - 368
524.202 Da
MTGDTYTAHAGAKF
364 - 377
1470.668 Da
Relative Uptake (Da)
Exposure Time (minutes)

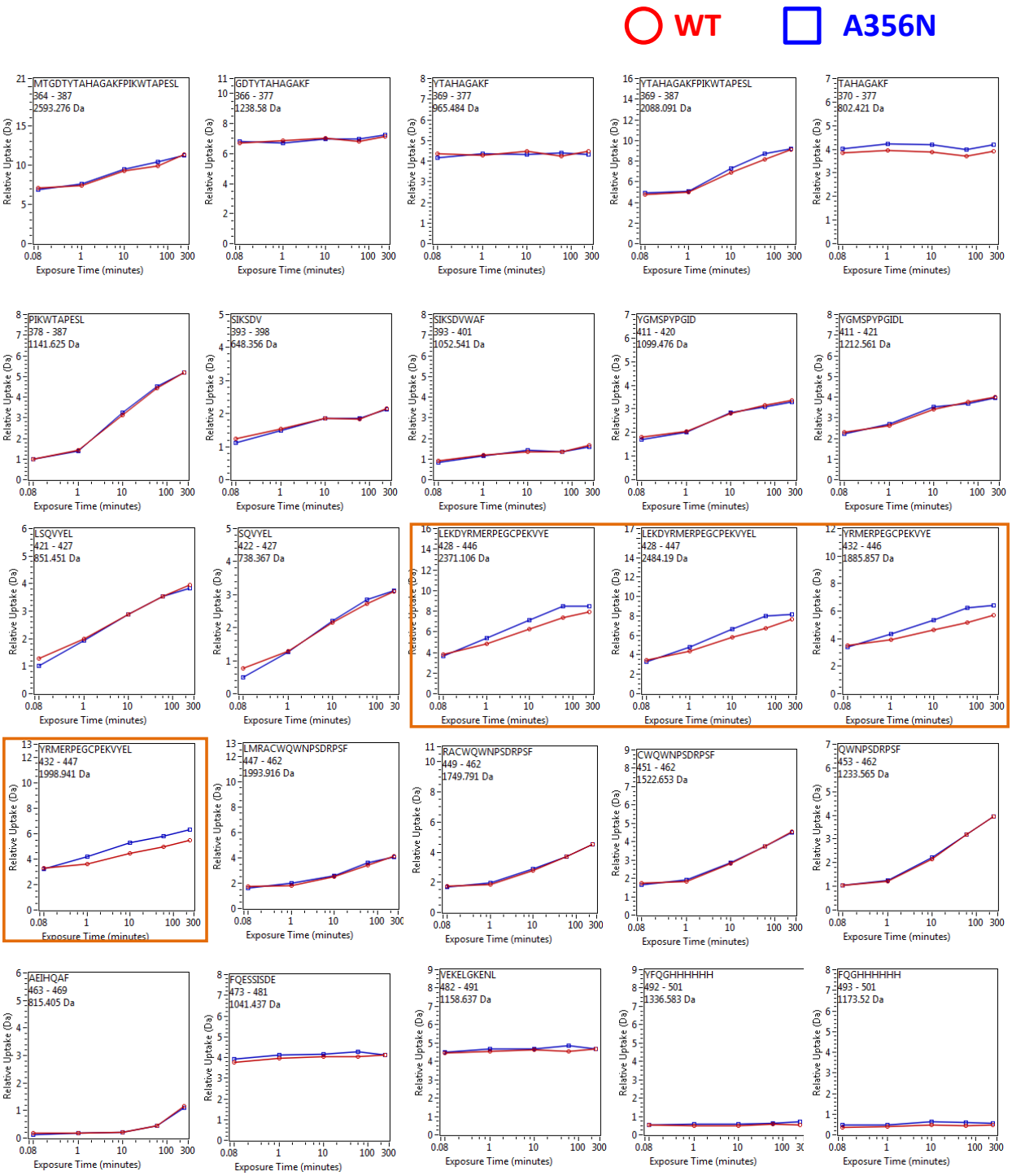
WT
A356N
MTGDTYTAHAGAKFPIKWTAPESL
364 - 387
2593.276 Da
GDTYTAHAGAKF
366 - 377
1238.58 Da
YTAHAGAKF
369 - 377
965.484 Da
YTAHAGAKFPIKWTAPESL
369 - 387
2088.091 Da
TAHAGAKF
370 - 377
802.421 Da
PIKWTAPESL
378 - 387
1141.625 Da
SIKSDV
393 - 398
648.356 Da
SIKSDVWAF
393 - 401
1052.541 Da
YGMSPYPGID
411 - 420
1099.476 Da
YGMSPYPGIDL
411 - 421
1212.561 Da
LSQVYEL
421 - 427
851.451 Da
SQVYEL
422 - 427
738.367 Da
LEKDYRMERPEGCPEKVYE
428 - 446
2371.106 Da
LEKDYRMERPEGCPEKVYEL
428 - 447
2484.19 Da
YRMERPEGCPEKVYE
432 - 446
1885.857 Da
YRMERPEGCPEKVYEL
432 - 447
1998.941 Da
LMRACWQWNPSDRPSF
447 - 462
1993.916 Da
RACWQWNPSDRPSF
449 - 462
1749.791 Da
CWQWNPSDRPSF
451 - 462
1522.653 Da
QWNPSDRPSF
453 - 462
1233.565 Da
AEIHQAF
463 - 469
815.405 Da
FQESSISDE
473 - 481
1041.437 Da
VEKELGKENL
482 - 491
1158.637 Da
YFQGHHHHHH
492 - 501
1336.583 Da
FQGHHHHHH
493 - 501
1173.52 Da
Relative Uptake (Da)
Exposure Time (minutes)

Figure 20B

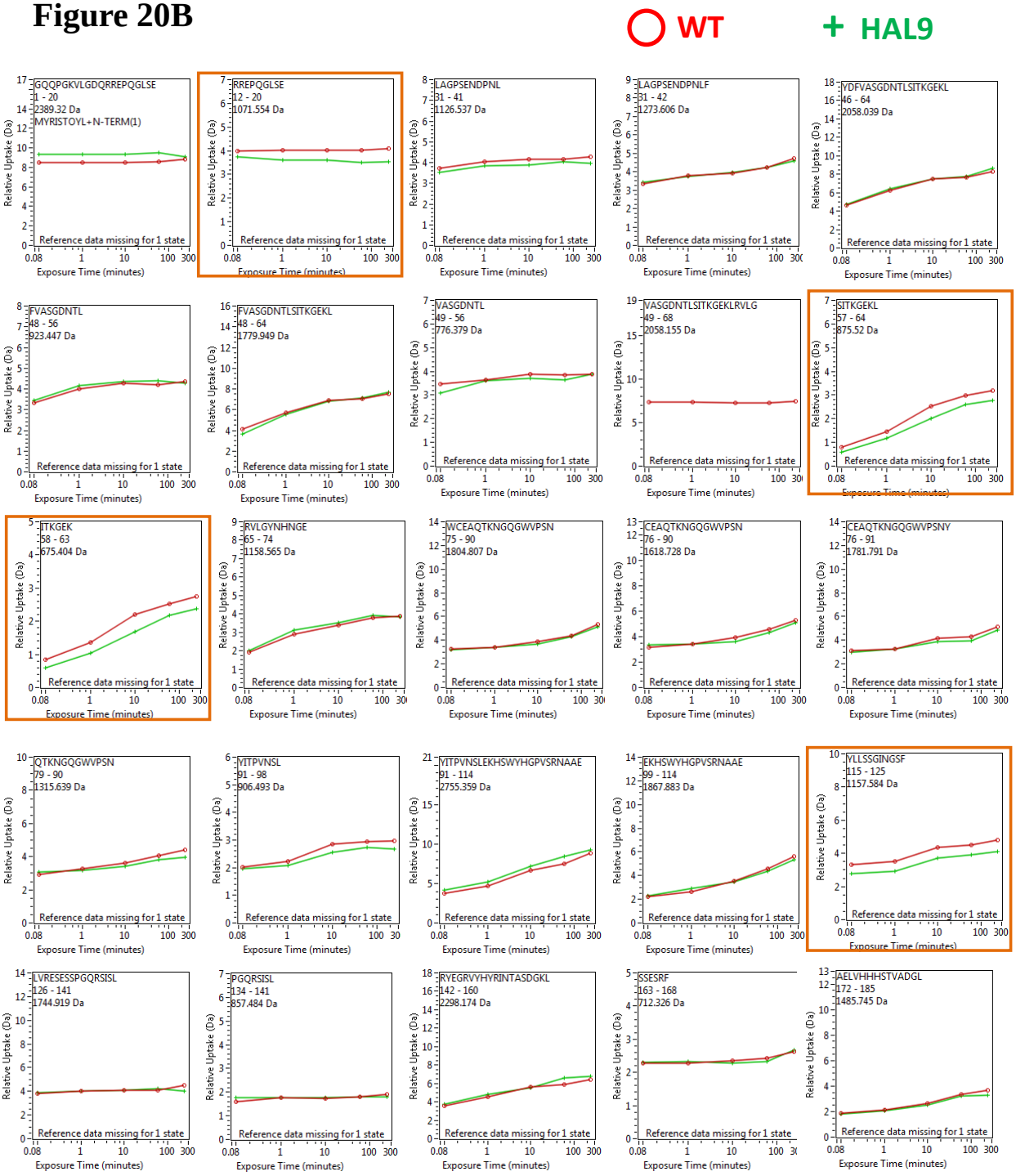
WT
HAL9
GQQPGKVLGDQRREPQGLSE
1 - 20
2389.32 Da
MYRISTOYL+N-TERM(1)
RREPQGLSE
12 - 20
1071.554 Da
LAGPSENDPNL
31 - 41
1126.537 Da
LAGPSENDPNLF
31 - 42
1273.606 Da
YDFVASGDNTLSITKGEKL
46 - 64
2058.039 Da
FVASGDNTL
48 - 56
923.447 Da
FVASGDNTLSITKGEKL
48 - 64
1779.949 Da
VASGDNTL
49 - 56
776.379 Da
VASGDNTLSITKGEKLRVLG
49 - 68
2058.155 Da
SITKGEKL
57 - 64
875.52 Da
ITKGEK
58 - 63
675.404 Da
RVLGYNHNGE
65 - 74
1158.565 Da
WCEAQTKNGQGWVPSN
75 - 90
1804.807 Da
CEAQTKNGQGWVPSN
76 - 90
1618.728 Da
CEAQTKNGQGWVPSNY
76 - 91
1781.791 Da
QTKNGQGWVPSN
79 - 90
1315.639 Da
YITPVNSL
91 - 98
906.493 Da
YITPVNSLEKHSWYHGPVSRNAAE
91 - 114
2755.359 Da
EKHSWYHGPVSRNAAE
99 - 114
1867.883 Da
YLLSSGINGSF
115 - 125
1157.584 Da
LVRESESSPGQRSISL
126 - 141
1744.919 Da
PGQRSISL
134 - 141
857.484 Da
RYEGRVYHYRINTASDGKL
142 - 160
2298.174 Da
SSESRF
163 - 168
712.326 Da
AELVHHHSTVADGL
172 - 185
1485.745 Da
Relative Uptake (Da)
Exposure Time (minutes)
Reference data missing for 1 state

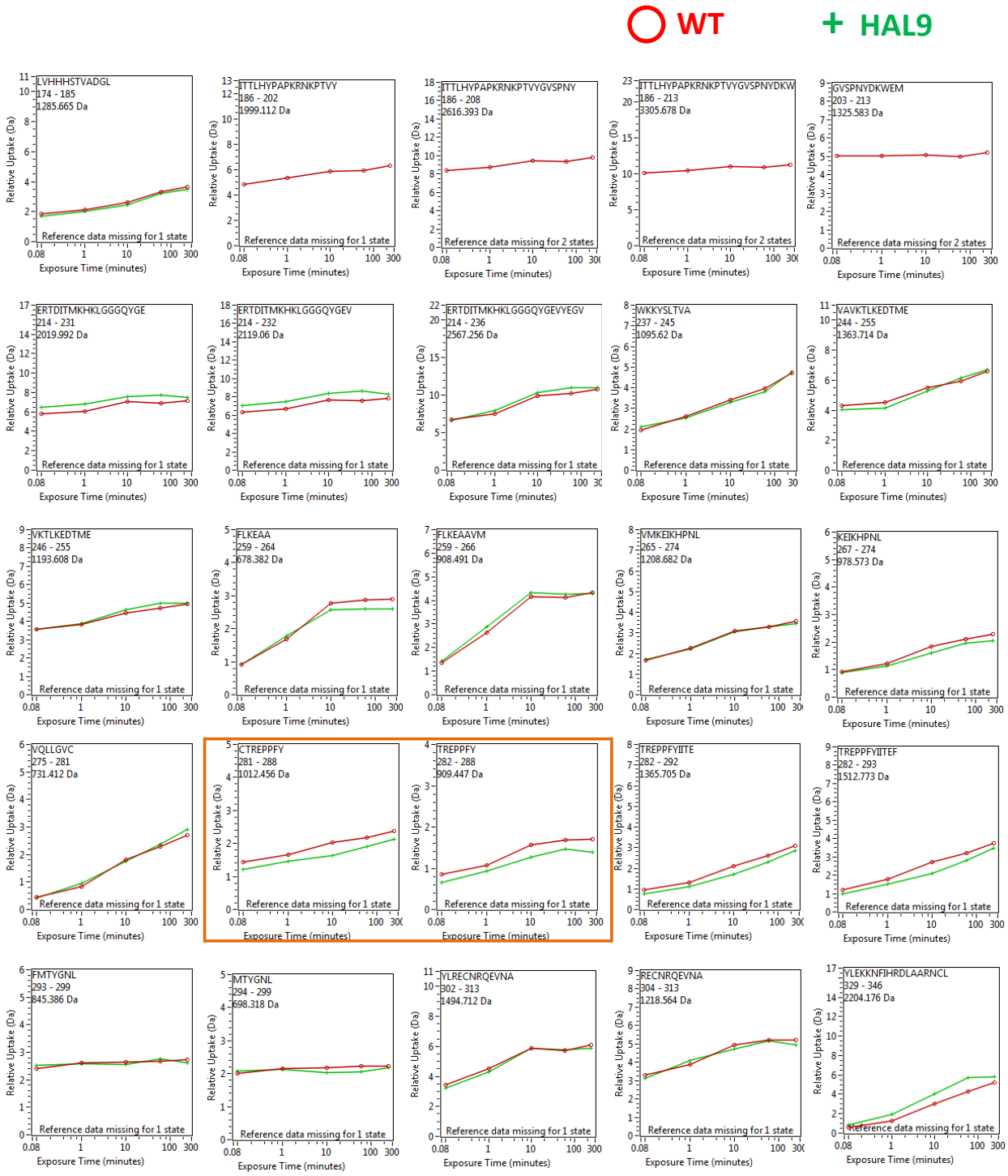
WT
HAL9
LVHHHSTVADGL
174 - 185
1285.665 Da
ITTLHYPAPKRNKPTVY
186 - 202
1999.112 Da
ITTLHYPAPKRNKPTVYGVSPNY
186 - 208
2616.393 Da
ITTLHYPAPKRNKPTVYGVSPNYDKW
186 - 213
3305.678 Da
GVSPNYDKWEM
203 - 213
1325.583 Da
ERTDITMKHKLGGGQYGE
214 - 231
2019.992 Da
ERTDITMKHKLGGGQYGEV
214 - 232
2119.06 Da
ERTDITMKHKLGGGQYGEVYEGV
214 - 236
2567.256 Da
WKKYSLTVA
237 - 245
1095.62 Da
VAVKTLKEDTME
244 - 255
1363.714 Da
VKTLKEDTME
246 - 255
1193.608 Da
FLKEAA
259 - 264
678.382 Da
FLKEAAVM
259 - 266
908.491 Da
VMKEIKHPNL
265 - 274
1208.682 Da
KEIKHPNL
267 - 274
978.573 Da
VQLLGVC
275 - 281
731.412 Da
CTREPPFY
281 - 288
1012.456 Da
TREPPFY
282 - 288
909.447 Da
TREPPFYIITE
282 - 292
1365.705 Da
TREPPFYIITEF
282 - 293
1512.773 Da
FMTYGNL
293 - 299
845.386 Da
MTYGNL
294 - 299
698.318 Da
YLRECNRQEVNA
302 - 313
1494.712 Da
RECNRQEVNA
304 - 313
1218.564 Da
YLEKKNFIHRDLAARNCL
329 - 346
2204.176 Da
Reference data missing for 1 state
Reference data missing for 2 states
Relative Uptake (Da)
Exposure Time (minutes)

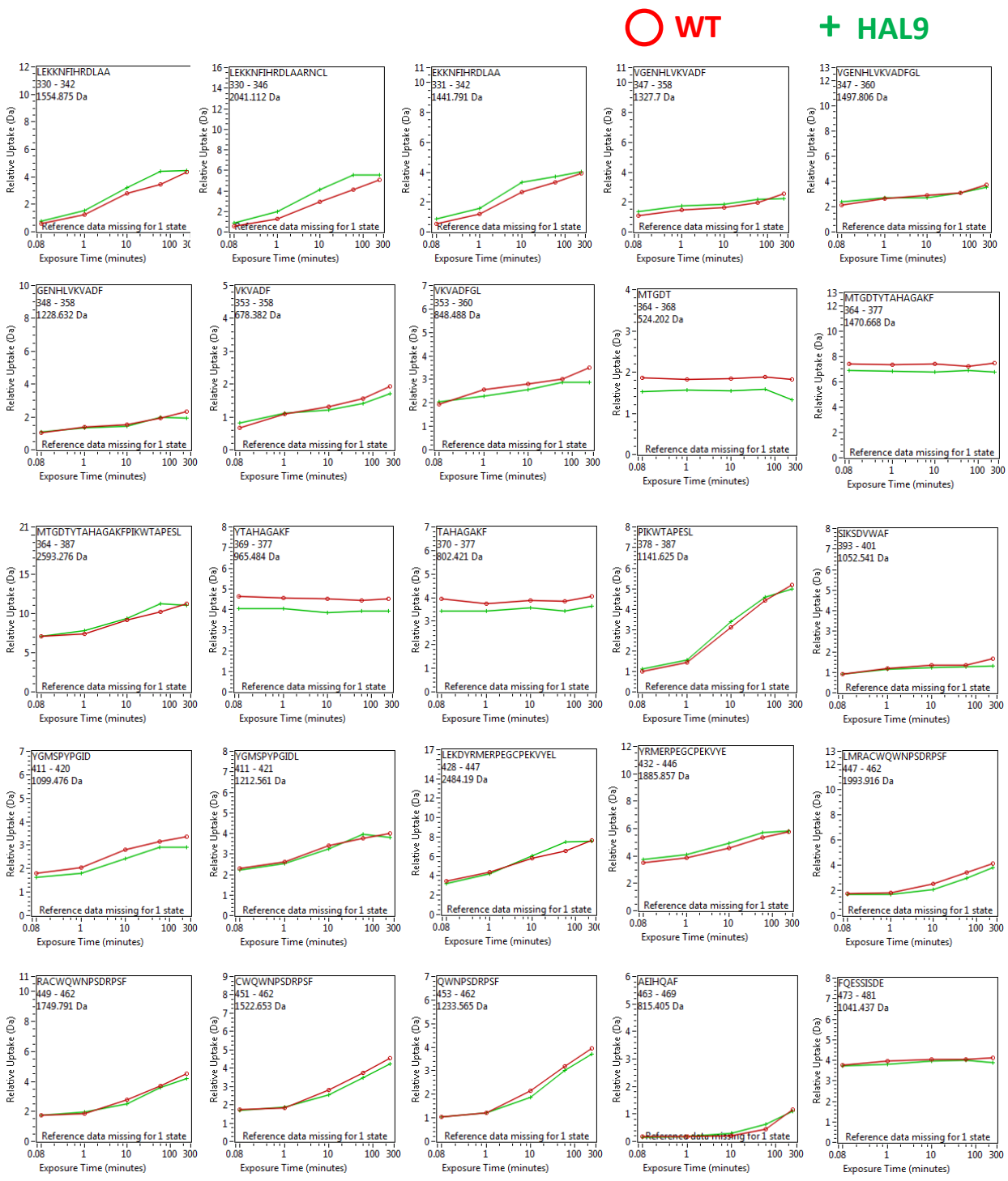
WT
HAL9
LEKKNFIHRDLAA
330 - 342
1554.875 Da
LEKKNFIHRDLAARNCL
330 - 346
2041.112 Da
EKKNFIHRDLAA
331 - 342
1441.791 Da
VGENHLVKVADF
347 - 358
1327.7 Da
VGENHLVKVADFGL
347 - 360
1497.806 Da
GENHLVKVADF
348 - 358
1228.632 Da
VKVADF
353 - 358
678.382 Da
VKVADFGL
353 - 360
848.488 Da
MTGDT
364 - 368
524.202 Da
MTGDTYTAHAGAKF
364 - 377
1470.668 Da
MTGDTYTAHAGAKFPIKWTAPESL
364 - 387
2593.276 Da
YTAHAGAKF
369 - 377
965.484 Da
TAHAGAKF
370 - 377
802.421 Da
PIKWTAPESL
378 - 387
1141.625 Da
SIKSDVWAF
393 - 401
1052.541 Da
VGMSPYPGID
411 - 420
1099.476 Da
VGMSPYPGIDL
411 - 421
1212.561 Da
LEKDYRMERPEGCPEKVYEL
428 - 447
2484.19 Da
YRMERPEGCPEKVYE
432 - 446
1885.857 Da
LMRACWQWNPSDRPSF
447 - 462
1993.916 Da
RACWQWNPSDRPSF
449 - 462
1749.791 Da
CWQWNPSDRPSF
451 - 462
1522.653 Da
QWNPSDRPSF
453 - 462
1233.565 Da
AEIHQAF
463 - 469
815.405 Da
FQESSISDE
473 - 481
1041.437 Da
Relative Uptake (Da)
Exposure Time (minutes)
Reference data missing for 1 state

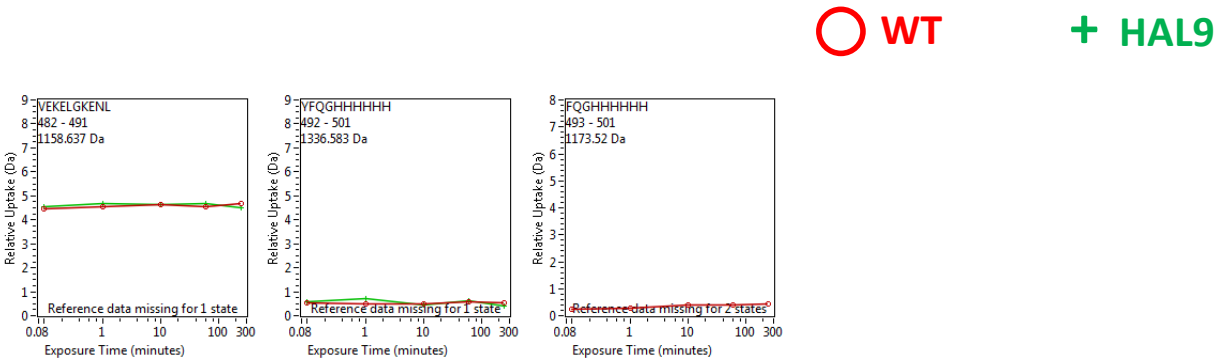
WT
HAL9
VEKELGKENL
482 - 491
1158.637 Da
YFQGHHHHHH
492 - 501
1336.583 Da
FQGHHHHHH
493 - 501
1173.52 Da
Relative Uptake (Da)
Reference data missing for 1 state
Reference data missing for 2 states
Exposure Time (minutes)
0.08
1
10
100
300

Figure 20C

X A356N HAL9-A356N

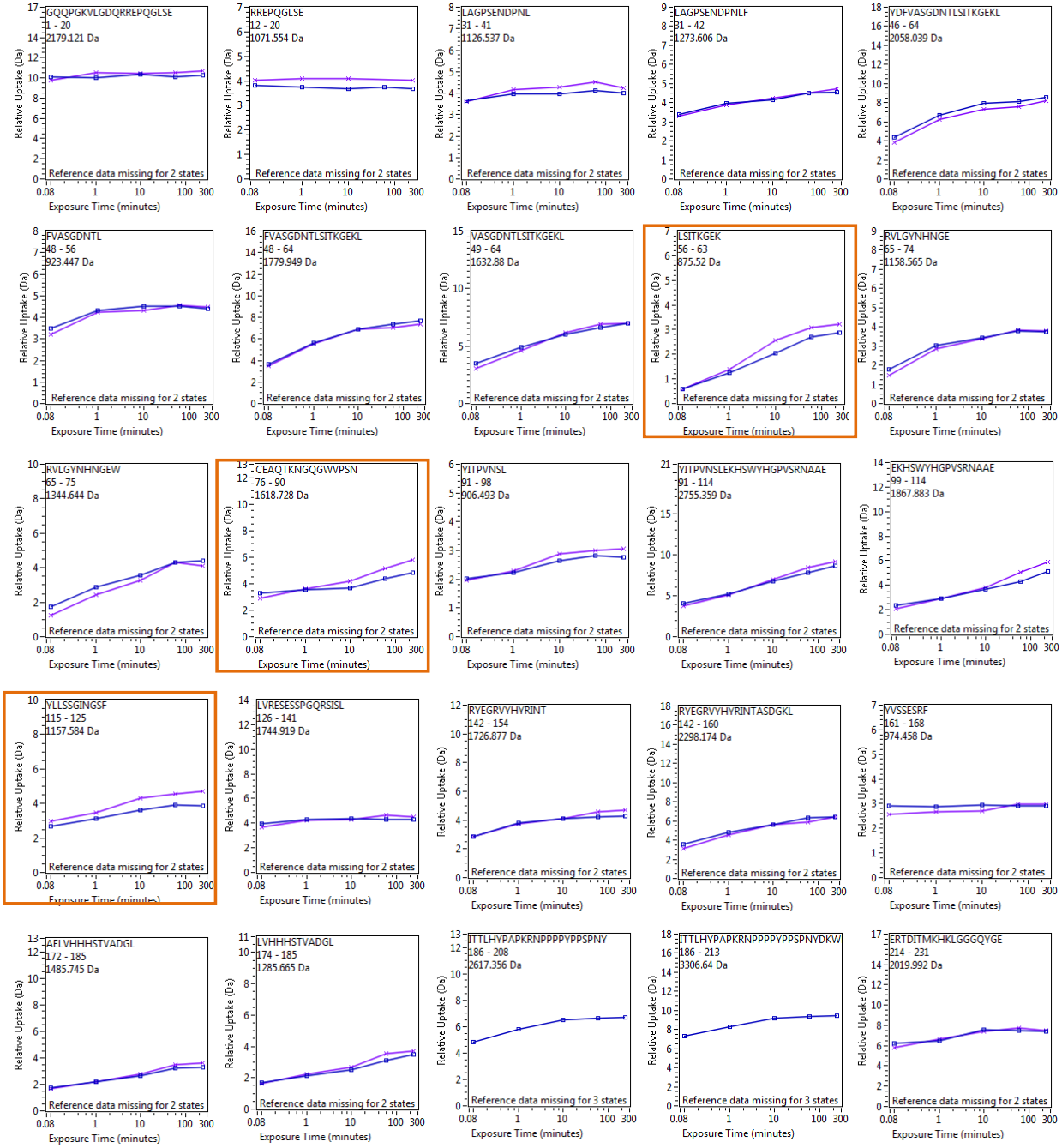

X A356N HAL9-A356N

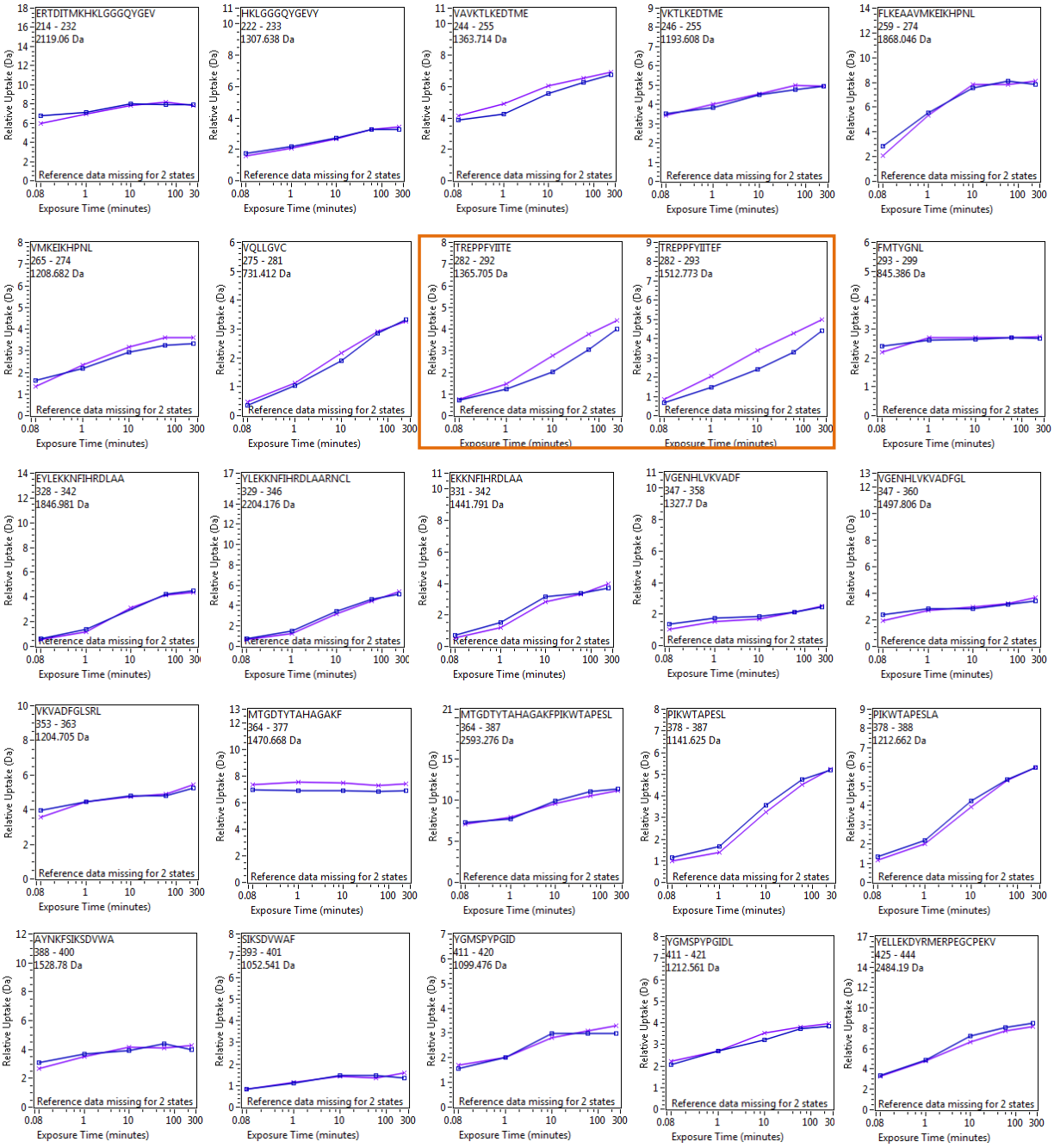

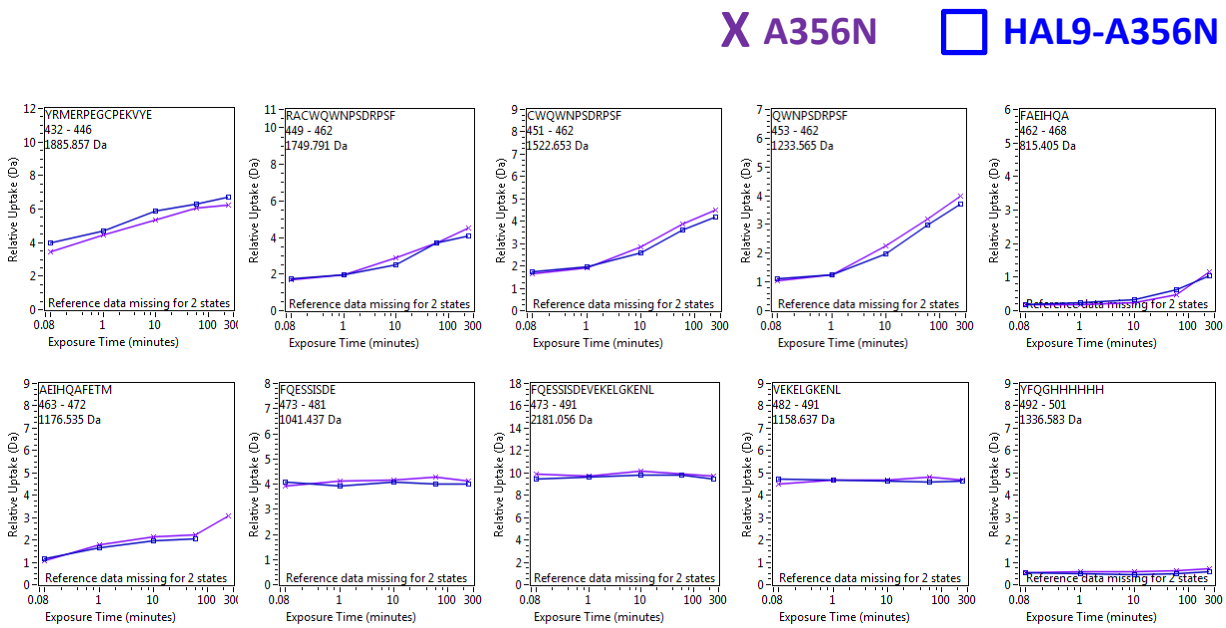

Figure 20: Comparative deuterium uptake curves for peptic peptides derived from c-ABL core proteins. Deuterium uptake graphs were generated using the DynamX software package (Waters Corp.). The cumulative error of measuring deuterium uptake in these assays is approximately ± 0.20 Da. Peptides displaying significant differences in deuterium uptake are outlined in orange. A, ABL-WT vs. A356N; B, WT vs. HAL9; C, A356N vs. HAL9-A356N. The sequence, numbering (ABL-1b) and mass of each peptide are shown.

Comparison of exchange in peptic peptides derived from WT ABL versus the active A356N mutant identified revealed nine peptides with more rapid deuterium uptake in the mutant, supporting the idea that disruption of the myristate binding pocket results in a more open, mobile structure. Most of the increases in deuterium incorporation observed in the A356N mutant localize to the N-lobe of the kinase domain (mapped to the structure of downregulated ABL in Figure 21). The peptide corresponding to ABL residues 282-293 (301-312 in ABL 1a numbering) not only showed more deuterium uptake in the A356N mutant, but the spectra indicate the presence of two populations of peptides, one of which is labeled more rapidly than the other (Figure 22). The half-life of conversion between the two populations in the mutant was around 10 minutes, whereas the conversion took much longer for the WT protein. These results indicate that the mutant was much more dynamic in this region and underwent partial unfolding of the EX1 type (Weis et al., 2006). Analysis of exchange into four overlapping peptides in this region shows that just four amino acids (sequence Ile-Ile-Thr-Glu) are responsible for the altered dynamics of the A356N mutant. These residues are located in the tip of the two-strand β-hairpin pointing into the ATP-binding site, and include the gatekeeper threonine (Thr315; ABL-1a numbering). Because this region is located at a great distance from the site of the activating mutation, these results support an allosteric connection between the myristic acid binding site in the C-lobe and part of the active site derived from the N-lobe. These observations are consistent with previous HX MS studies in which GNF-2 binding to the myristic acid binding pocket in the C-lobe decreased deuterium uptake in the ATP binding site (Zhang et al., 2010; Iacob et al., 2011). In addition to peptides derived from the N-lobe, peptide 432-446 (451-465 in ABL-1a) also displayed more deuterium uptake in A356N compared to WT. This peptide is located in the

α-helix adjacent to the site of the mutation in the kinase domain C-lobe, indicating that the A356N mutation also causes a local increase in solvent accessibility.

Comparison of exchange between the WT and HAL9 forms of the c-ABL core revealed several regions with less deuterium uptake in HAL9, strengthening the idea that enhanced SH3 interaction with the linker stabilizes the downregulated conformation of the kinase domain (Figures 20 and 21). The regions that showed reduced deuterium uptake in HAL9 included peptide 57-64 (76-83 in ABL-1a), which includes the N-terminal portion of the RT loop of the SH3 domain, SH2 domain peptide 115-125 (134-144 in ABL-1a), which is part of the α-helix that contacts the kinase domain C-lobe, and peptide 282-293 (ABL-1a 301-312) from the N-lobe of the kinase domain. The latter peptide overlaps with the same one that is more mobile in the A356N mutant as described above. Reduction of deuterium incorporation in these HAL9 regions supports the hypothesis that increasing SH3:linker interaction results in global stabilization of the inactive ABL core conformation.

A final comparison of HX MS data from the active A356N mutant with A356N-HAL9 showed that HAL9 substitution completely reverses the activating effects of A356N (Figures 21 and 22). Overall, the A356N-HAL9 protein had a very similar HX MS profile to that of HAL9 alone, with reduced deuterium uptake in SH3 domain peptides 56-63 and 76-90 (ABL-1a 75-82 and 95-109), and in the SH2 domain peptide 115-125 (ABL-1a 134-144) which contacts the kinase domain C-lobe. This peptide contains Tyr115 (ABL-1a Tyr158) which when mutated to aspartate increases ABL kinase activity (Figure 12). As discussed above, HAL9 substitution completely reversed kinase activation resulting from this SH2 domain mutation, consistent with global control of ABL kinase core conformation by SH3 interaction with the linker.

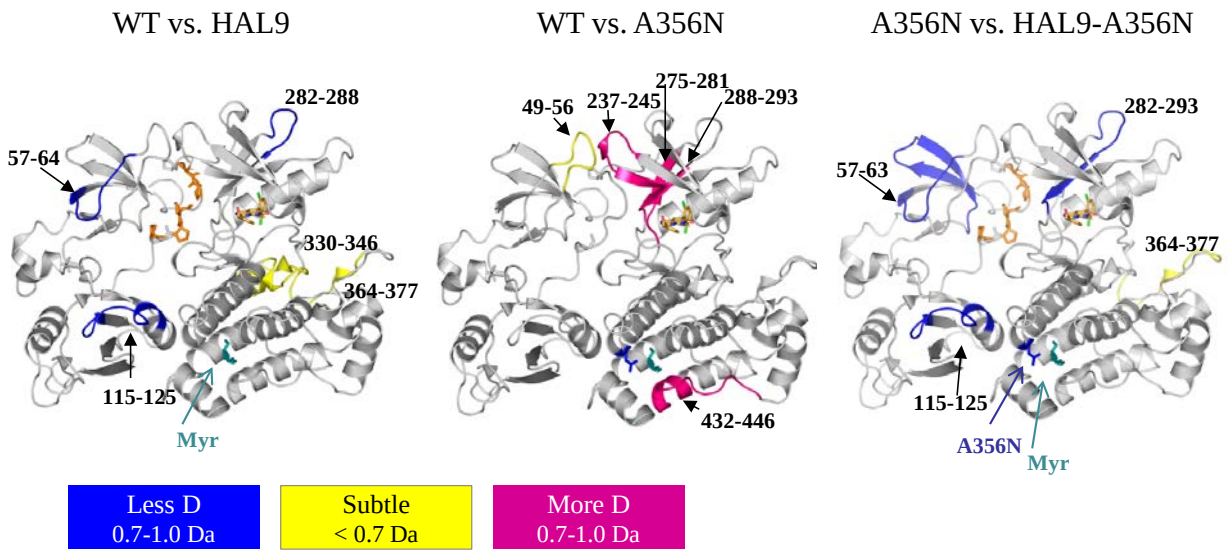

Figure 21: High-affinity linkers reduce hydrogen exchange in the c-ABL myristic acid binding pocket, the SH3 domain, and the kinase domain N-lobe. Regions of altered hydrogen exchange are indicated for the WT c-ABL core vs. HAL9 (left), WT vs. the A356N myristic acid binding pocket mutant (middle) and HAL9 vs. HAL9-A356N (right). Differences in deuterium uptake are color-coded, with blue indicating peptides with a significant reduction in uptake between 0.7-1.0 Da and yellow indicating peptides that displayed subtle changes (less than 0.7 Da difference between curves) in HAL9 vs. WT and in HAL9-A356N vs. A356N. Magenta indicates peptides with more deuterium uptake (0.7-1.0 Da) in the A356N sample when compared with WT. The cumulative error of measuring deuterium uptake in these assays is ± 0.20 Da. Proline residues that were introduced in HAL9 and HAL9-A356N are colored orange and rendered as sticks. The A356N mutation is represented in blue sticks. The locations of the peptides are modeled on the structure of the myristoylated, downregulated c-ABL core (PDB entry 2F0O).

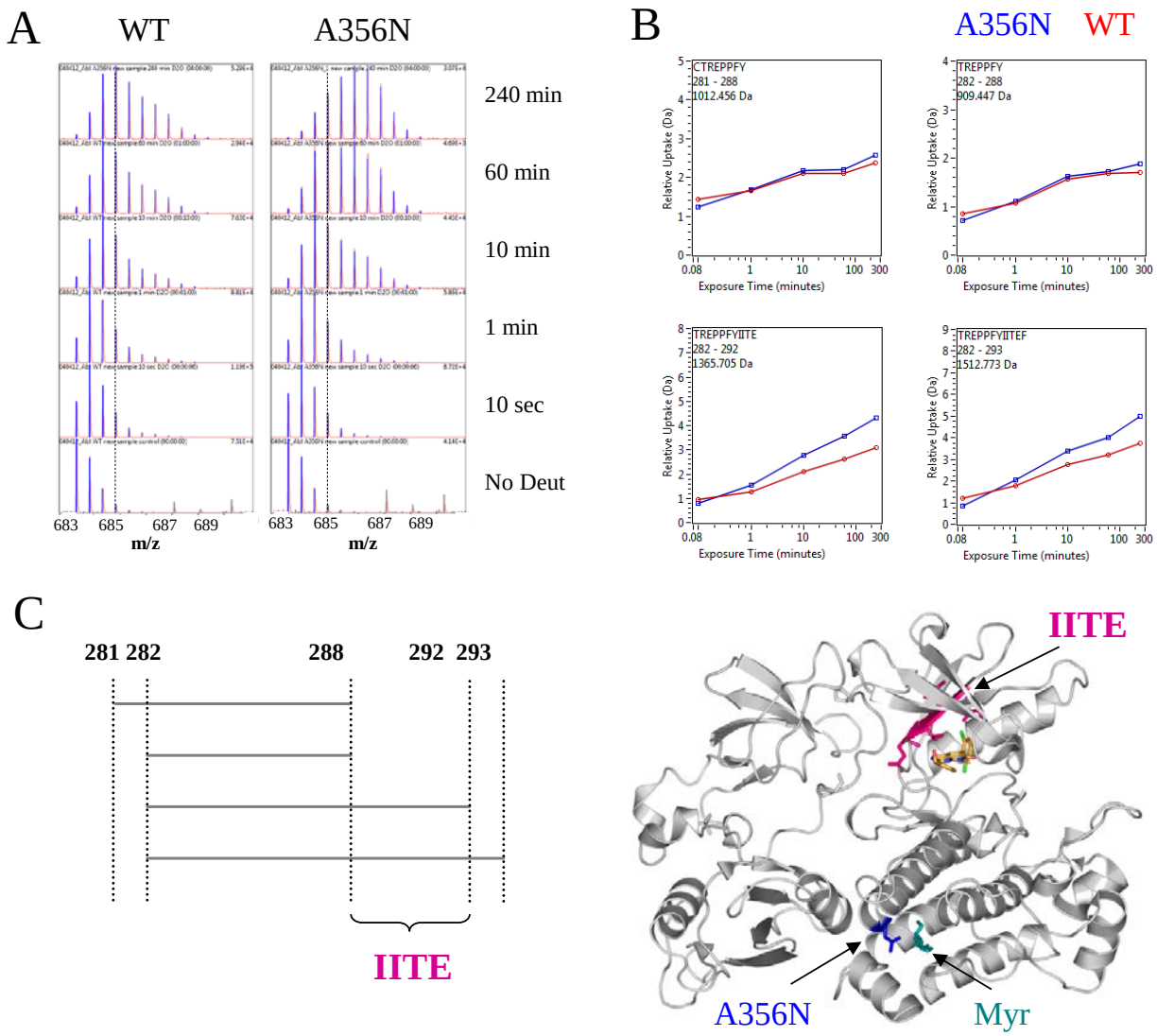

Figure 22: A kinase domain N-lobe peptide encompassing the gatekeeper residue is sensitive to A356N mutation in the myristate binding pocket. **(A)** Mass spectra of deuterium incorporation into the ABL N-lobe peptide 282-293 were recorded over the time intervals shown. The start of the unfolding in this peptide from the A356N mutant is readily observed after 10 min. **(B,C)** Comparison of the deuterium uptake curves corresponding to four overlapping peptides across the 282-293 region identify a four amino acids peptide flanking the gatekeeper position (IITE) as responsible for the dynamic and conformational changes in A356N mutant. The position of this peptide in the crystal structure of the c-ABL core (PDB: 2FO0) is shown at the lower right.

2.4 DISCUSSION

The discovery that the tyrosine kinase activity of BCR-ABL is the driving force behind CML led to the development of imatinib, a Type II ATP-competitive inhibitor of ABL as the first-line treatment for this rare form of leukemia (Druker, 2004). Imatinib revolutionized CML therapy and laid the foundation for targeting kinase activity as a therapeutic approach to other forms of cancer. However, despite the clinical success of imatinib, long term therapy often leads to the emergence of drug resistance and disease relapse (Nardi et al., 2004). Imatinib resistance results from kinase domain mutations that impact drug binding [e.g., gatekeeper T315I; (Gorre et al., 2001)] or from mutations outside of kinase domain which induce an active site conformation incompatible with drug binding (Azam et al., 2003). The second-generation ATP- competitive ABL inhibitors nilotinib and dasatinib have been approved for therapy of imatinib-resistant CML (Rix et al., 2007). However, these drugs are also associated with resistance and do not overcome the T315I imatinib-resistance mutation.

The need to overcome the gatekeeper mutation and to target ABL kinase activity more specifically led to the discovery of allosteric kinase inhibitors. GNF-2, the prototype of this inhibitor family, targets the myristate binding pocket in the C-lobe to stabilize the inactive conformation of the kinase domain (Iacob et al., 2011; Zhang et al., 2010; Adrian et al., 2006). GNF-2 inhibits some imatinib-resistant forms of BCR-ABL, with T315I as a notable exception. This observation suggests that the T315I mutation uncouples the active site from allosteric control by myristate-binding pocket. However, when combined with nilotinib or dasatinib, GNF-2 and related compounds overcome T315I mutations both in vitro and in vivo (Zhang et al., 2010). Combinations of GNF-2-type allosteric inhibitors and ATP competitive drugs also dramatically decrease the rate of experimental drug resistance, strongly suggesting that other

therapeutic approaches targeting natural mechanisms of kinase regulation may be of value in combating drug resistance. In this study, we focused on the potential of the SH3:linker interaction as an alternative allosteric regulator of kinase activity. Our approach was inspired by mounting evidence that the ABL SH3 and SH2 domains maintain regulatory control over the ABL kinase domain even in the context of the active BCR-ABL kinase. Indeed, imatinib resistance can arise from mutations in these regulatory domains as well as phosphorylation of the SH3 domain by Src-family kinases (Azam et al., 2003; Pene-Dumitrescu and Smithgall, 2010).

Previous HX MS studies have shown that the ABL linker remains bound to the SH3 domain even in the absence of kinase domain, supporting a prominent role for this interaction in ABL kinase regulation (Chen et al., 2008a). Our goal was to enhance SH3 interaction through systematic substitution of linker amino acid residues with proline without disturbing the overall structure of the downregulated c-ABL core. Using HXMS, we first showed enhanced SH3:linker engagement as a function of increased linker proline content in small proteins consisting of the NCap, SH3, SH2 and linker regions. Within the context of the larger ABL core protein, most of the HAL modifications maintained or reduced phosphorylation of key regulatory tyrosines relative to wild-type protein. Among these, the HAL9 protein, with five additional linker prolines, showed the greatest enhancement of SH3:linker interaction without disturbing overall kinase regulation.

The long-range allosteric influence of SH3:linker interaction on ABL kinase regulation became readily apparent when HAL9 was combined with mutations known to activate the c-ABL core. Particularly striking was the observation that HAL9 substitution completely reversed the activating effect of the A356N mutation in the myristic acid binding pocket. In contrast, HAL9 only partially reversed the activity of a non-myristoylated (G2A) ABL core protein,

suggesting that G2A and A356N produce distinct active conformations of the c-ABL core despite their functional relationship. In the case of the non-myristoylated ABL-G2A mutant, small-angle X-ray (Nagar et al., 2006) scattering supports a dramatic reorientation of the SH2 domain onto the N-lobe of the kinase, where it stabilizes an active kinase domain conformation (Filippakopoulos et al., 2008). This active 'top-hat' conformation is also supported by previous HX MS studies of non-myristoylated ABL core proteins (Iacob et al., 2009). On the other hand, HX MS of the ABL-A356N core protein presented here revealed no changes in deuterium incorporation at the SH2:C-lobe interface, the NCap or the SH2-kinase linker, indicating that ABL-A356N does not adopt the top hat conformation. These differences in active conformation help to explain why HAL9 completely reverses the activity of the A356N mutation. In this case, the overall structure of the ABL core is likely to be maintained, with the SH3 domain bound to the linker and the myristoylated NCap bound to its C-lobe binding pocket. Enhanced SH3:linker interaction via HAL9 substitution may compensate for allosteric uncoupling resulting from the A356N mutation. Indeed, HX MS studies showed that introduction of HAL9 decreased deuterium incorporation in the C-lobe at the site of the A356N mutation, the N-lobe adjacent to the active site as well as the SH3 and SH2 domains. These HX MS data also support an allosteric connection between the SH3 domain, the myristic acid binding pocket, and the active site.

The allosteric impact of HAL9 was observed not only with the ABL kinase core protein but also within the context of full-length BCR-ABL. Using human TF-1 myeloid cells transformed with BCR-ABL as a model system, we found that HAL9 substitution enhanced sensitivity to imatinib both in terms of BCR-ABL kinase activity and apoptosis. These data provide direct evidence that SH3:linker interaction maintains control over BCR-ABL kinase activity. The enhancement in the apparent potency of imatinib against the HAL9 form of BCR-

ABL most likely results from restructuring of the kinase domain in the downregulated conformation required for drug binding.

In addition to imatinib, enhanced SH3:linker interaction dramatically sensitized BCR-ABL-transformed TF-1 cells to the allosteric inhibitors GNF-2 and GNF-5, both in terms of kinase inhibition and the apoptotic response. These results support a three-way allosteric connection between the SH3 domain, the myristic acid binding pocket, and the active site. This point is underscored by the observation that HAL9 substitution also sensitized the T315I mutant of BCR-ABL to GNF-2.

In summary, our data show that the SH3:linker interface is a key node controlling the overall dynamics and regulation of the c-ABL kinase core, and that this regulatory influence is retained in the context of the BCR-ABL oncoprotein. Furthermore, the combination of HX MS, biochemical and biological studies strongly support allosteric interplay between the SH3:linker interface, the myristic acid binding pocket in the C-lobe, and the active site. Enhanced SH3:linker interaction sensitizes BCR-ABL to both Type II ATP competitive inhibitors such as imatinib as well as allosteric inhibitors targeting the C-lobe hydrophobic pocket. Our work strongly supports future drug discovery campaigns to identify small molecules that stabilize SH3:linker interaction as allosteric inhibitors of both wild-type and drug resistant forms of BCR-ABL.

2.5 MATERIALS AND METHODS

2.5.1 Cell culture

The human GM-CSF-dependent myeloid leukemia cell line TF-1 was obtained from the American Type Culture Collection (ATCC) and maintained in RPMI 1640 supplemented with 10% fetal bovine serum (FBS), 100 U/ml penicillin G, 100 µg/ml streptomycin sulfate, 0.25 µg/ml amphotericin (Antibiotic-Antimycotic, Invitrogen) and 1 ng/ml human recombinant GM-CSF. Sf9 insect cells were maintained in Grace's medium (Gibco) supplemented with 10% FBS. 293T cells were obtained from the ATCC and cultured in Dulbecco's Modified Eagle's medium (DMEM) containing 10% FBS and antibiotic-antimycotic.

2.5.2 Expression and purification of ABL-SH3-SH2-HAL proteins

The high affinity linker mutants HAL1 (K241P), HAL2 (V244P), HAL4 (T243P) and HAL5 (G246P) were created by site-directed mutagenesis using the QuikChange method (Stratagene) and the pET-14b/SH32L plasmid as a template. This plasmid was previously used to express wild-type ABL SH3-SH2-linker (32L) protein for HXMS analysis (Chen et al., 2008a).The pET-14b-HAL1 and HAL4 vectors were then used in subsequent round of mutagenesis to generate HAL3 (K241P, V244P) and HAL6 (T243P, G246P), respectively. The pET-14b-HAL3 vector was used to generate HAL7 (K241P, T243P, V244P) while the pET-14b-HAL7 vector was used to create HAL8 (K241P, T243P, V244P, G246P). The HAL8 construct was then used to create HAL9 (K241P, T243P, V244P, G246P, V247P) and subsequently HAL10 (K241P, T243P,

V244P, G246P, V247P, S248P). All ABL 32L proteins were expressed in *E. coli* Rosetta2 (Novagen) and purified using affinity chromatography with Ni-NTA agarose beads (Qiagen). Following cleavage of the hexahistidine tag at the N-terminus by human thrombin protease, the proteins were further purified by size exclusion chromatography. The theoretical mass for each protein matched the measured mass to within 0.5 Da by electrospray mass spectrometry (data not shown).

2.5.3 Expression and purification of NCap-c-ABL core proteins

The NCap-ABL core encompasses residues 1-531 of human c-ABL-1b with an internal deletion of residues 15-56 and a C-terminal cleavage site for the tobacco etch virus (TEV) protease followed by a hexahistidine tag. All ten HAL sequences were introduced into the NCap-ABL core using a two-step PCR-based strategy and the corresponding ABL SH3-SH2-HAL constructs as templates. The NCap-ABL core coding sequence with modified linkers were assembled in the cloning vector pSP72 (Promega) and subsequently subcloned into pCDNA3.1 (Invitrogen) for transient expression in 293T cells and pVL1392 (BD Biosciences) for expression in Sf9 insect cells. The pVL1392/*NCap-ABL* constructs were used to create high-titer recombinant baculovirus in Sf9 insect cells using linearized Baculogold DNA and the manufacturer's protocol (BD Biosciences). For protein production, Sf9 cells were grown in monolayers on large plates and co-infected with NCap-Abl and YopH phosphatase baculoviruses. YopH phosphatase promotes a downregulated conformation of NCap-Abl that allows high-yield purification from Sf9 cells. Sf9-cells were grown for an additional 72 h, harvested by centrifugation, and resuspended in 20 mM Tris-HCL (pH 8.3), 10% glycerol and 5 mM β-mercaptoethanol. Pellets were lysed by sonication and the lysates were clarified by centrifugation at 16,000 rpm for 30

min. The proteins were purified from the supernatant using a combination of ion exchange and affinity chromatography as described previously (Iacob et al., 2009). Upon purification, proteins were dialyzed against 20 mM Tris-HCl (pH 8.3) containing 100 mM NaCl and 3 mM DTT.

2.5.4 Transient expression of c-ABL core proteins in 293T cells

Human 293T cells (1 x 10^6) were plated in 60 mm dishes and incubated at 37 ºC overnight, followed by transfection with 2.5 µg plasmid DNA and X-tremeGENE9 DNA transfection reagent (Roche). Cells were lysed by sonication 24 h later in ice-cold RIPA buffer supplemented with protease and phosphatase inhibitors as described (Briggs and Smithgall, 1999). Cell lysates were clarified by centrifugation at 16,000 rpm for 10 min at 4 ºC and protein concentrations were determined using the Bradford Assay reagent (Pierce). Aliquots of total protein were heated directly in SDS sample buffer and separated by SDS-PAGE. For immunoprecipitation, protein concentrations were first normalized in lysis buffer, followed by addition of 1 µg of anti-His antibody (Abcam) and 20 µl of G-Sepharose (50% slurry; GE Healthcare). Following incubation at 4 ºC overnight, immunoprecipitates were washed three times in RIPA buffer and heated in SDS sample buffer. Following SDS-PAGE, proteins were transferred to nitrocellulose membranes (Bio Rad) for immunoblot analysis. Immunoreactive proteins were visualized and quantitated with appropriate infrared (IR) dye-labeled secondary antibodies using the Odyssey imaging system (LI-COR Biosciences). Antibodies used in this part of the study include ABL polyclonal (sc-131; Santa Cruz Biotechnology), ABL monoclonal (sc-23; Santa Cruz), phospho-ABL (Tyr412, Tyr245, Tyr89; Cell Signaling Technology) and anti-phosphotyrosine (pY99; Santa Cruz).

2.5.5 Construction of Bcr-Abl HAL vectors and retroviral transduction of the human myeloid leukemia cell line, TF-1

Oligonucleotides (648 bp) spanning the HAL9 and BCR-ABL kinase domain mutations E255V, Y253H and T315I plus flanking restriction sites were commercially synthesized (DNA 2.0). Each of these DNA fragments was then swapped for the corresponding region of wild-type BCR-ABL and subcloned into the retroviral vector pMSCV-neo (Clontech). BCR-ABL kinase domain mutations were generated by site directed mutagenesis as described above. Following DNA sequence verification of all constructs, retroviral stocks were produced by co-transfection of 293T cells with each pMSCV/Bcr-Abl plasmid and an amphotropic packaging vector as described previously (Meyn, III et al., 2006). TF-1 cells ($1 \text{ X } 10^6$) were incubated with 5 ml of viral stock in the presence of 4 µg/ml Polybrene (Sigma-Aldrich) and centrifuged at 3000 rpm for 3 h at room temperature. Following infection, cells were washed, transferred to regular medium for 24 h and then put under G418 selection (800 µg/ml) for 14 days. Following selection time, cells were maintained in medium supplemented with 400 µg/ml G418.

2.5.6 Proliferation and apoptosis assays

Proliferation of TF-1 cells was assayed in the absence of GM-CSF using the Cell Titer-Blue Cell Viability assay (Promega) according to the manufacturer's protocol. Fluorescence intensity was then measured using a Gemini XS microplate spectrofluorimeter (Molecular Devices) at 544/590

nm excitation and emission wavelengths, respectively. Caspase activation was measured using the Apo-One Caspase 3/7 assay (Promega) according to manufacturer's protocol. Fluorescence intensity was measured on Gemini XS at 485/520 nm excitation and emission wavelengths, respectively.

2.5.7 Hydrogen exchange experiments

Hydrogen exchange experiments were performed essentially as described in Iacob et al (Iacob et al., 2009). Stock solutions of each ABL core protein (WT, HAL9, A356N, and A356N-HAL9) were prepared at 20 pmol/µL in 20 mM Tris-HCl (pH 7.96), 100 mM NaCl, 3 mM DTT in H_2O. Deuterium exchange was initiated by dilution of each protein 15-fold with an identical buffer prepared in D_2O at room temperature. At each deuterium exchange time point (ranging from 10 s to 4 h) an aliquot from the exchange reaction was removed and labeling was quenched by adjusting the pH to 2.5 with an equal volume of quench buffer (0.8 M guanidinium HCl, 0.8% formic acid) followed by freezing on dry ice. Samples were stored at -80 °C prior to pepsin digestion and mass analysis.

2.5.8 Mass analysis

Each frozen sample was thawed rapidly and injected into a custom Waters nanoACQUITY UPLC HDX Manager^{TM} (Waters Corp., Milford, MA, USA) and analyzed as previously described (Wales et al., 2008). The protein samples were digested using a Poroszyme immobilized pepsin cartridge (Applied Biosystems) which was accommodated within the UPLC

system. The cooling chamber of the UPLC system which housed all the chromatographic elements was held at 0.1 °C for the entire analysis. The injected peptides were trapped and desalted for 3 min at 100 µL/min and then separated over 6 min with an 8%-40% acetonitrile:water gradient at 40 µL/min. Chromatography was performed on a 1×100 mm Waters ACQUITY UPLC C18 BEH column containing 1.7 µm particles and the back pressure averaged 8800 psi at 0.1 °C. The average amount of back-exchange using this experimental setup was 18% to 25%, based on analysis of highly deuterated peptide standards. Deuterium levels were not corrected for back-exchange and are therefore reported as relative (Wales and Engen, 2006). However, all comparisons were done under identical experimental conditions thus negating the need for back-exchange correction. The UPLC step was performed with protonated solvents, thereby allowing deuterium to be replaced with hydrogen from side chains and the amino/carboxyl termini which exchange much faster than amide linkages (Englander and Kallenbach, 1983). All experiments were performed in duplicate and the error of determining the deuterium levels was ± 0.20 Da in this experimental setup consistent with previously obtained values (Burkitt and O'Connor, 2008).

Mass spectra were obtained with a Waters XEVO G2 TOF equipped with a standard ESI source. The instrument was configured as follows: capillary at 3.2 kV, trap collision energy at 6 V, sampling cone at 35 V, source temperature of 80 °C and desolvation temperature of 175 °C. Mass spectra were acquired over an m/z range of 100 to 2000. Mass accuracy was ensured by calibration with 500 fmol/µL GFP, and was less than 10 ppm throughout all experiments. The mass spectra were processed with the software package DynamX^{TM} (Waters) by centroiding an isotopic distribution corresponding to the +2, +3, or +4 charge state of each peptide. Deuteration levels were calculated by subtracting the centroid of the isotopic distribution for peptide ions of

undeuterated protein from the centroid of the isotopic distribution for peptide ions from the deuterium labeled sample. The resulting relative deuterium levels were automatically plotted versus the exchange-in time. Identification of the peptic fragments was accomplished through a combination of exact mass analysis and MS^E (Plumb et al., 2006) using Identity Software (Waters). MS^E was performed by a series of low-high collision energies ramping from 5–30 V, therefore ensuring proper fragmentation of all the peptic peptides eluting from the LC system.

2.5.9 Data Visualization

Peptic maps were obtained using the DynamX software package. Local changes in isotope exchange were mapped to the crystal structure of c-Abl (PDB: 2F0O) using PyMOL (Seeliger and de Groot, 2010)

3.0 OVERCOMING IMATINIB RESISTANCE WITH SELECTIVE SRC-FAMILY KINASE INHIBITORS IN CHRONIC MYELOGENOUS LEUKEMIA

3.1 ABSTRACT

Src family kinases (SFKs) are important mediators of BCR-ABL signal transduction and oncogenesis in CML. BCR-ABL binds to and activates multiple SFKs in CML cells, including HCK and LYN. In turn, active SFKs directly phosphorylate regulatory tyrosine residues in the SH3 domain, the SH2-kinase linker, and the BCR-derived portion of BCR-ABL. Given the important role SFKs in BCR-ABL-mediated signaling and drug resistance, we studied the effect of the SFK-selective inhibitor A-419259 on human TF-1 myeloid cells transformed with clinically relevant imatinib-resistant forms of BCR-ABL (E255V, Y253H and T315I). Proliferation of TF-1 cells transformed with BCR-ABL E255V and Y253H was markedly inhibited by A-419249. The anti-proliferative effects of the inhibitor correlated with suppression of overall SFK activity. However, TF-1 cells transformed with the Bcr-Abl gatekeeper mutant T315I were completely cross-resistant to A-419259. Surprisingly, SFK activity in TF-1 cells expressing BCR-ABL T315I was not inhibited by this compound. Immunoprecipitation experiments show that endogenous LYN remained active in A-419259-treated TF-1 cells transformed with BCR-ABL T315I. These results suggest that in general, SFKs are important targets to overcome imatinib resistance in CML. However, our data also suggest a new

mechanism of BCR-ABL T315I-induced resistance to drugs that target SFKs in CML. We speculate that this effect may be due to an acquired ability of BCR-ABL T315I to phosphorylate SFKs at novel sites that interfere with drug action.

3.2 INTRODUCTION

CML results from the neoplastic transformation of a hematopoietic stem cell (Sawyers, 1992). CML was the first cancer in which a specific chromosomal abnormality was linked to the pathogenesis of the disease. This hallmark chromosomal abnormality is referred to as the Philadelphia chromosome (Ph) which results from the reciprocal translocation between the long arms of chromosomes 9 and 22 [t(9;22)(q34;q11)] (Rowley, 1973; Rowley, 1980). This translocation fuses the *ABL* and *BCR* loci, creating a hybrid *BCR-ABL* gene that is expressed as a chimeric BCR-ABL protein with deregulated tyrosine kinase activity (Shtivelman et al., 1985). Clinically, CML is characterized by a chronic phase defined by an increase in proliferation of the transformed progenitor cells that retain their ability to differentiate. Within 5-8 years of disease onset, CML progresses to the accelerated phase marked by decreased maturation of the myeloid and lymphoid compartments. The final blast crisis phase is characterized by the accumulation of immature blast cells that have lost the ability to differentiate. In about 80 percent of cases, CML blasts have a myeloblastic phenotype and the remaining 20 percent have a lymphoblastic phenotype. This phase of the disease resembles acute leukemias and is often fatal (Kurzrock et al., 1988; Advani and Pendergast, 2002; Ren, 2005).

Since BCR-ABL tyrosine kinase activity is required for the initiation and maintenance of CML, it represents an ideal therapeutic target. Imatinib (STI571; Gleevec) is a 2-phenylaminopyrimidine inhibitor that targets the ATP binding site of the ABL kinase domain (Druker et al., 1996; Schindler et al., 2000). Treatment of CML with imatinib has been a remarkable clinical success, especially in the chronic phase of the disease. However, treatment failure in the blast crisis phase is often attributable to imatinib resistance caused by point mutations in the kinase domain of BCR-ABL(Azam et al., 2003). One of the most clinically challenging resistance mutations involves substitution of the 'gatekeeper' threonine with isoleucine (T315I) (Gorre et al., 2001; Shah et al., 2002). This threonine is located at the hinge region between the two lobes of the kinase domain and is termed the gatekeeper residue because it controls the access of inhibitors into a deep hydrophobic pocket near the active site (Nagar et al., 2002). A variety of small molecule kinase inhibitors that target the ATP binding site require threonine at this position for binding specificity. In the case of BCR-ABL, the hydroxyl group of threonine hydrogen bonds with imatinib as well as the second generation ATP competitive inhibitors nilotinib and dasatinib. Substitution of threonine with isoleucine results in the loss of this stabilizing hydrogen bond and steric hindrance between the bulky isoleucine side chain and the drugs thus prevents access to the hydrophobic pocket.

In addition to kinase domain mutations, a growing body of evidence suggests that SFKs play a clinically important role in BCR-ABL signal transduction and imatinib resistance as well. The first evidence linking BCR-ABL and SFKs in CML was shown by Danhauser-Riedl's group (Danhauser-Riedl et al., 1996). In this study, BCR-ABL associated with and increased the kinase activity of HCK and LYN in murine 32D cells transformed with BCR-ABL and in CML cell lines such as BV173, LAMA-84 and K562. The interaction between BCR-ABL and HCK is

mediated by SH3, SH2, kinase domain and C-terminal domains of BCR-ABL as well as SH3 and SH2 domains of HCK (Stanglmaier et al., 2003b; Lionberger et al., 2000).

Subsequent work has implicated SFKs in the phosphorylation of BCR-ABL on tyrosine sites that affect its regulation and oncogenicity. For example, Tyr177 in the BCR portion of the protein is phosphorylated by HCK and LYN, resulting in the recruitment and binding of the GRB2/SOS complex and subsequent activation of RAS/ERK signaling downstream (Warmuth et al., 1997; Meyn, III et al., 2006). In addition, kinase-dead HCK suppresses STAT5 activation and blocks BCR-ABL-induced transformation of myeloid cells, suggesting that HCK is a key intermediate linking BCR-ABL with this survival signaling pathway (Klejman et al., 2002; Lionberger et al., 2000). HCK, LYN and FYN directly phosphorylate tyrosine residues in the SH3 and SH2 domains as well as the SH2-kinase linker of BCR-ABL that have been implicated in the regulation of BCR-ABL kinase activity (Meyn, III et al., 2006). Substitution of these residues with phenylalanine impaired BCR-ABL-mediated transformation of myeloid progenitor cells to cytokine independence, suggesting an important function for SFK-mediated phosphorylation of BCR-ABL in vivo.

Previous work from our laboratory showed that A-419259, a SFK-selective inhibitor, blocks CML cell proliferation specifically in Ph+ cell lines and inhibited Erk and Stat5 activation (Lionberger et al., 2000; Wilson et al., 2002). This study suggested that BCR-ABL-mediated transformation of myeloid cells is dependent on SFK activity. More recent work from our laboratory showed that A-419259 induces growth arrest and apoptosis in CD34+ cells isolated from CML patients. In addition, expression of a form of HCK with engineered resistance to A-419259 protected CML cells from the antiapoptotic and antiproliferative effects of this SFK inhibitor. Furthermore, overexpression of HCK in CML cells induced resistance to imatinib and

sensitivity was restored upon inhibition of HCK kinase activity (Pene-Dumitrescu et al., 2008; Pene-Dumitrescu and Smithgall, 2010).

The literature discussed above supports an important role for SFKs in the pathogenesis of CML and drug resistance. In this study we investigated whether the SFK inhibitor A-419259 is effective against human myeloid cells transformed with three common imatinib-resistant forms of BCR-ABL (E255V, Y253H and T315I). We found that imatinib resistance due to mutations in the P-loop (E255V and Y253H) can be completely overcome with this inhibitor. However, cells transformed with the gatekeeper mutant, T315I, were completely resistant to the anti-proliferative effects of A-419259. Moreover, A-419259 treatment failed to inhibit SFKs in cells transformed with BCR-ABL T315I. The same cross-resistance phenomenon was observed upon expression of wild-type HCK in cells transformed with T315I BCR-ABL. A final series of experiments demonstrates that BCR-ABL T315I phosphorylates HCK much more aggressively than wild-type HCK in a defined system, suggesting that enhanced phosphorylation of HCK may be responsible for A-419259 resistance in BCR-ABL T315I-transformed cells. Our data also highlight the importance of SFKs in imatinib resistance, their importance as therapeutic targets and a possible new mechanism of resistance involving the gatekeeper mutation.

3.3 RESULTS

3.3.1 Transformation of TF-1 cells with imatinib-resistant BCR-ABL mutants

As a model system for the present study, we chose the human myeloid leukemia cell line, TF-1. Like normal myeloid progenitors, TF-1 cells require GM-CSF, IL-3 or other cytokines for growth and survival in culture. Our previous studies have shown that TF-1 cells are transformed into a cytokine-independent phenotype following retroviral transduction with wild-type BCR-ABL (Meyn, III et al., 2006). We transformed TF-1 cells with wild-type BCR-ABL as well as three imatinib-resistant BCR-ABL mutants that commonly arise in patients. These include the gatekeeper mutant, T315I, as well as two additional mutants that localize to the phosphate-binding 'P-loop' of the kinase domain active site (E255V, Y253H; Figure 23). To confirm the drug-resistant phenotype, we performed cell proliferation assays in the absence of GM-CSF and with increasing concentrations of imatinib over 72 hours (see Materials and Methods). As expected, proliferation of TF-1 cells expressing wild-type BCR-ABL was blocked by imatinib at 1 μM (Figure 24). In contrast, all three TF-1 cell populations transduced with the imatinib-resistant forms of BCR-ABL grew at the same rate in the presence of imatinib at the highest concentration tested (1 μM).

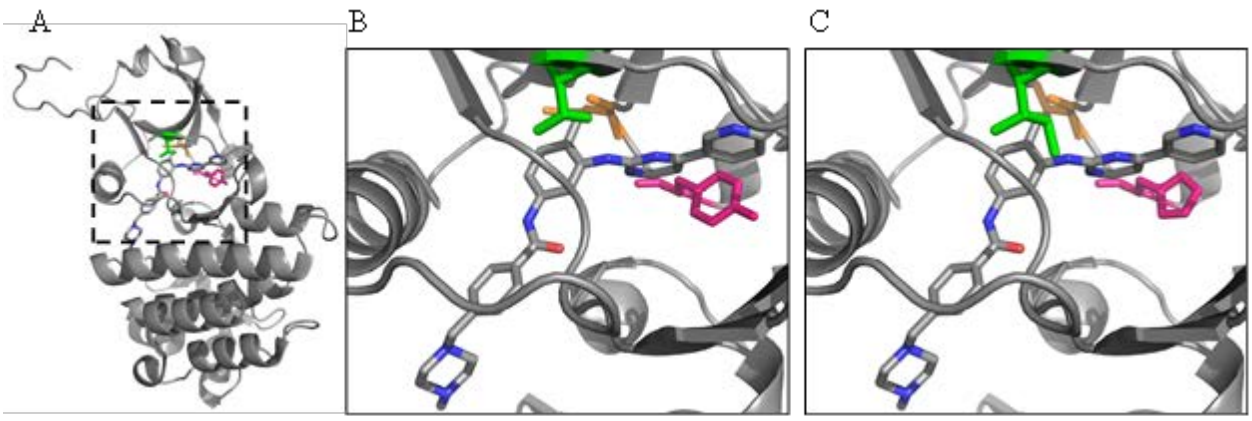

Figure 23: Imatinib resistant mutations. A, structure of ABL kinase domain with imatinib (PDB code 1IEP). The side chain of gatekeeper residue Thr315 is highlighted in green, side chain of Y253 is in pink and side chain of E255 is in orange. These three residues and imatinib are shown in the boxed area. **B,** close-up view of the three amino acids and their relationship with imatinib. **C,** close-up view of the boxed area with three mutants T315I, Y253H, E255V. This close-up view shows the steric clash of the isoleucine side chain at the gatekeeper residue and the loss of aromatic interaction at the Y253H residue.

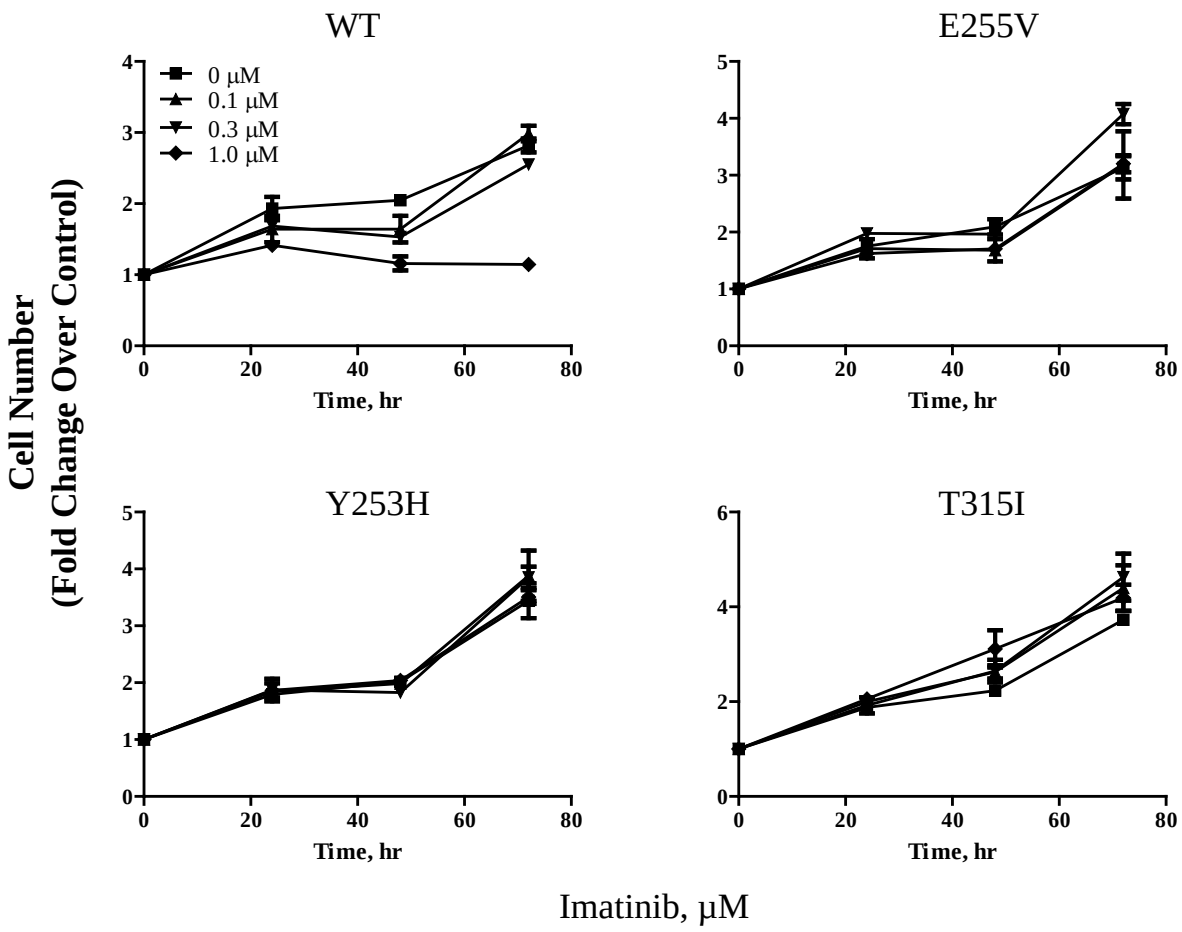

Figure 24: Effect of imatinib on TF-1 cells expressing wild-type and imatinib- resistant BCR-ABL mutants. Human TF-1 myeloid cells were transduced with wild-type (WT) BCR-ABL as well as imatinib resistant mutant E255V, Y253H, and T315I retroviruses. Transformed cells were plated in triplicate wells in the presence of the indicated concentrations of imatinib. Cell viability was measured at the indicated time points using Cell Titer Blue assay. Data are expressed as cell number fold change +/- SD.

3.3.2 Imatinib resistance due to kinase domain mutations E255V and Y253H but not T315I are overcome with the selective Src family kinase inhibitor, A-419259

We next investigated the sensitivity of the same panel of TF-1 cells to the effects of the SFK inhibitor, A-419259. Cell proliferation was inhibited in TF-1 cells expressing wild-type BCR-ABL in response to increasing concentrations of A-419259 over 72 hours (Figure 25), consistent with our previous reports (Wilson et al., 2002). Interestingly, cells expressing BCR-ABL imatinib resistant mutants E255V and Y253H also displayed growth arrest in response to A-419259 treatment. Cells expressing the E255V and Y253H mutant responded in a similar way to cells expressing wild-type BCR-ABL, and proliferation was almost completely blocked at a concentration of 1μM. However, TF-1 cells expressing the T315I mutant were completely resistant to the effects of A-419259 in terms of cell proliferation.

We next investigated the effects of A-419259 treatment on SFK and BCR-ABL protein-tyrosine phosphorylation in whole cell lysates by immunoblot analysis. SFK phosphorylation was assayed with a phosphospecific antibody directed against the activation loop phosphotyrosine (pY418), which correlates with kinase activity. Because BCR-ABL is phosphorylated on multiple tyrosines, phosphorylation was evaluated as overall phosphotyrosine content. As shown in Figure 26, in TF-1 cells transformed with wild-type, Y253H, and E255V BCR-ABL, endogenous SFK autophosphorylation was inhibited in a concentration-dependent manner. BCR-ABL phosphotyrosine content was also inhibited in these cells at higher A-419259 concentrations, consistent with our previous observations that SFKs phosphorylate BCR-ABL on multiple tyrosine residues both in vitro and in vivo (Meyn, III et al., 2006). These observations are consistent with the effect of A-419259 treatment on the proliferation of these

cell lines. In contrast, A-419259 treatment had no effect on SFK activation loop phosphorylation or BCR-ABL phosphotyrosine content in TF-1 cells expressing BCR-ABL T315I, suggesting that T315I confers cross-resistance to this SFK inhibitor.

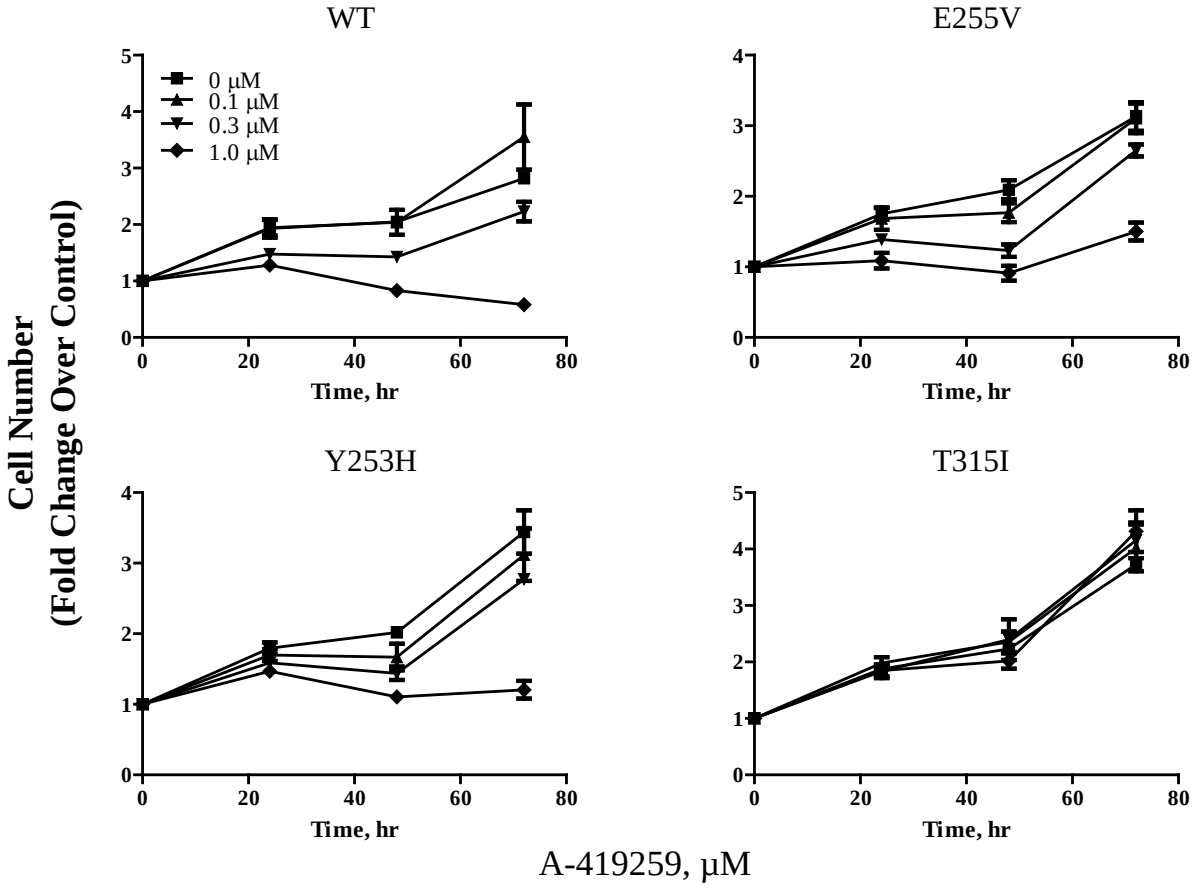

Figure 25: Sensitivity of TF-1 cells expressing wild-type and imatinib-resistant forms of BCR-ABL to the Src family kinase inhibitor A-419259. TF-1 cells were cultured in the presence of A-419259 at concentrations shown. Viable cells were assayed in triplicate using the cell Titer Blue assay at the indicated time points. Data are expressed as relative cell number +/- SD.

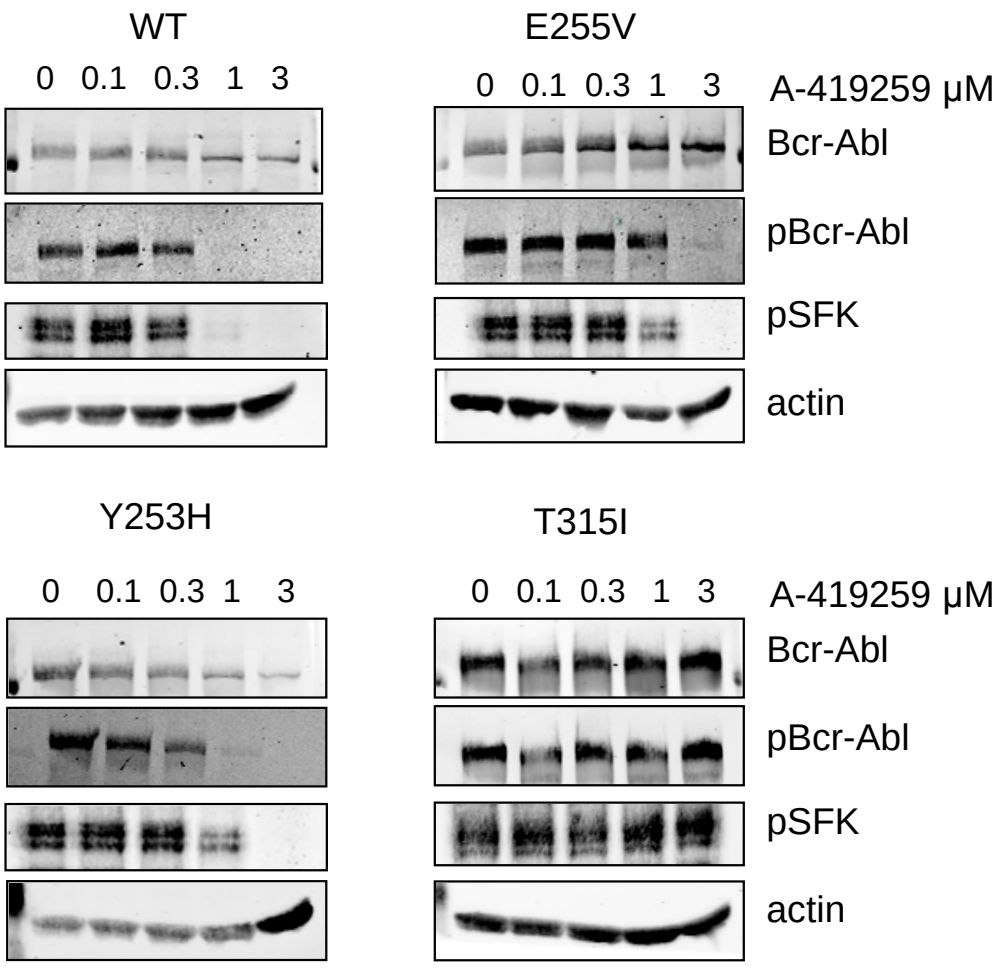

Figure 26: TF-1 cells expressing Bcr-Abl T315I are insensitive to the effects of SFK inhibitor A-419259. TF-1 cells expressing wild-type Bcr-Abl or imatinib-resistant mutants were treated with increasing concentrations of A-419259 for 16 h. Clarified cell lysates were assayed by immunoblotting analysis for expression of Bcr-Abl protein, Bcr-Abl phosphotyrosine content (pAbl), autophosphorylated SFKs (pSFK) and actin as a loading control.

3.3.3 The myeloid SFKs LYN and HCK acquire resistance to A-419259 in TF-1 cells transformed by BCR-ABL T315I

We first investigated whether the myeloid SFK LYN specifically showed resistance to A-419259 in BCR-ABL-T315I transformed TF-1 cells. LYN is strongly expressed in this cell line where it appears as a doublet due to expression of the LYN-A and LYN-B isoforms. Following treatment of TF-1 cells expressing BCR-ABL wild-type, E255V, Y253H or T315I with 1 μM A-419259, we immunoprecipitated LYN and analyzed its inhibitor responsiveness using the antibody to the activation loop phosphotyrosine residue (Figure 27A). In TF-1 cells expressing wild-type BCR-ABL, LYN activation loop phosphorylation was completely blocked by A-419259 treatment. Similar results were obtained with cells expressing BCR-ABL E255V and Y253H, with LYN activation loop phosphorylation dramatically decreased but not completely suppressed as in treated cells expressing wild-type BCR-ABL. In striking contrast, LYN activation loop phosphorylation was unaffected by A-419259 treatment in cells transformed with the BCR-ABL T315I mutant.

To determine whether A-419259 cross-resistance is specific to LYN or if it could be observed with other Src-family members linked to BCR-ABL, we overexpressed HCK in TF-1 cells transformed with the wild-type and T315I forms of BCR-ABL. Phosphorylation of HCK at the activation loop tyrosine was almost completely inhibited by 1 μM A-419259 in cells expressing wild-type BCR-ABL, similar to the effects observed with endogenous LYN. However, HCK activation loop phosphorylation was resistant to the effects of A-419259 in cells expressing BCR-ABL T315I (Figure 27B).

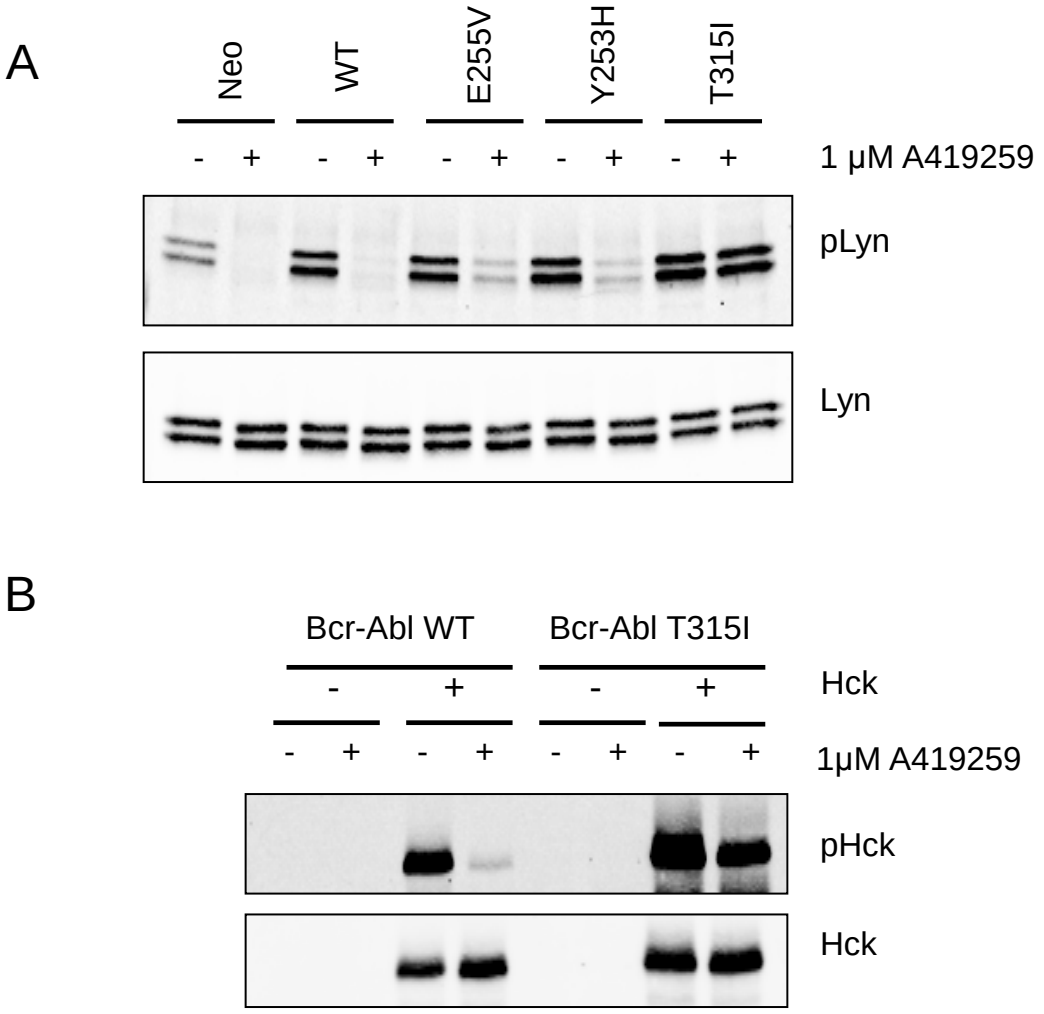

Figure 27: Endogenous LYN and exogenous HCK are cross-resistant to the SFK inhibitor A-419259 in cells expressing BCR-ABL T315I. A) TF-1 cells expressing wild-type (WT) and imatinib-resistant BCR-ABL (E255V, Y253H, T315I) were grown overnight in the presence of 1 µM A-419259. Endogenous LYN was immunoprecipitated from clarified lysates and analyzed by immunoblotting with antibodies to LYN protein and to the phosphorylated activation loop (pLYN). LYN is expressed as two isoforms from two separate loci, LYN-A and LYN-B. **B)** TF-1 cells expressing BCR-ABL wild-type and T315I were transduced with HCK retrovirus. TF-1 cells expressing both BCR-ABL and HCK were treated with 1 µM A-419259 for 16 h. HCK was immunoprecipitated from clarified extracts and analyzed by immunoblotting with antibodies to HCK as well as its phosphorylated activation loop (pHCK).

3.3.4 HCK is a direct substrate for the ABL kinase

Results presented in the preceding sections show that SFKs become resistant to the effects of A-419259 in cells transformed with the BCR-ABL imatinib-resistant mutant, T315I. Previous studies have shown that this gatekeeper mutation alters the catalytic properties of the ABL kinase domain, resulting in enhanced kinase activity (Iacob et al., 2009; Azam et al., 2008). These findings suggest a mechanism of cross-resistance in which BCR-ABL T315I directly phosphorylates HCK or LYN, thereby affecting inhibitor action. To investigate this possibility without interference from endogenous mammalian cell kinases, we turned to Sf9 insect cells. Here we expressed kinase-dead HCK either alone or together with wild-type or T315I ABL kinase core proteins, and analyzed the extent of HCK phosphorylation by immunoblotting with the activation loop phosphospecifc antibody. As shown in Figure 28, kinase-dead HCK was phosphorylated by both ABL proteins, but the extent of phosphorylation was dramatically higher upon co-expression of HCK with ABL T315I compared to wild-type ABL. This is the first evidence to demonstrate that SFKs can be directly phosphorylated by ABL kinase. These data support a previously unrecognized consequence of the BCR-ABL T315I mutation in terms of SFK phosphorylation, which may account in part for the observed cross-resistance to A-419259.

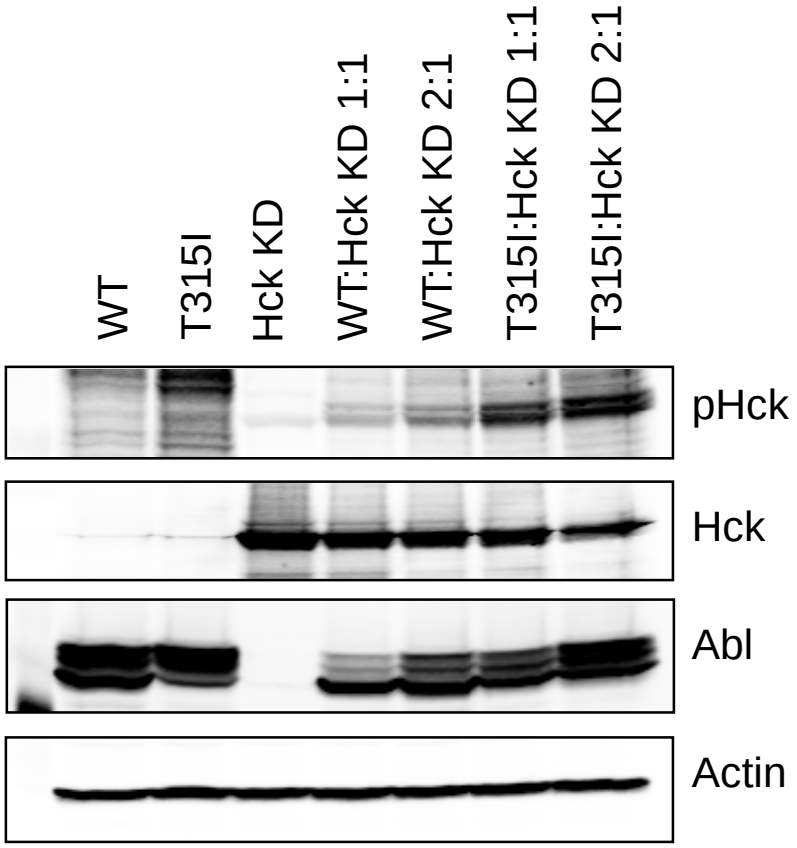

Figure 28: Kinase-dead HCK is phosphorylated by wild-type and T315I ABL in Sf9 insect cells. Sf9 insect cells were infected with wild-type and T315I c-ABL core baculoviruses either alone or co-infected with kinase dead HCK (HCK KD) baculovirus at a 1:1 (WT/TI: HCK KD) or 2:1 (WT/TI:HCK KD) virus ratio. Following 24 h infection, clarified lysates were analyzed by immunoblotting with antibodies to the phosphorylated activation loop (pHCK), HCK, ABL and actin as loading control.

3.4 DISCUSSION

To date, there is strong evidence supporting the crucial role of Src-family kinases in many aspects of CML pathogenesis (Li, 2008). Cross-talk between SFKs and BCR-ABL promotes oncogenic signaling downstream (Danhauser-Riedl et al., 1996; Lionberger et al., 2000; Warmuth et al., 1997; Klejman et al., 2002). SFKs interact with and phosphorylate BCR-ABL leading to recruitment of adaptor proteins to BCR-ABL and subsequent activation of downstream signaling. Phosphorylation of BCR-ABL by SFKs also interferes with regulation of the kinase domain and desensitization to targeted therapies (Warmuth et al., 1997; Meyn, III et al., 2006). In turn BCR-ABL induces expression and activation of SFKs that play important roles in the progression of the disease to blast crisis. SFKs also contribute to clinical CML drug resistance in the absence of BCR-ABL kinase domain mutations. For example, work from our group has shown that over-expression of HCK is sufficient to induce imatinib resistance in CML cell lines (Pene-Dumitrescu and Smithgall, 2010). Similarly, elevated LYN expression and activity have been observed in samples from patients after imatinib and nilotinib therapy failure and in the absence of BCR-ABL kinase domain mutations (Okabe et al., 2011; Ptasznik et al., 2004; Gioia et al., 2011). Based on these data, SFKs represent an important therapeutic target in CML.

Previous work from our group has shown that global inhibition of SFK activity with the ATP-competitive pyrrolo-pyrimidine A-419259 leads to growth arrest and apoptosis in CML cell lines and in primary CD34+ CML cells (Lionberger et al., 2000; Wilson et al., 2002; Pene-Dumitrescu et al., 2008). In addition, expression of an HCK mutant with engineered resistance to

A-419259 protects CML cells against the antiproliferative and apoptotic effects of this compound, providing important evidence that SFKs are the primary target for this inhibitor in CML cells (Pene-Dumitrescu and Smithgall, 2010). In the present study, we extended our investigation of A-419259 to human TF-1 myeloid cells transformed with clinically relevant imatinib-resistant forms of BCR-ABL (E255V, Y253H and T315I). Proliferation of TF-1 cells transformed with BCR-ABL E255V and Y253H was markedly inhibited by A-419249. The anti-proliferative effects of the inhibitor correlated with suppression of overall SFK activity and a reduction on BCR-ABL phosphotyrosine content. However, TF-1 cells transformed with the BCR-ABL gatekeeper mutant T315I were completely cross-resistant to A-419259. Surprisingly, endogenous SFKs present in the T315I-transformed cells were not inhibited by this compound. Immunoprecipitation experiments identified LYN as an endogenous myeloid SFK resistant to A-419259 in TF-1 cells expressing Bcr-Abl T315I. We also showed that the same mechanism of resistance occurred upon over-expression of HCK in the TF-1/BCR-ABL-T315I cells.

These observations suggest a cross-resistance mechanism in which BCR-ABLT315I acquires the ability to phosphorylate SFKs and induce drug-resistance. In support of this mechanism, we showed that kinase-dead HCK was strongly phosphorylated by an ABLT315I core protein in insect cells, while wild-type ABL was less effective at doing so. This observation is consistent with recent reports that gatekeeper mutations alter the kinetic, dynamic and signaling properties of both ABL and BCR-ABL kinases. Future studies will determine whether BCR-ABLT315I-mediated resistance of HCK, LYN or other SFKs to A-419259 is due to differences in the extent of HCK phosphorylation, differential phosphorylation at drug-sensitive sites, or both. Alternatively, T315I mutation may enhance the expression of P-glycoprotein (Pgp), the ATP-dependent xenobiotic transport protein associated with the multi-drug resistant

phenotype. Future studies will investigate the role of Pgp expression as a possible mechanism conferring cross-resistance to A-419259.

In summary, data presented here suggest that selective inhibitors of SFKs may have translational use in the treatment of some types of imatinib-resistant CML, including cases with kinase domain mutations other than T315I or where SFKs such as HCK and LYN are over-expressed. However our data also revealed a new mechanism of BCR-ABL T315I-induced resistance to drugs that target SFKs in addition to BCR-ABL, and may help to explain why drug resistant CML linked to the BCR-ABL T315I mutation is so difficult to manage, even with broader spectrum inhibitors such as dasatinib which target both BCR-ABL and SFKs.

3.5 MATERIALS AND METHODS

3.5.1 Cell Culture

The human GM-CSF-dependent myeloid leukemia cell line TF-1 was obtained from the American Type Culture Collection (ATCC) and maintained in RPMI 1640 supplemented with 10% fetal bovine serum (FBS), 100 U/ml penicillin G, 100 µg/ml streptomycin sulfate, 0.25 µg/ml amphotericin (Antibiotic-Antimycotic, Invitrogen) and 1 ng/ml human recombinant GM-CSF. Sf9 insect cells were maintained in Grace's medium (Gibco) supplemented with 10% FBS.

3.5.2 Mutagenesis of the ABL kinase domain and transformation of TF-1 cells with BCR-ABL retroviruses

Imatinib-resistant BCR-ABL kinase domain mutants E255V, Y253H and T315I were created by site-directed mutagenesis of a wild-type p210 BCR-ABL cDNA as described elsewhere (O'Hare T). The nucleotide sequences of the mutant cDNAs were confirmed by automated DNA sequence analysis. Wild-type and imatinib-resistant mutant forms of Bcr-Abl were subcloned into the retroviral vector pMSCV-neo (Clontech).

To make retroviral stocks, 293T cells were co-transfected with each retroviral construct and an amphotropic packaging vector as described (Briggs SD). TF-1 cells (10^6) were incubated with 5 ml of viral supernatant in the presence of 4 μg/ml polybrene and centrifuged at 2400 rpm for 3 h at room temperature to enhance infection. Cell populations were selected with 800 μg/ml G418 for 10-14 days. Following selection, cells were maintained in medium supplemented with 400 μg/ml G418.

3.5.3 Cell proliferation assays

Proliferation of Bcr-Abl-transformed TF-1 cells was assayed in the absence of GM-CSF using the CellTiter-Blue Cell Viability assay (Promega) according to the manufacturer's protocol. Cells were plated in triplicate and incubated with increasing concentrations of imatinib, A-419259 or DMSO for up to 72 hours. Fluorescence intensity was measured using a Gemini XS microplate spectrofluorimeter (Molecular Devices) at 544/590 nm excitation and emission

wavelengths, respectively. All experiments were performed in triplicate and data are presented as the mean +/- SD for each timepoint.

3.5.4 Immunoblotting and Immunoprecipitation

To analyze protein expression and tyrosine phosphorylation, TF-1 cells expressing different BCR-ABL mutants were treated with the indicated concentration of A-419259 for 16 hours. Cells were collected by centrifugation, washed with PBS and lysed by sonication in ice-cold RIPA buffer supplemented with protease and phosphatase inhibitors as described. Cell lysates were clarified by centrifugation at 16,000 rpm for 10 min at 4 ºC and protein concentrations were determined using the Bradford Assay reagent (Pierce). Aliquots of total protein were heated directly in SDS sample buffer and separated by SDS-PAGE. For immunoprecipitation of LYN or HCK, protein concentrations were first normalized in lysis buffer, followed by addition of 1 µg of anti-LYN or anti-HCK antibodies. Following SDS-PAGE, proteins were transferred to nitrocellulose membranes (BioRad) for immunoblot analysis. Immunoreactive proteins were visualized and quantitated with appropriate infrared (IR) dye-labeled secondary antibodies using the Odyssey imaging system (LI-COR Biosciences). Antibodies used in this part of the study include ABL polyclonal (sc-131; Santa Cruz Biotechnology), Abl monoclonal (sc-23; Santa Cruz), phospho-Abl (Tyr412; Cell Signaling Technology), anti-phosphotyrosine (pY99; Santa Cruz), actin (source), phospho-Src (Tyr418; source).

3.5.5 Retroviral transduction of TF-1 cells

Wild-type Hck was subcloned into the retroviral expression vector pMSCV-puro. Retroviral stocks were produced from the resulting construct in 293T cells using an amphotropic packaging vector as described above. TF-1 cells expressing wild-type and T315I BCR-ABL mutant were plated in 6 well plates at 1X 10^6 cells/well in 5 ml of viral supernatant in the presence of 4 µg/ml Polybrene (hexadimethrine bromide) and centrifuged at 2400 rpm for 3 hours at room temperature. After infection cells were placed under puromycin selection (1µg/ml) for 10 days. After the selection time, cells were maintained in medium with G418 (400 µg/ml) and puromycin (0.5 µg/ml). The protein expression and phosphorylation status of HCK was determined by immunoprecipitation as described in the above section.

3.5.6 Expression in Sf9 insect cells

Using site directed mutagenesis, the Lys269 to Asp (K269D) mutation was introduced into the coding sequence of human HCK (QuickChange XL Site-directed Mutagenesis Kit, Stratagene). The NCap-c-ABL wild-type and T315I constructs encompass residues 1-531 of human c-ABL-1b with residues 15-56 deleted and containing c-terminal tobacco etch virus (TEV) protease cleavage site followed by hexahistidine tag. HCK-KD and the NCap-c-ABL constructs were cloned into pVL1392 (BD biosciences) and each plasmid was used to create high-titer recombinant baculovirus in Sf9 insect cells using Baculogold DNA and the manufacturer's protocol (BD Biosciences). To determine activation loop phosphorylation of HCK, 2.5 X 10^6 Sf9 cells were plated in 60 mm dishes in Grace's medium supplemented with 10% FBS. Cells were then infected with wild-type and T315I c-ABL core viruses alone or co-infected with kinase dead

HCK virus at 1:1 or 2:1 (ABL/HCK) ratio. Twenty-four hours later, clarified cell lysates were analyzed by immunoblotting with antibodies to the phosphorylated activation loop of HCK (pY418), HCK, ABL and actin.

4.0 OVERALL DISCUSSION

4.1 SUMMARY OF FINDINGS AND SIGNIFICANCE

Despite the unprecedented response rates with imatinib, resistance to imatinib has been inevitable (Roychowdhury and Talpaz, 2011). Based on extensive work on imatinib-induced resistance, it is evident that resistance mechanisms can be BCR-ABL-dependent or independent. Fifty percent of the BCR-ABL dependent mechanisms of resistance relate to kinase domain mutations. To date more than 100 kinase mutations have been identified that map not only onto the drug binding site but also on other regions of the protein (Quintas-Cardama et al., 2009). The mutations arising in the SH3, SH2, SH2-Kinase linker, SH3-SH2 connector and the kinase domains induce allosteric conformational changes that interfere with drug binding (Azam et al., 2003; Shah et al., 2002; Sherbenou et al., 2010). These studies paved the way to the design of second generation tyrosine kinase inhibitors either with more potency than imatinib (nilotinib) or drugs that also target the active conformation of the protein (dasatinib). However, the second generation drugs cannot overcome the most recalcitrant gatekeeper mutations and also lead to resistance. A third generation of tyrosine kinase inhibitor in clinical trials, ponatinib, binds to the ATP binding site of the inactive conformation of the protein and accommodates the isoleucine side chain of the gatekeeper mutant T315I (Ohanian et al., 2012; Zhou et al., 2011).

Prior to this study, the use of allosteric inhibitors that target BCR-ABL kinase at a distance from the active site has gained a lot of attention as an alternative strategy to overcome resistance (Zhang et al., 2009). One such example is GNF-2, which targets the C-lobe myristic acid binding pocket of the ABL protein (Adrian et al., 2006). This compound and its analogs have shown inhibitory effects on most BCR-ABL mutants with the notable exception of the T315I mutation. This observation suggests that T315I uncouples the active site from allosteric control by the myristate binding pocket in the C-lobe. However, when combined with nilotinib or dasatinib, GNF-2 and related compounds overcome T315I mutations.

Recently work from our group has shown that phosphorylation of BCR-ABL on Tyr89 in the SH3 domain causes imatinib resistance. Furthermore, dynamics analyses revealed that phosphorylation of this residue disrupts intramolecular SH3:linker binding, an interaction necessary for negative regulation of c-ABL kinase activity (Chen et al., 2008b; Meyn, III et al., 2006; Pene-Dumitrescu and Smithgall, 2010). These studies support the idea that mutations occurring outside the active site allosterically induce an active conformation of the kinase domain which is less compatible with imatinib binding. Also, these studies suggest that the SH3 domain may have a regulatory effect in the context of active BCR-ABL kinase. Therefore, in the first aim of my thesis, I attempted to determine the role of SH3:linker interaction as an alternate allosteric regulator involved in stabilizing a single conformation of the kinase domain and its impact in sensitizing the kinase to currently established inhibitors.

In addition, to date, there is a wealth of literature supporting the crucial role of SFKs in many aspects of CML pathogenesis and BCR-ABL-independent mechanisms of resistance (Ptasznik et al., 2004) .Based on these observations, SFKs represent important therapeutic targets in CML. Therefore, in the second aim of my thesis, I sought to understand the effect of global

inhibition of SFK activity with Src-selective inhibitor A-419259 in clinically relevant imatinib resistant BCR-ABL mutants.

4.1.1 SH3:linker interaction as an allosteric regulator of ABL and BCR-ABL kinases

To understand the contribution of the SH3:linker interaction in allosteric regulation of ABL and BCR-ABL kinases, we worked with our collaborators to strengthen this interaction by the sequential substitution of linker residues with proline, and referred to these modifications as *High Affinity Linkers* (HAL). This approach was used previously by our group to strengthen the SH3:linker interaction in HCK (Lerner et al., 2005). However, unlike in HCK where substitution of two lysine residues tightened the SH3:linker interaction, substitution of at least 4 residues (HAL8) in ABL linker was necessary to tighten this interaction in small ABL proteins comprised of the NCap, SH3, SH2 and the linker regions. The increase in proline content correlated with an increase in the affinity of the SH3 for the linker as seen by HX MS. Next, I introduced these substitutions in the core of ABL (NCap-SH3-SH2-Linker-Kinase domain) and expressed the resulting proteins in 293T cells. Within the context of the larger protein, HAL9 (5 prolines) enhanced the SH3:linker interaction without disturbing overall kinase regulation as determined by the comparative phosphorylation of key tyrosines relative to the wild-type kinase core. To understand the long-range allosteric impact of enhanced SH3:linker interaction in the context of mutations that activate the kinase, I combined HAL9 and the activating mutations A356N, G2A , T315I, Y158D and determined the extent of reversal of activation. The A356N and G2A mutations are functionally similar in that they exclude the NCap from the myristic acid binding

pocket by inhibiting binding (A356N) or by inhibiting myristoylation of the Ncap (G2A). Enhancement of SH3:linker interaction, completely reversed the activating effects of A356N mutation while partially reversing activating effects of non-myristoylated G2A mutation. These observations suggest that these two proteins have distinct active conformations. In the case of G2A, previous small-angle X-ray scattering and HX MS studies support a "top hat" conformation for the non-myristoylated ABL core protein in which the SH2 domain is reoriented to interact with the N-lobe of the kinase (Nagar et al., 2006; Filippakopoulos et al., 2008; Iacob et al., 2009). Though in the SAXS study the locations of the SH3 and the linker domains were not determined, in such a highly reoriented conformation HAL9 might not compensate for the activating effects of G2A. However, our HX MS results in this study indicate that A356N mutation does not lead to the "top hat" conformation because there were no changes in deuterium incorporation in ABL-A356N at the SH2:C-lobe interface, the NCap or the linker regions. The dynamic and conformational changes of ABL-A356N are represented by increases in deuterium incorporation at the site of A356N mutation and in a peptide encompassing the gatekeeper residue in the N-lobe. Interestingly, these changes are completely reversed by HAL9 substitution. Thus, the extent to which HAL9 compensates for the activating effects of mutations is dependent on differences in active conformations of the ABL core protein.

In the context of the ABL gatekeeper mutation (T315I), we have previously shown that this mutation induces local conformational changes at the site of the mutation and in the SH3 domain in the myristoylated core of the protein (Iacob et al., 2009). Also, T315I is shown to uncouple the active site from allosteric regulation by the myristic acid binding site inhibitors. Interestingly, in this study I show that HAL9 partially reverses the activating effects of T315I. Furthermore, HAL9 also reverses the activating effects of Y158D mutation that occurs at the

SH2:kinase interface. This suggests that SH3:linker interaction can allosterically regulate SH2 and C-lobe kinase domains.

To understand the allosteric regulation by HAL9 in the context of full length BCR-ABL, I introduced wild-type and HAL9-BCR-ABL in TF-1 cells. HAL9 sensitized the cells to the effects of imatinib, suggesting that HAL9 induced restructuring of the BCR-ABL kinase to the downregulated conformation that favors drug binding. However, HAL9 did not sensitize TF-1 cells expressing BCR-ABL T315I to the effects of imatinib. This does not necessarily suggest that HAL9 does not induce downregulated conformation of BCR-ABLT315I. However, this may suggest that even in the downregulated conformation of the protein the hydrogen bonding between the threonine hydroxyl group and imatinib is absolutely necessary for the binding stability of imatinib and its effects. This observation could be clarified in the future with ponatinib. Ponatinib binds to the ATP binding site and prefers the “DFG-out” conformation, it does not require the hydroxyl side chain of threonine for stable binding and it can accommodate the isoleucine side chain of T315I mutant. Hence, it is predicted that HAL9 would induce the downregulated conformation of the ABL core in BCR-ABL-T315I and would enhance the sensitivity to the effects of ponatinib. Interestingly, enhanced SH3:linker interaction dramatically sensitized wild-type and T315I BCR-ABL expressing TF-1 cells to the effects of the allosteric inhibitors GNF-2 and GNF-5. These results support an allosteric connection between the SH3 domain, the active site, and the myristic acid binding pocket.

The results presented in chapter 2 are significant also because they shed light on the role of the intermolecular interactions in the ABL core region within the context of constitutively active BCR-ABL kinase. Unlike in c-ABL core protein, the role of intermolecular interactions in BCR-ABL is less clear and controversial. BCR fusion is sufficient to activate ABL however it

does not necessarily displace SH3 and SH2 domains from their regulatory positions. In support of this hypothesis, it is well established that imatinib prefers the inactive conformation of the kinase domain, and that mutations arising in SH3 and SH2 domains are associated with imatinib resistance (Schindler et al., 2000; Sherbenou et al., 2010). These observations support the hypothesis that the SH3 and SH2 domains maintain contact with the kinase domain in BCR-ABL. In addition, Smith et al showed that BCR coiled-coil domain mutations that disrupt BCR-ABL oligomerization impair its kinase activity. However disruption of SH3:linker interaction restores the kinase activity (Smith et al., 2003). This suggests that SH3 maintains negative regulatory interaction in BCR-ABL. We have also established that HCK mediated phosphorylation of Y89 in the SH3 domain in CML cells correlates with imatinib resistance, providing further evidence that SH3:linker interaction maintains its negative regulatory effect in BCR-ABL (Pene-Dumitrescu and Smithgall, 2010). The data in the current study clearly show that enhancing the SH3:linker interaction (HAL9) in the context of BCR-ABL does not impact its kinase or transforming activity yet enhances drug sensitivity to compounds that prefer the inactive conformation of the kinase domain.

On the other hand, a recent structural study showed that the SH2 domain of the c-ABL core undergoes major conformational rearrangement and moves from a negative regulatory position to a new position that promotes SH2 interaction with the N-lobe of the kinase (Nagar et al., 2006). In this “top hat” conformation, the kinase is stabilized in its active state. This highly mutated and active ABL protein structure was deduced mostly from small X-ray scattering, and though the position of the SH3 domain was not identified, the data suggest that it is also displaced. Hence, this study disputes that SH3 and SH2 domains maintain their interaction at the back of the active kinase domain. More recently, Grebien et al showed that this “top hat”

conformation is critical for maintaining a fully active kinase domain (Grebien et al., 2011). They also showed that disruption of the "top hat" conformation by mutations at the SH2:N-lobe interface enhances sensitivity to nilotinib which favors the inactive conformation of the kinase. However, in the study by Grebien et al, disrupting the SH2:N-lobe interaction, either by mutation or by monobody targeting, reduced kinase activity only partially. In light of these observations, the data in Chapter 2 dispute the absolute requirement for "top hat" conformation in BCR-ABL in order to be "kinase active" and support the concept that BCR-ABL samples multiple active states that may be independent from each other.

In summary, results presented in Chapter 2, showed for the first time that SH3:linker interaction is a crucial allosteric regulatory interface controlling the overall dynamics and regulation of c-ABL core protein as well as BCR-ABL. Combining biophysical, biochemical and biological methodologies and techniques, this study showed that there is allosteric interplay between SH3:linker interface, the myristic acid binding pocket and the active site as well as an interplay between the SH3:linker interface, the SH2:kinase interface and the active site. This work strongly supports that a unique regulatory interaction (SH3:linker) at a distance from the active site represents a target for stabilization by small molecules that could then favor a downregulated conformation and sensitization to conformationally-selective inhibitors such as imatinib and nilotinib.

4.1.2 BCR-ABL T315I and resistance to Src-selective inhibitor

In the second aim of my thesis work, I set out to understand the effects of global inhibition of SFK activity with the ATP-competitive pyrrolo-pyrimidine inhibitor-A-419259 in cells transformed with clinically relevant BCR-ABL mutations. The mutations at residues Y253,

E255and T315 are very common and account for about 60-70% of the kinase domain mutations in clinically observed imatinib-resistant CML cases (Quintas-Cardama et al., 2009). I observed that proliferation of TF-1 cells expressing wild-type and two of the mutant BCR-ABLs (E255V, Y253H) is markedly inhibited by A-419259. These results are in agreement with previous work from our group that showed inhibition of SFK activity with A-419259 leads to growth arrest and apoptosis in primary CML cells and CML cell lines (Pene-Dumitrescu et al., 2008; Wilson et al., 2002). Surprisingly, neither proliferation nor SFK activity is inhibited by this compound in TF-1 cells expressing BCR-ABL T315I mutant. These observations suggest a cross-resistance mechanism acquired by BCR-ABL T315I to phosphorylate SFKs and induce drug resistance. This unexpected finding has important implications in the use of SFK inhibitors or dual ABL/SRC kinase inhibitors as therapeutics in CML. The data in Chapter 3 indicate that the use of dual inhibitors that do not overcome T315I activity may not be therapeutically beneficial.

In support of the cross-resistance mechanism, I show that endogenous LYN and exogenously expressed HCK remain phosphorylated in the presence of the inhibitor in cells expressing BCR-ABL T315I but not the wild-type oncoprotein. Furthermore, I show that kinase dead HCK is strongly phosphorylated by ABL T315I. These observations support a role of ABL T315I in phosphorylating SFK members in the presence of Src-selective inhibitors and further investigations are necessary to determine whether this cross-resistance mechanism is due to differences in the extent of phosphorylation, differential phosphorylation at drug binding sites, and/or differential phosphorylation at allosteric sites.

4.2 FUTURE DIRECTIONS

4.2.1 Identify chemical sensitizers of ABL SH3:linker interaction

The current frontline therapy for CML is imatinib. When imatinib resistance emerges, patients are treated with second generation tyrosine kinase inhibitors dasatinib or nilotinib. This strategy of sequential therapy can potentially select for cells harboring kinase domain mutations in the same allele leading to compound mutations. Compound mutations may be less sensitive to third generation drugs and may have different oncogenic potency. To prevent occurrence of compound mutations, combination therapy of the aforementioned compounds or a combination of ATP-competitive inhibitors with allosteric inhibitors may be initiated at diagnosis. In both cases, and upon availability of these drugs, it is necessary to address the tolerability of combination of tyrosine kinase inhibitors. Hence, it is crucial to have available allosteric inhibitors that could be used in combination with currently available drugs to enhance sensitivity and to reduce emergence of resistance. Thus, as a next logical step following the confirmation that SH3:linker interface is a key node controlling overall regulation of ABL and BCR-ABL kinases, I propose identifying small molecules that reproduce the HAL9 effect. This would require a development of an approach amenable to high throughput screening of small molecules that would influence the SH3:linker interaction as a new approach to inhibit BCR-ABL activity. Previous dynamics studies of the ABL SH3-SH2-linker region showed that the ABL SH3 domain exhibits a cooperative unfolding-refolding behavior and that this behavior can be quenched when bound to the linker or high affinity peptides. This same behavior was observed in the presence of the kinase domain in the core of ABL protein. Based on my observations with the ABL-HAL system, our group is currently pursuing a fluorescence polarization (FP) assay using

ABL SH3-SH2-linker recombinant protein and a fluorescently tagged high affinity peptide ligand for the ABL SH3 domain. In the presence of the fluorescently tagged high affinity peptide, SH3:peptide interaction will stabilize the fluorescence and result in an FP signal. Thus small molecules capable of enhancing SH3:linker interaction would prevent the interaction of fluorescently tagged peptide with the SH3 domain and result in diminished FP signal. Following identification of hits with ABL-SH3-SH2-linker protein in FP assay, I propose to test the compounds for their ability to sensitize the transiently expressed c-ABL protein in 293T cells to inhibition by drugs that prefer the "DFG-out" conformation such as imatinib as well as by allosteric inhibitors such as GNF-2/5. Furthermore, to test the effects of the compound in the context of BCR-ABL, I propose to study their impact in TF-1 cells expressing wild-type BCR-ABL as well as clinically relevant mutations. I also propose to investigate the frequency with which TF-1 cells expressing wild-type BCR-ABL would become resistant to lead compound alone or in combination with ATP-competitive inhibitors such as imatinib. This would be an important parameter in considering combination therapy. I also propose to study the mechanism of action of the lead compounds that show activity both in vitro and in cell-based assays. One way to define the mechanism of SH3:linker enhancement is by determining the X-ray crystal structure of NCap-ABL-HAL9 and compare to the structure of wild-type NCap-ABL. I predict two possible outcomes: first, the enhanced interaction by HAL9 compared to the wild-type may simply result in enhanced packing of SH3 in the back of the kinase. Second, HAL9 may induce an alternative downregulatory conformation involving other regions of the protein besides the SH3:linker interface. These studies would help in the understanding of structural differences induced by HAL9 modification. One could also crystalize the wild-type protein with the lead compound and compare the structural differences with that of the HAL9 structure. Alternatively,

instead of investigating differences in a static structural view, I propose studying the impact of the lead compound on ABL dynamics using HX MS. Using this methodology, one could determine global changes in ABL dynamics as well as regional changes in the presence and absence of the compound. I predict that a lead compound that enhances SH3:linker interaction, would lengthen SH3 unfolding half-life compared to the protein in the absence of the compound. The compound might also reduce deuterium incorporation at the SH2:C-lobe interface and/or the N-lobe as shown for the HAL9 core protein.

4.2.2 Determine the mechanism of acquired Src-kinase resistance to A-419259 in the presence of ABL-T315I

The data presented in chapter 3 of this work supports the use of SFK inhibitors in CML to overcome BCR-ABL kinase domain mutations other than T315I. I show that ABL-T315I acquires the ability to phosphorylate SFKs and induce drug-resistance. To further investigate the suggested mechanism of resistance, I propose to determine whether ABL T315I phosphorylates HCK or LYN on sites that are not phosphorylated by wild-type ABL or other imatinib-resistant mutants. The prediction is that these sites would either be in direct contact with the drug binding site or would allosterically modify the drug binding site. I also propose to investigate whether the extent of phosphorylation by wild-type or T315I is different or if both mechanisms (extent of phosphorylation and phosphorylation at different sites) contribute to the acquired resistance. To test these possibilities, one could purify HCK and LYN recombinant proteins and analyze their intact mass in the presence and absence of recombinant wild-type ABL protein and imatinib resistant mutants (T315I, E255Vand Y253H). If the cross-resistance mechanism is due to differences in the extent of phosphorylation, then it is predicted that T315I would phosphorylate

the SFKs more extensively. To determine if the cross-resistance is due to differential phosphorylation of SFKs by ABL wild-type versus ABL T315I, it is possible to identify the phosphopeptides by mass spectrometry and investigate if the phosphorylated tyrosines map onto the drug binding or allosteric site. Following identification of residues involved in differential phosphorylation, I propose to substitute these residues with phenylalanine and determine re-sensitization to the effects of A-419259 in vitro and in cell-based assays.

Alternatively, the observed mechanism of resistance can be due to cellular mechanisms of drug efflux. Expression of P-glycoprotein (Pgp), the ATP-dependent xenobiotic transport protein associated with the multi-drug resistant phenotype in many types of tumors, has been implicated in the BCR-ABL independent resistance to imatinib (Illmer et al., 2004). This observation suggests that the T315I mutation may enhance the ability of BCR-ABL to induce Pgp expression as a possible mechanism conferring cross-resistance to A-419259. To rule out the involvement of Pgp in the cross-resistance of TF-1 BCR-ABL T315I cells to A-419259, I would propose to test the effects of the Pgp blocker verapamil on the sensitivity of TF-1 BCR-ABL T315I cells to A-419259 in proliferation assay. The prediction is that, if Pgp is not involved in this cross-resistance mechanism, its inhibition would not reverse A-419259 resistance in cells expressing BCR-ABL T315I.

4.3 CLOSING REMARKS

The discovery of imatinib and its significant activity in all phases of CML represent a true milestone in the cancer therapeutics field. However, despite the impressive success of imatinib, clinical relapse due to drug resistance is inevitable. Therefore, new therapies targeting imatinib-resistant mutants particularly the T315I are needed. The major challenge in developing new kinase inhibitors is to achieve highly selective, efficacious inhibitors with minimal potential for development of drug resistance. In this context, discovery and design of allosteric inhibitors have been gaining much attention. Allosteric inhibitors bind outside the ATP-binding site of a certain kinase, exploit a unique regulatory mechanism of the kinase and modulate its activity (Zhang et al., 2009). However, to date there are only handful of well characterized allosteric inhibitors such as the MEK1 and MEK2 inhibitor CI-1040 (Ohren et al., 2004), the inhibitor of nuclear factor-kB kinase inhibitor BMS-345541(McIntyre et al., 2003) and BCR-ABL inhibitor GNF-2 (Adrian et al., 2006). Furthermore, identification of allosteric sites in kinases that could be targeted remains as much challenging as designing allosteric inhibitors. In this context, the work presented in this dissertation identifies SH3:linker interaction as an unique allosteric site that induces long range conformational changes in the kinase domain and enhances potency of drugs that target the ATP binding site and/or myristic acid binding pocket. This remarkable allosteric network linking the SH3 domain, the myristic binding pocket and the active site of the c-ABL core was revealed by dynamic studies using HX MS. As such, this work underscores the importance of this technique in providing structural basis for biological observations. The data presented in this work also revealed a novel finding about the status of the negative regulatory

domains in active BCR-ABL kinase. While the dogmatic view supports the displacement of these domains from their negative regulatory positions in the active kinase, this work challenges that view and clearly shows that enhancing SH3:linker interaction in the context of constitutively active BCR-ABL, does not impair the kinase activity yet confers enhanced drug sensitivity. In addition, this work also revealed a new mechanism of BCR-ABL T315I-induced resistance to drugs that target SFKs. This finding suggests that the use of dual ABL/SRC kinase inhibitors that do not overcome T315I activity may not be therapeutically beneficial. Therefore, this study supports future drug discovery campaigns to identify allosteric inhibitors that stabilize SH3:linker interaction as a new strategy to inhibit wild-type and drug resistant mutants.

BIBLIOGRAPHY

Adrian,F.J., Ding,Q., Sim,T., Velentza,A., Sloan,C., Liu,Y., Zhang,G., Hur,W., Ding,S., Manley,P., Mestan,J., Fabbro,D., and Gray,N.S. (2006). Allosteric inhibitors of Bcr-abl-dependent cell proliferation. Nat. Chem. Biol. *2*, 95-102.

Advani,A.S. and Pendergast,A.M. (2002). Bcr-Abl variants: biological and clinical aspects. Leuk. Res. *26*, 713-720.

Agrawal,M., Garg,R.J., Kantarjian,H., and Cortes,J. (2010). Chronic myeloid leukemia in the tyrosine kinase inhibitor era: what is the "best" therapy? Curr. Oncol. Rep. *12*, 302-313.

American Cancer Society. American Cancer Society. Cancer Facts and Figures 2012. 1-1-2012. Ref Type: Report

Azam,M., Latek,R.R., and Daley,G.Q. (2003). Mechanisms of autoinhibition and STI-571/imatinib resistance revealed by mutagenesis of BCR-ABL. Cell *112*, 831-843.

Azam,M., Seeliger,M.A., Gray,N.S., Kuriyan,J., and Daley,G.Q. (2008). Activation of tyrosine kinases by mutation of the gatekeeper threonine. Nat. Struct. Mol. Biol. *15*, 1109-1118.

Ban,K., Gao,Y., Amin,H.M., Howard,A., Miller,C., Lin,Q., Leng,X., Munsell,M., Bar-Eli,M., Arlinghaus,R.B., and Chandra,J. (2008). BCR-ABL1 mediates up-regulation of Fyn in chronic myelogenous leukemia. Blood *111*, 2904-2908.

Barila,D. and Superti-Furga,G. (1998). An intramolecular SH3-domain interaction regulates c-Abl activity. Nat. Genet. *18*, 280-282.

Barnes,D.J., Palaiologou,D., Panousopoulou,E., Schultheis,B., Yong,A.S., Wong,A., Pattacini,L., Goldman,J.M., and Melo,J.V. (2005). Bcr-Abl expression levels determine the rate of development of resistance to imatinib mesylate in chronic myeloid leukemia. Cancer Res. *65*, 8912-8919.

Baskaran,R., Chiang,G.G., and Wang,J.Y. (1996). Identification of a binding site in c-Ab1 tyrosine kinase for the C-terminal repeated domain of RNA polymerase II. Mol. Cell Biol. *16*, 3361-3369.

Beissert,T., Hundertmark,A., Kaburova,V., Travaglini,L., Mian,A.A., Nervi,C., and Ruthardt,M. (2008). Targeting of the N-terminal coiled coil oligomerization interface by a helix-2 peptide inhibits unmutated and imatinib-resistant BCR/ABL. Int. J. Cancer *122*, 2744-2752.

Boveri,T. (2008). Concerning the origin of malignant tumours by Theodor Boveri. Translated and annotated by Henry Harris. J. Cell Sci. *121 Suppl 1*, 1-84.

Brasher,B.B., Roumiantsev,S., and Van Etten,R.A. (2001). Mutational analysis of the regulatory function of the c-Abl Src homology 3 domain. Oncogene *20*, 7744-7752.

Brasher,B.B. and Van Etten,R.A. (2000). c-Abl has high intrinsic tyrosine kinase activity that is stimulated by mutation of the Src homology 3 domain and by autophosphorylation at two distinct regulatory tyrosines. J. Biol. Chem. *275*, 35631-35637.

Briggs,S.D. and Smithgall,T.E. (1999). SH2-kinase linker mutations release Hck tyrosine kinase and transforming activities in rat-2 fibroblasts. J. Biol. Chem. *274*, 26579-26583.

Bruecher-Encke,B., Griffin,J.D., Neel,B.G., and Lorenz,U. (2001). Role of the tyrosine phosphatase SHP-1 in K562 cell differentiation. Leukemia *15*, 1424-1432.

Buchdunger,E., Zimmermann,J., Mett,H., Meyer,T., Muller,M., Druker,B.J., and Lydon,N.B. (1996). Inhibition of the Abl protein-tyrosine kinase in vitro and in vivo by a 2-phenylaminopyrimidine derivative. Cancer Res. *56*, 100-104.

Buchdunger,E., Zimmermann,J., Mett,H., Meyer,T., Muller,M., Regenass,U., and Lydon,N.B. (1995). Selective inhibition of the platelet-derived growth factor signal transduction pathway by a protein-tyrosine kinase inhibitor of the 2-phenylaminopyrimidine class. Proc. Natl. Acad. Sci. U. S. A *92*, 2558-2562.

Burkitt,W. and O'Connor,G. (2008). Assessment of the repeatability and reproducibility of hydrogen/deuterium exchange mass spectrometry measurements. Rapid Commun. Mass Spectrom. *22*, 3893-3901.

Cao,X., Tanis,K.Q., Koleske,A.J., and Colicelli,J. (2008). Enhancement of ABL kinase catalytic efficiency by a direct binding regulator is independent of other regulatory mechanisms. J. Biol. Chem. *283*, 31401-31407.

Carlesso,N., Frank,D.A., and Griffin,J.D. (1996). Tyrosyl phosphorylation and DNA binding activity of signal transducers and activators of transcription (STAT) proteins in hematopoietic cell lines transformed by Bcr/Abl. J. Exp. Med. *183*, 811-820.

Chen,S., Brier,S., Smithgall,T.E., and Engen,J.R. (2007). The Abl SH2-kinase linker naturally adopts a conformation competent for SH3 domain binding. Protein Sci. *16*, 572-581.

Chen,S., Dumitrescu,T.P., Smithgall,T.E., and Engen,J.R. (2008a). Abl N-terminal cap stabilization of SH3 domain dynamics. Biochemistry *47*, 5795-5803.

Chen,S., O'Reilly,L.P., Smithgall,T.E., and Engen,J.R. (2008b). Tyrosine phosphorylation in the SH3 domain disrupts negative regulatory interactions within the c-Abl kinase core. J. Mol. Biol. *383*, 414-423.

Choi,H.G., Zhang,J., Weisberg,E., Griffin,J.D., Sim,T., and Gray,N.S. (2012). Development of 'DFG-out' inhibitors of gatekeeper mutant kinases. Bioorg. Med. Chem. Lett. *22*, 5297-5302.

Colicelli,J. (2010). ABL tyrosine kinases: evolution of function, regulation, and specificity. Sci. Signal. *3*, re6.

Coluccia,A.M., Vacca,A., Dunach,M., Mologni,L., Redaelli,S., Bustos,V.H., Benati,D., Pinna,L.A., and Gambacorti-Passerini,C. (2007). Bcr-Abl stabilizes beta-catenin in chronic myeloid leukemia through its tyrosine phosphorylation. EMBO J. *26*, 1456-1466.

Cong,F., Spencer,S., Cote,J.F., Wu,Y., Tremblay,M.L., Lasky,L.A., and Goff,S.P. (2000). Cytoskeletal protein PSTPIP1 directs the PEST-type protein tyrosine phosphatase to the c-Abl kinase to mediate Abl dephosphorylation. Mol. Cell *6*, 1413-1423.

Copland,M., Hamilton,A., Elrick,L.J., Baird,J.W., Allan,E.K., Jordanides,N., Barow,M., Mountford,J.C., and Holyoake,T.L. (2006). Dasatinib (BMS-354825) targets an earlier progenitor population than imatinib in primary CML but does not eliminate the quiescent fraction. Blood *107*, 4532-4539.

Cortes,J.E., Kim,D.W., Kantarjian,H.M., Brummendorf,T.H., Dyagil,I., Griskevicus,L., Malhotra,H., Powell,C., Gogat,K., Countouriotis,A.M., and Gambacorti-Passerini,C. (2012). Bosutinib Versus Imatinib in Newly Diagnosed Chronic-Phase Chronic Myeloid Leukemia: Results From the BELA Trial. J. Clin. Oncol.

Cortez,D., Kadlec,L., and Pendergast,A.M. (1995). Structural and signaling requirements for BCR-ABL-mediated transformation and inhibition of apoptosis. Mol. Cell. Biol. *15*, 5531-5541.

Cortez,D., Stoica,G., Pierce,J.H., and Pendergast,A.M. (1996). The BCR-ABL tyrosine kinase inhibits apoptosis by activating a Ras-dependent signaling pathway. Oncogene *13*, 2589-2594.

Cox,S., Radzio-Andzelm,E., and Taylor,S.S. (1994). Domain movements in protein kinases. Curr. Opin. Struct. Biol. *4*, 893-901.

Crossman,L.C., Druker,B.J., Deininger,M.W., Pirmohamed,M., Wang,L., and Clark,R.E. (2005). hOCT 1 and resistance to imatinib. Blood *106*, 1133-1134.

Dai,H., Marbach,P., Lemaire,M., Hayes,M., and Elmquist,W.F. (2003). Distribution of STI-571 to the brain is limited by P-glycoprotein-mediated efflux. J. Pharmacol. Exp. Ther. *304*, 1085-1092.

Dai,Z. and Pendergast,A.M. (1995). Abi-2, a novel SH3-containing protein interacts with the c-Abl tyrosine kinase and modulates c-Abl transforming activity. Genes and Development *9*, 2569-2582.

Daley,G.Q., Van Etten,R.A., and Baltimore,D. (1990). Induction of chronic myelogenous leukemia in mice by the $p210^{bcr\text{-}abl}$ gene of the Philadelphia chromosome. Science *247*, 824-830.

Danhauser-Riedl,S., Warmuth,M., Druker,B.J., Emmerich,B., and Hallek,M. (1996). Activation of Src kinases $p53/56^{lyn}$ and $p59^{hck}$ by $p210^{bcr/abl}$ in myeloid cells. Cancer Res. *56*, 3589-3596.

de Groot,R.P., Raaijmakers,J.A., Lammers,J.W., and Koenderman,L. (2000). STAT5-Dependent CyclinD1 and Bcl-xL expression in Bcr-Abl-transformed cells. Mol. Cell Biol. Res. Commun. *3*, 299-305.

de,J.R., Haataja,L., Voncken,J.W., Heisterkamp,N., and Groffen,J. (1995). Tyrosine phosphorylation of murine Crkl. Oncogene *11*, 1469-1474.

Deininger,M.W., Goldman,J.M., and Melo,J.V. (2000). The molecular biology of chronic myeloid leukemia. Blood *96*, 3343-3356.

Delbaldo,C., Chatelut,E., Re,M., Deroussent,A., Seronie-Vivien,S., Jambu,A., Berthaud,P., Le,C.A., Blay,J.Y., and Vassal,G. (2006). Pharmacokinetic-pharmacodynamic relationships of imatinib and its main metabolite in patients with advanced gastrointestinal stromal tumors. Clin. Cancer Res. *12*, 6073-6078.

Diehl,J.A., Cheng,M., Roussel,M.F., and Sherr,C.J. (1998). Glycogen synthase kinase-3beta regulates cyclin D1 proteolysis and subcellular localization. Genes Dev. *12*, 3499-3511.

Dorey,K., Engen,J.R., Kretzschmar,J., Wilm,M., Neubauer,G., Schindler,T., and Superti-Furga,G. (2001). Phosphorylation and structure-based functional studies reveal a positive and a negative role for the activation loop of the c-Abl tyrosine kinase. Oncogene *20*, 8075-8084.

Druker,B.J. (2004). Imatinib as a paradigm of targeted therapies. Adv. Cancer Res. *91*, 1-30.

Druker,B.J., Tamura,S., Buchdunger,E., Ohno,S., Segal,G.M., Fanning,S., Zimmermann,J., and Lydon,N.B. (1996). Effects of a selective inhibitor of the Abl tyrosine kinase on the growth of Bcr-Abl positive cells. Nat. Med. *2*, 561-566.

Engen,J.R. (2009). Analysis of protein conformation and dynamics by hydrogen/deuterium exchange MS. Anal. Chem. *81*, 7870-7875.

Englander,S.W. and Kallenbach,N.R. (1983). Hydrogen exchange and structural dynamics of proteins and nucleic acids. Q. Rev. Biophys. *16*, 521-655.

Ernst,T., Erben,P., Muller,M.C., Paschka,P., Schenk,T., Hoffmann,J., Kreil,S., La,R.P., Hehlmann,R., and Hochhaus,A. (2008). Dynamics of BCR-ABL mutated clones prior to hematologic or cytogenetic resistance to imatinib. Haematologica *93*, 186-192.

Fava,C., Rege-Cambrin,G., and Saglio,G. (2012). Chronic Myeloid Leukemia: State of the Art in 2012. Curr. Oncol. Rep.

Feller,S.M., Knudsen,B., and Hanafusa,H. (1994). c-Abl kinase regulates the protein binding activity of c-Crk. EMBO J. *13*, 2341-2351.

Feller,S.M., Posern,G., Voss,J., Kardinal,C., Sakkab,D., Zheng,J., and Knudsen,B.S. (1998). Physiological signals and oncogenesis mediated through Crk family adapter proteins. J. Cell Physiol *177*, 535-552.

Ferrao,P.T., Frost,M.J., Siah,S.P., and Ashman,L.K. (2003). Overexpression of P-glycoprotein in K562 cells does not confer resistance to the growth inhibitory effects of imatinib (STI571) in vitro. Blood *102*, 4499-4503.

Filippakopoulos,P., Kofler,M., Hantschel,O., Gish,G.D., Grebien,F., Salah,E., Neudecker,P., Kay,L.E., Turk,B.E., Superti-Furga,G., Pawson,T., and Knapp,S. (2008). Structural coupling of SH2-kinase domains links Fes and Abl substrate recognition and kinase activation. Cell *134*, 793-803.

Frank,D.A. and Varticovski,L. (1996). BCR/abl leads to the constitutive activation of Stat proteins, and shares an epitope with tyrosine phosphorylated Stats. Leukemia *10*, 1724-1730.

Franz,W.M., Berger,P., and Wang,J.Y.J. (1989). Deletion of an N-terminal regulatory domain of the c-abl tyrosine kinase activates its oncogenic potential. EMBO J. *8*, 137-147.

Gambacorti-Passerini,C., le,C.P., Zucchetti,M., and D'Incalci,M. (2002). Binding of imatinib by alpha(1)-acid glycoprotein. Blood *100*, 367-368.

Gao,Y., Howard,A., Ban,K., and Chandra,J. (2009). Oxidative stress promotes transcriptional up-regulation of Fyn in BCR-ABL1-expressing cells. J. Biol. Chem. *284*, 7114-7125.

Gesbert,F. and Griffin,J.D. (2000). Bcr/Abl activates transcription of the Bcl-X gene through STAT5. Blood *96*, 2269-2276.

Gioia,R., Leroy,C., Drullion,C., Lagarde,V., Etienne,G., Dulucq,S., Lippert,E., Roche,S., Mahon,F.X., and Pasquet,J.M. (2011). Quantitative phosphoproteomics revealed interplay between Syk and Lyn in the resistance to nilotinib in chronic myeloid leukemia cells. Blood *118*, 2211-2221.

Goga,A., Liu,X., Hambuch,T.M., Senechal,K., Major,E., Berk,A.J., Witte,O.N., and Sawyers,C.L. (1995a). p53 dependent growth suppression by the c-Abl nuclear tyrosine kinase. Oncogene *11*, 791-799.

Goga,A., McLaughlin,J., Afar,D.E.H., Saffran,D.C., and Witte,O.N. (1995b). Alternative signals to RAS for hematopoietic transformation by the BCR-ABL oncogene. Cell *82*, 981-988.

Gorre,M.E., Mohammed,M., Ellwood,K., Hsu,N., Paquette,R., Rao,P.N., and Sawyers,C.L. (2001). Clinical resistance to STI-571 cancer therapy caused by BCR-ABL gene mutation or amplification. Science *293*, 876-880.

Graham,S.M., Jorgensen,H.G., Allan,E., Pearson,C., Alcorn,M.J., Richmond,L., and Holyoake,T.L. (2002). Primitive, quiescent, Philadelphia-positive stem cells from patients with chronic myeloid leukemia are insensitive to STI571 in vitro. Blood *99*, 319-325.

Grebien,F., Hantschel,O., Wojcik,J., Kaupe,I., Kovacic,B., Wyrzucki,A.M., Gish,G.D., Cerny-Reiterer,S., Koide,A., Beug,H., Pawson,T., Valent,P., Koide,S., and Superti-Furga,G. (2011). Targeting the SH2-kinase interface in Bcr-Abl inhibits leukemogenesis. Cell *147*, 306-319.

Griswold,I.J., MacPartlin,M., Bumm,T., Goss,V.L., O'Hare,T., Lee,K.A., Corbin,A.S., Stoffregen,E.P., Smith,C., Johnson,K., Moseson,E.M., Wood,L.J., Polakiewicz,R.D., Druker,B.J., and Deininger,M.W. (2006). Kinase domain mutants of Bcr-Abl exhibit altered

transformation potency, kinase activity, and substrate utilization, irrespective of sensitivity to imatinib. Mol. Cell Biol. *26*, 6082-6093.

Groffen,J., Stephenson,J.R., Heisterkamp,N., de Klein,A., Bartram,C.R., and Grosfeld,G. (1984). Philadelphia chromosomal breakpoints are clustered within a limited region, *bcr*, on chromosome 22. Cell *36*, 93-99.

Grosso,S., Puissant,A., Dufies,M., Colosetti,P., Jacquel,A., Lebrigand,K., Barbry,P., Deckert,M., Cassuto,J.P., Mari,B., and Auberger,P. (2009). Gene expression profiling of imatinib and PD166326-resistant CML cell lines identifies Fyn as a gene associated with resistance to BCR-ABL inhibitors. Mol. Cancer Ther. *8*, 1924-1933.

Hanks,S.K. (2003). Genomic analysis of the eukaryotic protein kinase superfamily: a perspective. Genome Biol. *4*, 111.

Hanks,S.K., Quinn,A.M., and Hunter,T. (1988). The protein kinase family: Conserved features and deduced phylogeny of the catalytic domain. Science *241*, 42-52.

Hantschel,O., Nagar,B., Guettler,S., Kretzschmar,J., Dorey,K., Kuriyan,J., and Superti-Furga,G. (2003). A myristoyl/phosphotyrosine switch regulates c-Abl. Cell *112*, 845-857.

Hantschel,O. and Superti-Furga,G. (2004). Regulation of the c-Abl and Bcr-Abl tyrosine kinases. Nat. Rev. Mol. Cell Biol. *5*, 33-44.

Hantschel,O., Warsch,W., Eckelhart,E., Kaupe,I., Grebien,F., Wagner,K.U., Superti-Furga,G., and Sexl,V. (2012). BCR-ABL uncouples canonical JAK2-STAT5 signaling in chronic myeloid leukemia. Nat. Chem. Biol. *8*, 285-293.

Harper,P.S. (2006). The discovery of the human chromosome number in Lund, 1955-1956. Hum. Genet. *119*, 226-232.

Hehlmann,R., Berger,U., and Hochhaus,A. (2005). Chronic myeloid leukemia: a model for oncology. Ann. Hematol. *84*, 487-497.

Hehlmann,R., Hochhaus,A., and Baccarani,M. (2007). Chronic myeloid leukaemia. Lancet *370*, 342-350.

Heisterkamp,N. and Groffen,J. (2002). Philadelphia-positive leukemia: a personal perspective. Oncogene *21*, 8536-8540.

Hochhaus,A., Kreil,S., Corbin,A.S., La,R.P., Muller,M.C., Lahaye,T., Hanfstein,B., Schoch,C., Cross,N.C., Berger,U., Gschaidmeier,H., Druker,B.J., and Hehlmann,R. (2002). Molecular and chromosomal mechanisms of resistance to imatinib (STI571) therapy. Leukemia *16*, 2190-2196.

Hochrein,J.M., Lerner,E.C., Schiavone,A.P., Smithgall,T.E., and Engen,J.R. (2006). An examination of dynamics crosstalk between SH2 and SH3 domains by hydrogen/deuterium exchange and mass spectrometry. Protein Sci. *15*, 65-73.

Holtz,M.S., Forman,S.J., and Bhatia,R. (2005). Nonproliferating CML CD34+ progenitors are resistant to apoptosis induced by a wide range of proapoptotic stimuli. Leukemia *19*, 1034-1041.

Holtz,M.S., Slovak,M.L., Zhang,F., Sawyers,C.L., Forman,S.J., and Bhatia,R. (2002). Imatinib mesylate (STI571) inhibits growth of primitive malignant progenitors in chronic myelogenous leukemia through reversal of abnormally increased proliferation. Blood *99*, 3792-3800.

Hubbard,S.R., Wei,L., Ellis,L., and Hendrickson,W.A. (1994). Crystal structure of the tyrosine kinase domain of the human insulin receptor. Nature *372*, 746-754.

Huse,M. and Kuriyan,J. (2002). The conformational plasticity of protein kinases. Cell *109*, 275-282.

Iacob,R.E., Pene-Dumitrescu,T., Zhang,J., Gray,N.S., Smithgall,T.E., and Engen,J.R. (2009). Conformational disturbance in Abl kinase upon mutation and deregulation. Proc. Natl. Acad. Sci. U. S. A *106*, 1386-1391.

Iacob,R.E., Zhang,J., Gray,N.S., and Engen,J.R. (2011). Allosteric interactions between the myristate- and ATP-site of the Abl kinase. PLoS. One. *6*, e15929.

Ilaria,R.L., Jr. and Van Etten,R.A. (1996). P210 and $P190^{BCR/ABL}$ induce the tyrosine phosphorylation and DNA binding activity of multiple specific STAT family members. J. Biol. Chem. *271*, 31704-31710.

Illmer,T., Schaich,M., Platzbecker,U., Freiberg-Richter,J., Oelschlagel,U., von,B.M., Pursche,S., Bergemann,T., Ehninger,G., and Schleyer,E. (2004). P-glycoprotein-mediated drug efflux is a resistance mechanism of chronic myelogenous leukemia cells to treatment with imatinib mesylate. Leukemia *18*, 401-408.

Inokuchi,K. (2006). Chronic myelogenous leukemia: from molecular biology to clinical aspects and novel targeted therapies. J. Nihon Med. Sch *73*, 178-192.

Jain,S.K., Susa,M., Keeler,M.L., Carlesso,N., Druker,B., and Varticovski,L. (1996). PI 3-kinase activation in BCR/abl-transformed hematopoietic cells does not require interaction of p85 SH2 domains with p210 BCR/abl. Blood *88*, 1542-1550.

Kantarjian,H.M., Baccarani,M., Jabbour,E., Saglio,G., and Cortes,J.E. (2011). Second-generation tyrosine kinase inhibitors: the future of frontline CML therapy. Clin. Cancer Res. *17*, 1674-1683.

Kelliher,M.A., McLaughlin,J., Witte,O.N., and Rosenberg,N. (1990). Induction of a chronic myelogenous leukemia-like syndrome in mice with v-abl and BCR/ABL. Proc. Natl. Acad. Sci. U. S. A *87*, 6649-6653.

Kharas,M.G., Deane,J.A., Wong,S., O'Bosky,K.R., Rosenberg,N., Witte,O.N., and Fruman,D.A. (2004). Phosphoinositide 3-kinase signaling is essential for ABL oncogene-mediated transformation of B-lineage cells. Blood *103*, 4268-4275.

Kharbanda,S., Bharti,A., Pei,D., Wang,J., Pandey,P., Ren,R., Weichselbaum,R., Walsh,C.T., and Kufe,D. (1996). The stress response to ionizing radiation involoves c-Abl-dependent phosphorylation of SHPTP1. Proc. Natl. Acad. Sci. U. S. A *93*, 6898-6901.

Klejman,A., Schreiner,S.J., Nieborowska-Skorska,M., Slupianek,A., Wilson,M.B., Smithgall,T.E., and Skorski,T. (2002). The Src family kinase Hck couples Bcr-Abl to Stat5 activation in myeloid cells. EMBO J. *21*, 5766-5774.

Knighton,D.R., Zheng,J.H., Ten Eyck,L.F., Xuong,N.H., Taylor,S.S., and Sowadski,J.M. (1991). Structure of a peptide inhibitor bound to the catalytic subunit of cyclic adenosine monophosphate-dependent protein kinase. Science *253*, 414-420.

Kornev,A.P., Haste,N.M., Taylor,S.S., and Eyck,L.F. (2006). Surface comparison of active and inactive protein kinases identifies a conserved activation mechanism. Proc. Natl. Acad. Sci. U. S. A *103*, 17783-17788.

Koschmieder,S., Gottgens,B., Zhang,P., Iwasaki-Arai,J., Akashi,K., Kutok,J.L., Dayaram,T., Geary,K., Green,A.R., Tenen,D.G., and Huettner,C.S. (2005). Inducible chronic phase of myeloid leukemia with expansion of hematopoietic stem cells in a transgenic model of BCR-ABL leukemogenesis. Blood *105*, 324-334.

Kuriyan,J. and Cowburn,D. (1997). Modular peptide recognition domains in eukaryotic signaling. Annu. Rev. Biophys. Biomol. Struct. *26*, 259-288.

Kurzrock,R., Gutterman,J.U., and Talpaz,M. (1988). The molecular genetics of Philadelphia chromosome-positive leukemias. N. Engl. J. Med. *319*, 990-998.

Ladbury,J.E., Lemmon,M.A., Zhou,M., Green,J., Botfield,M.C., and Schlessinger,J. (1995). Measurement of the binding of tyrosyl phosphopeptides to SH2 domains: A reappraisal. Proc. Natl. Acad. Sci. USA *92*, 3199-3203.

le,C.P., Kreuzer,K.A., Na,I.K., Lupberger,J., Holdhoff,M., Appelt,C., Schwarz,M., Muller,C., Gambacorti-Passerini,C., Platzbecker,U., Bonnet,R., Ehninger,G., and Schmidt,C.A. (2002). Determination of alpha-1 acid glycoprotein in patients with Ph+ chronic myeloid leukemia during the first 13 weeks of therapy with STI571. Blood Cells Mol. Dis. *28*, 75-85.

le,C.P., Mologni,L., Cleris,L., Marchesi,E., Buchdunger,E., Giardini,R., Formelli,F., and Gambacorti-Passerini,C. (1999). In vivo eradication of human BCR/ABL-positive leukemia cells with an ABL kinase inhibitor. J. Natl. Cancer Inst. *91*, 163-168.

Lerner,E.C., Trible,R.P., Schiavone,A.P., Hochrein,J.M., Engen,J.R., and Smithgall,T.E. (2005). Activation of the Src Family Kinase Hck without SH3-Linker Release. J. Biol. Chem. *280*, 40832-40837.

Levinson,N.M., Kuchment,O., Shen,K., Young,M.A., Koldobskiy,M., Karplus,M., Cole,P.A., and Kuriyan,J. (2006a). A Src-like inactive conformation in the abl tyrosine kinase domain. PLoS. Biol. *4*, e144.

Levinson,N.M., Kuchment,O., Shen,K., Young,M.A., Koldobskiy,M., Karplus,M., Cole,P.A., and Kuriyan,J. (2006b). A Src-like inactive conformation in the abl tyrosine kinase domain. PLoS. Biol. *4*, e144.

Li,S. (2008). Src-family kinases in the development and therapy of Philadelphia chromosome-positive chronic myeloid leukemia and acute lymphoblastic leukemia. Leuk. Lymphoma *49*, 19-26.

Li,Y., Clough,N., Sun,X., Yu,W., Abbott,B.L., Hogan,C.J., and Dai,Z. (2007). Bcr-Abl induces abnormal cytoskeleton remodeling, beta1 integrin clustering and increased cell adhesion to fibronectin through the Abl interactor 1 pathway. J. Cell Sci. *120*, 1436-1446.

Lin,J., Sun,T., Ji,L., Deng,W., Roth,J., Minna,J., and Arlinghaus,R. (2007). Oncogenic activation of c-Abl in non-small cell lung cancer cells lacking FUS1 expression: inhibition of c-Abl by the tumor suppressor gene product Fus1. Oncogene *26*, 6989-6996.

Lionberger,J.M., Wilson,M.B., and Smithgall,T.E. (2000). Transformation of Myeloid Leukemia Cells to Cytokine Independence by Bcr-Abl Is Suppressed by Kinase-defective Hck. J. Biol. Chem. *275*, 18581-18585.

Lombardo,L.J., Lee,F.Y., Chen,P., Norris,D., Barrish,J.C., Behnia,K., Castaneda,S., Cornelius,L.A., Das,J., Doweyko,A.M., Fairchild,C., Hunt,J.T., Inigo,I., Johnston,K., Kamath,A., Kan,D., Klei,H., Marathe,P., Pang,S., Peterson,R., Pitt,S., Schieven,G.L., Schmidt,R.J., Tokarski,J., Wen,M.L., Wityak,J., and Borzilleri,R.M. (2004). Discovery of N-(2-chloro-6-methyl- phenyl)-2-(6-(4-(2-hydroxyethyl)- piperazin-1-yl)-2-methylpyrimidin-4-ylamino)thiazole-5-carboxamide (BMS-354825), a dual Src/Abl kinase inhibitor with potent antitumor activity in preclinical assays. J. Med. Chem. *47*, 6658-6661.

Lugo,T.G., Pendergast,A.M., Muller,A.J., and Witte,O.N. (1990). Tyrosine kinase activity and transforming potency of *bcr-abl* oncogene products. Science *247*, 1079-1082.

Mahon,F.X., Deininger,M.W., Schultheis,B., Chabrol,J., Reiffers,J., Goldman,J.M., and Melo,J.V. (2000). Selection and characterization of BCR-ABL positive cell lines with differential sensitivity to the tyrosine kinase inhibitor STI571: diverse mechanisms of resistance. Blood *96*, 1070-1079.

Marcsisin,S.R. and Engen,J.R. (2010). Hydrogen exchange mass spectrometry: what is it and what can it tell us? Anal. Bioanal. Chem. *397*, 967-972.

Martinelli,G., Soverini,S., Rosti,G., and Baccarani,M. (2005). Dual tyrosine kinase inhibitors in chronic myeloid leukemia. Leukemia *19*, 1872-1879.

Mayer,B.J. and Baltimore,D. (1994). Mutagenic analysis of the roles of SH2 and SH3 domains in regulation of the Abl tyrosine kinase. Mol. Cell. Biol. *14*, 2883-2894.

McIntyre,K.W., Shuster,D.J., Gillooly,K.M., Dambach,D.M., Pattoli,M.A., Lu,P., Zhou,X.D., Qiu,Y., Zusi,F.C., and Burke,J.R. (2003). A highly selective inhibitor of I kappa B kinase, BMS-

345541, blocks both joint inflammation and destruction in collagen-induced arthritis in mice. Arthritis Rheum. *48*, 2652-2659.

McWhirter,J.R., Galasso,D.L., and Wang,J.Y.J. (1993). A coiled-coil oligomerization domain of *bcr* is essential for the transforming function of *bcr-abl* oncoproteins. Mol. Cell. Biol. *13*, 7587-7595.

Melnick,J.S., Janes,J., Kim,S., Chang,J.Y., Sipes,D.G., Gunderson,D., Jarnes,L., Matzen,J.T., Garcia,M.E., Hood,T.L., Beigi,R., Xia,G., Harig,R.A., Asatryan,H., Yan,S.F., Zhou,Y., Gu,X.J., Saadat,A., Zhou,V., King,F.J., Shaw,C.M., Su,A.I., Downs,R., Gray,N.S., Schultz,P.G., Warmuth,M., and Caldwell,J.S. (2006). An efficient rapid system for profiling the cellular activities of molecular libraries. Proc. Natl. Acad. Sci. U. S. A *103*, 3153-3158.

Meyn,M.A., III, Wilson,M.B., Abdi,F.A., Fahey,N., Schiavone,A.P., Wu,J., Hochrein,J.M., Engen,J.R., and Smithgall,T.E. (2006). Src family kinases phosphorylate the Bcr-Abl SH3-SH2 region and modulate Bcr-Abl transforming activity. J. Biol. Chem. *281*, 30907-30916.

Musacchio,A., Saraste,M., and Wilmanns,M. (1994). High-resolution crystal structures of tyrosine kinase SH3 domains complexed with proline-rich peptides. Nat. Struct. Biol. *1*, 546-551.

Nagar,B. (2007). c-Abl tyrosine kinase and inhibition by the cancer drug imatinib (Gleevec/STI-571). J. Nutr. *137*, 1518S-1523S.

Nagar,B., Bornmann,W.G., Pellicena,P., Schindler,T., Veach,D.R., Miller,W.T., Clarkson,B., and Kuriyan,J. (2002). Crystal Structures of the Kinase Domain of c-Abl in Complex with the Small Molecule Inhibitors PD173955 and Imatinib (STI-571). Cancer Res. *62*, 4236-4243.

Nagar,B., Hantschel,O., Seeliger,M., Davies,J.M., Weis,W.I., Superti-Furga,G., and Kuriyan,J. (2006). Organization of the SH3-SH2 unit in active and inactive forms of the c-Abl tyrosine kinase. Mol. Cell *21*, 787-798.

Nagar,B., Hantschel,O., Young,M.A., Scheffzek,K., Veach,D., Bornmann,W., Clarkson,B., Superti-Furga,G., and Kuriyan,J. (2003). Structural basis for the autoinhibition of c-Abl tyrosine kinase. Cell *112*, 859-871.

Nardi,V., Azam,M., and Daley,G.Q. (2004). Mechanisms and implications of imatinib resistance mutations in BCR-ABL. Curr. Opin. Hematol. *11*, 35-43.

Nowell,P.C. (1962). The minute chromosome (Phl) in chronic granulocytic leukemia. Blut *8*, 65-66.

Nowell,P.C. (2007). Discovery of the Philadelphia chromosome: a personal perspective. J. Clin. Invest *117*, 2033-2035.

O'Hare,T., Walters,D.K., Stoffregen,E.P., Jia,T., Manley,P.W., Mestan,J., Cowan-Jacob,S.W., Lee,F.Y., Heinrich,M.C., Deininger,M.W., and Druker,B.J. (2005). In vitro activity of Bcr-Abl

inhibitors AMN107 and BMS-354825 against clinically relevant imatinib-resistant Abl kinase domain mutants. Cancer Res. *65*, 4500-4505.

Obsilova,V., Vecer,J., Herman,P., Pabianova,A., Sulc,M., Teisinger,J., Boura,E., and Obsil,T. (2005). 14-3-3 Protein interacts with nuclear localization sequence of forkhead transcription factor FoxO4. Biochemistry *44*, 11608-11617.

Oda,T., Heaney,C., Hagopian,J.R., Okuda,K., Griffin,J.D., and Druker,B.J. (1994). Crkl is the major tyrosine-phosphorylated protein in neutrophils from patients with chronic myelogenous leukemia. J. Biol. Chem. *269*, 22925-22928.

Ohanian,M., Cortes,J., Kantarjian,H., and Jabbour,E. (2012). Tyrosine kinase inhibitors in acute and chronic leukemias. Expert. Opin. Pharmacother. *13*, 927-938.

Ohren,J.F., Chen,H., Pavlovsky,A., Whitehead,C., Zhang,E., Kuffa,P., Yan,C., McConnell,P., Spessard,C., Banotai,C., Mueller,W.T., Delaney,A., Omer,C., Sebolt-Leopold,J., Dudley,D.T., Leung,I.K., Flamme,C., Warmus,J., Kaufman,M., Barrett,S., Tecle,H., and Hasemann,C.A. (2004). Structures of human MAP kinase kinase 1 (MEK1) and MEK2 describe novel noncompetitive kinase inhibition. Nat. Struct. Mol. Biol. *11*, 1192-1197.

Okabe,S., Tauchi,T., Tanaka,Y., and Ohyashiki,K. (2011). Dasatinib preferentially induces apoptosis by inhibiting Lyn kinase in nilotinib-resistant chronic myeloid leukemia cell line. J. Hematol. Oncol. *4*, 32.

Pap,M. and Cooper,G.M. (1998). Role of glycogen synthase kinase-3 in the phosphatidylinositol 3-Kinase/Akt cell survival pathway. J. Biol. Chem. *273*, 19929-19932.

Pawson,T. and Gish,G. (1992). SH2 and SH3 domains: from structure to function. Cell *71*, 359-362.

Pawson,T. and Schlessingert,J. (1993). SH2 and SH3 domains. Curr. Biol. *3*, 434-442.

Pear,W.S., Miller,J.P., Xu,L., Pui,J.C., Soffer,B., Quackenbush,R.C., Pendergast,A.M., Bronson,R., Aster,J.C., Scott,M.L., and Baltimore,D. (1998). Efficient and rapid induction of a chronic myelogenous leukemia-like myeloproliferative disease in mice receiving P210 bcr/abl-transduced bone marrow. Blood *92*, 3780-3792.

Pendergast,A.M. (2002). The Abl family kinases: mechanisms of regulation and signaling. Adv. Cancer Res. *85*, 51-100.

Pendergast,A.M., Quilliam,L.A., Cripe,L.D., Bassing,C.H., Dai,Z., Li,N., Batzer,A., Rabun,K.M., Der,C.J., Schlessinger,J., and Gishizky,M.L. (1993). *BCR-ABL*-induced oncogenesis is mediated by direct interaction with the SH2 domain of the GRB-2 adaptor protein. Cell *75*, 175-185.

Pene-Dumitrescu,T., Peterson,L.F., Donato,N.J., and Smithgall,T.E. (2008). An inhibitor-resistant mutant of Hck protects CML cells against the antiproliferative and apoptotic effects of the broad-spectrum Src family kinase inhibitor A-419259. Oncogene *27*, 7055-7069.

Pene-Dumitrescu,T. and Smithgall,T.E. (2010). Expression of a Src family kinase in chronic myelogenous leukemia cells induces resistance to imatinib in a kinase-dependent manner. J. Biol. Chem. *285*, 21446-21457.

Peng,Z., Yuan,Y., Li,Y.J., Wang,H.X., Shi,J., Cao,W.X., Luo,H.W., Deng,J.R., and Feng,W.L. (2012). Targeting BCR tyrosine177 site with novel SH2-DED causes selective leukemia cell death in vitro and in vivo. Int. J. Biochem. Cell Biol. *44*, 861-868.

Pisabarro,M.T., Serrano,L., and Wilmanns,M. (1998). Crystal structure of the abl-SH3 domain complexed with a designed high-affinity peptide ligand: implications for SH3-ligand interactions. J. Mol. Biol. *281*, 513-521.

Pluk,H., Dorey,K., and Superti-Furga,G. (2002). Autoinhibition of c-Abl. Cell *108*, 247-259.

Plumb,R.S., Johnson,K.A., Rainville,P., Smith,B.W., Wilson,I.D., Castro-Perez,J.M., and Nicholson,J.K. (2006). UPLC/MS(E); a new approach for generating molecular fragment information for biomarker structure elucidation. Rapid Commun. Mass Spectrom. *20*, 1989-1994.

Ptasznik,A., Nakata,Y., Kalota,A., Emerson,S.G., and Gewirtz,A.M. (2004). Short interfering RNA (siRNA) targeting the Lyn kinase induces apoptosis in primary, and drug-resistant, BCR-ABL1(+) leukemia cells. Nat. Med. *10*, 1187-1189.

Puil,L., Liu,J., Gish,G., Mbamalu,G., Bowtell,D., Pelicci,P.G., Arlinghaus,R., and Pawson,T. (1994). Bcr-Abl oncoproteins bind directly to activators of the Ras signalling pathway. EMBO J. *13*, 764-773.

Quintas-Cardama,A. and Cortes,J. (2009). Molecular biology of bcr-abl1-positive chronic myeloid leukemia. Blood *113*, 1619-1630.

Quintas-Cardama,A., Kantarjian,H., and Cortes,J. (2007). Flying under the radar: the new wave of BCR-ABL inhibitors. Nat. Rev. Drug Discov. *6*, 834-848.

Quintas-Cardama,A., Kantarjian,H.M., and Cortes,J.E. (2009). Mechanisms of primary and secondary resistance to imatinib in chronic myeloid leukemia. Cancer Control *16*, 122-131.

Ramaraj,P., Singh,H., Niu,N., Chu,S., Holtz,M., Yee,J.K., and Bhatia,R. (2004). Effect of mutational inactivation of tyrosine kinase activity on BCR/ABL-induced abnormalities in cell growth and adhesion in human hematopoietic progenitors. Cancer Res. *64*, 5322-5331.

Ren,R. (2002). The molecular mechanism of chronic myelogenous leukemia and its therapeutic implications: studies in a murine model. Oncogene *21*, 8629-8642.

Ren,R. (2005). Mechanisms of BCR-ABL in the pathogenesis of chronic myelogenous leukaemia. Nat. Rev. Cancer *5*, 172-183.

Rix,U., Hantschel,O., Durnberger,G., Remsing Rix,L.L., Planyavsky,M., Fernbach,N.V., Kaupe,I., Bennett,K.L., Valent,P., Colinge,J., Kocher,T., and Superti-Furga,G. (2007). Chemical

proteomic profiles of the BCR-ABL inhibitors imatinib, nilotinib, and dasatinib reveal novel kinase and nonkinase targets. Blood *110*, 4055-4063.

Rowley,J.D. (1973). A new consistent chromosomal abnormality in chronic myelogenous leukemia identified by quinacrine fluorescence and G Giemsa staining. Nature *243*, 290-293.

Rowley,J.D. (1980). Ph1-positive leukaemia, including chronic myelogenous leukaemia. Clin. Haematol. *9*, 55-86.

Roychowdhury,S. and Talpaz,M. (2011). Managing resistance in chronic myeloid leukemia. Blood Rev. *25*, 279-290.

Samanta,A., Perazzona,B., Chakraborty,S., Sun,X., Modi,H., Bhatia,R., Priebe,W., and Arlinghaus,R. (2011). Janus kinase 2 regulates Bcr-Abl signaling in chronic myeloid leukemia. Leukemia *25*, 463-472.

Samanta,A.K., Lin,H., Sun,T., Kantarjian,H., and Arlinghaus,R.B. (2006). Janus kinase 2: a critical target in chronic myelogenous leukemia. Cancer Res. *66*, 6468-6472.

Sato,M., Maruoka,M., Yokota,N., Kuwano,M., Matsui,A., Inada,M., Ogawa,T., Ishida-Kitagawa,N., and Takeya,T. (2011). Identification and functional analysis of a new phosphorylation site (Y398) in the SH3 domain of Abi-1. FEBS Lett. *585*, 834-840.

Sattler,M., Mohi,M.G., Pride,Y.B., Quinnan,L.R., Malouf,N.A., Podar,K., Gesbert,F., Iwasaki,H., Li,S., Van Etten,R.A., Gu,H., Griffin,J.D., and Neel,B.G. (2002). Critical role for Gab2 in transformation by BCR/ABL. Cancer Cell *1*, 479-492.

Sattler,M., Salgia,R., Okuda,K., Uemura,N., Durstin,M.A., Pisick,E., Xu,G., Li,J.L., Prasad,K.V., and Griffin,J.D. (1996). The proto-oncogene product p120CBL and the adaptor proteins CRKL and c-CRK link c-ABL, p190BCR/ABL and p210BCR/ABL to the phosphatidylinositol-3' kinase pathway. Oncogene *12*, 839-846.

Savage,D.G. and Antman,K.H. (2002a). Imatinib mesylate--a new oral targeted therapy. N. Engl. J. Med. *346*, 683-693.

Savage,D.G. and Antman,K.H. (2002b). Imatinib mesylate--a new oral targeted therapy. N. Engl. J. Med. *346*, 683-693.

Sawyers,C.L. (1992). The *bcr-abl* gene in chronic myelogenous leukemia. Cancer Surveys *15*, 37-51.

Sawyers,C.L. (1999). Chronic myeloid leukemia. N. Engl. J. Med. *340*, 1330-1340.

Schindler,T., Bornmann,W., Pellicena,P., Miller,W.T., Clarkson,B., and Kuriyan,J. (2000). Structural mechanism for STI-571 inhibition of abelson tyrosine kinase. Science *289*, 1938-1942.

Schwetz,B.A. (2001). From the Food and Drug Administration. JAMA *286*, 35.

Sebastien Brier and John R.Engen (2008). Hydrogen Exchange Mass Spectrometry: Principles and Capabilities. In Mass Spectrometry Analysis for Protein-Protein Interactions and Dynamics, Mark Chance, ed. Wiley & Sons, Inc.), pp. 11-43.

Seeliger,D. and de Groot,B.L. (2010). Ligand docking and binding site analysis with PyMOL and Autodock/Vina. J. Comput. Aided Mol. Des *24*, 417-422.

Shah,N.P., Nicoll,J.M., Nagar,B., Gorre,M.E., Paquette,R.L., Kuriyan,J., and Sawyers,C.L. (2002). Multiple BCR-ABL kinase domain mutations confer polyclonal resistance to the tyrosine kinase inhibitor imatinib (STI571) in chronic phase and blast crisis chronic myeloid leukemia. Cancer Cell *2*, 117-125.

Shah,N.P., Tran,C., Lee,F.Y., Chen,P., Norris,D., and Sawyers,C.L. (2004). Overriding imatinib resistance with a novel ABL kinase inhibitor. Science *305*, 399-401.

Sherbenou,D.W., Hantschel,O., Kaupe,I., Willis,S., Bumm,T., Turaga,L.P., Lange,T., Dao,K.H., Press,R.D., Druker,B.J., Superti-Furga,G., and Deininger,M.W. (2010). BCR-ABL SH3-SH2 domain mutations in chronic myeloid leukemia patients on imatinib. Blood.

Shi,Y., Alin,K., and Goff,S.P. (1995). Abl-interactor-1, a novel SH3 protein binding to the carboxy-terminal portion of the Abl protein, suppresses v-abl transforming activity. Genes Dev. *9*, 2583-2597.

Shtivelman,E., Lifshitz,B., Gale,R.P., and Canaani,E. (1985). Fused transcript of *abl* and *bcr* genes in chronic myelogenous leukemia. Nature *315*, 550-554.

Shtivelman,E., Lifshitz,B., Gale,R.P., Roe,B.A., and Canaani,E. (1986). Alternative splicing of RNAs transcribed from the human abl gene and from the bcr-abl fused gene. Cell *47*, 277-284.

Sillaber,C., Gesbert,F., Frank,D.A., Sattler,M., and Griffin,J.D. (2000). STAT5 activation contributes to growth and viability in Bcr/Abl-transformed cells. Blood *95*, 2118-2125.

Skorski,T., Bellacosa,A., Nieborowska-Skorska,M.N., Majewski,M., Martinez,R., Choi,J.K., Trotta,R., Wlodarski,P., Perrotti,D., Chan,T.O., Wasik,M.A., Tsichlis,P.N., and Calabretta,B. (1997). Transformation of hematopoietic cells by BCR/ABL requires activation of a PI-3K/Akt-dependent pathway. EMBO J. *16*, 6151-6161.

Smith,J.M., Katz,S., and Mayer,B.J. (1999). Activation of the Abl tyrosine kinase in vivo by Src homology 3 domains from the Src homology 2/Src homology 3 adaptor Nck. J. Biol. Chem. *274*, 27956-27962.

Smith,K.M., Yacobi,R., and Van Etten,R.A. (2003). Autoinhibition of Bcr-Abl through its SH3 domain. Mol. Cell *12*, 27-37.

Smithgall,T.E. (1995). SH2 and SH3 domains: potential targets for anti-cancer drug design. J. Pharmacol. Toxicol. Methods *34*, 125-132.

Stanglmaier,M., Warmuth,M., Kleinlein,I., Reis,S., and Hallek,M. (2003a). The interaction of the Bcr-Abl tyrosine kinase with the Src kinase Hck is mediated by multiple binding domains. Leukemia *17*, 283-289.

Stanglmaier,M., Warmuth,M., Kleinlein,I., Reis,S., and Hallek,M. (2003b). The interaction of the Bcr-Abl tyrosine kinase with the Src kinase Hck is mediated by multiple binding domains. Leukemia *17*, 283-289.

Steelman,L.S., Abrams,S.L., Whelan,J., Bertrand,F.E., Ludwig,D.E., Basecke,J., Libra,M., Stivala,F., Milella,M., Tafuri,A., Lunghi,P., Bonati,A., Martelli,A.M., and McCubrey,J.A. (2008). Contributions of the Raf/MEK/ERK, PI3K/PTEN/Akt/mTOR and Jak/STAT pathways to leukemia. Leukemia *22*, 686-707.

Steelman,L.S., Pohnert,S.C., Shelton,J.G., Franklin,R.A., Bertrand,F.E., and McCubrey,J.A. (2004). JAK/STAT, Raf/MEK/ERK, PI3K/Akt and BCR-ABL in cell cycle progression and leukemogenesis. Leukemia *18*, 189-218.

Sun,X., Li,Y., Yu,W., Wang,B., Tao,Y., and Dai,Z. (2008). MT1-MMP as a downstream target of BCR-ABL/ABL interactor 1 signaling: polarized distribution and involvement in BCR-ABL-stimulated leukemic cell migration. Leukemia *22*, 1053-1056.

Superti-Furga,G. and Courtneidge,S.A. (1995). Structure-function relationships in Src family and related protein tyrosine kinases. BioEssays *17*, 321-330.

ten,H.J., Kaartinen,V., Fioretos,T., Haataja,L., Voncken,J.W., Heisterkamp,N., and Groffen,J. (1994). Cellular interactions of CRKL, and SH2-SH3 adaptor protein. Cancer Res. *54*, 2563-2567.

Thomas,J., Wang,L., Clark,R.E., and Pirmohamed,M. (2004). Active transport of imatinib into and out of cells: implications for drug resistance. Blood *104*, 3739-3745.

Van Etten,R.A. (1999). Cycling, stressed-out and nervous: cellular functions of c-Abl. Trends Cell Biol. *9*, 179-186.

Van Etten,R.A., Jackson,P., and Baltimore,D. (1989). The mouse type IV c-*abl* gene product is a nuclear protein, and activation of its transforming ability is associated with cytoplasmic localization. Cell *58*, 669-678.

Van Etten,R.A., Jackson,P.K., Baltimore,D., Sanders,M.C., Matsudaira,P.T., and Janmey,P.A. (1994). The COOH terminus of the c-Abl tyrosine kinase contains distinct F- and G-actin binding domains with bundling activity. J. Cell Biol. *124*, 325-340.

Voncken,J.W., Kaartinen,V., Pattengale,P.K., Germeraad,W.T., Groffen,J., and Heisterkamp,N. (1995). BCR/ABL P210 and P190 cause distinct leukemia in transgenic mice. Blood *86*, 4603-4611.

Wales,T.E. and Engen,J.R. (2006). Hydrogen exchange mass spectrometry for the analysis of protein dynamics. Mass Spectrom. Rev. *25*, 158-170.

Wales,T.E., Fadgen,K.E., Gerhardt,G.C., and Engen,J.R. (2008). High-speed and high-resolution UPLC separation at zero degrees Celsius. Anal. Chem. *80*, 6815-6820.

Warmuth,M., Bergmann,M., Priess,A., Hauslmann,K., Emmerich,B., and Hallek,M. (1997). The Src family kinase Hck interacts with Bcr-Abl by a kinase- independent mechanism and phosphorylates the Grb2-binding site of Bcr. J. Biol. Chem. *272*, 33260-33270.

Weis,D.D., Wales,T.E., Engen,J.R., Hotchko,M., and Ten Eyck,L.F. (2006). Identification and characterization of EX1 kinetics in H/D exchange mass spectrometry by peak width analysis. J. Am. Soc. Mass Spectrom. *17*, 1498-1509.

Weisberg,E., Manley,P., Mestan,J., Cowan-Jacob,S., Ray,A., and Griffin,J.D. (2006). AMN107 (nilotinib): a novel and selective inhibitor of BCR-ABL. Br. J. Cancer *94*, 1765-1769.

Weisberg,E., Manley,P.W., Breitenstein,W., Bruggen,J., Cowan-Jacob,S.W., Ray,A., Huntly,B., Fabbro,D., Fendrich,G., Hall-Meyers,E., Kung,A.L., Mestan,J., Daley,G.Q., Callahan,L., Catley,L., Cavazza,C., Azam,M., Neuberg,D., Wright,R.D., Gilliland,D.G., and Griffin,J.D. (2005). Characterization of AMN107, a selective inhibitor of native and mutant Bcr-Abl. Cancer Cell *7*, 129-141.

Weisberg,E., Manley,P.W., Cowan-Jacob,S.W., Hochhaus,A., and Griffin,J.D. (2007). Second generation inhibitors of BCR-ABL for the treatment of imatinib-resistant chronic myeloid leukaemia. Nat. Rev. Cancer *7*, 345-356.

Wen,S.T. and Van Etten,R.A. (1997). The PAG gene product, a stress-induced protein with antioxidant properties, is an Abl SH3-binding protein and a physiological inhibitor of c-Abl tyrosine kinase activity. Genes Dev. *11*, 2456-2467.

Wilson,M.B., Schreiner,S.J., Choi,H.-J., Kamens,J.S., and Smithgall,T.E. (2002). Selective pyrrolo-pyrimidine inhibitors reveal a necessary role for Src family kinases in Bcr-Abl signal transduction and oncogenesis. Oncogene *21*, 8075-8088.

Wong,S. and Witte,O.N. (2004). The BCR-ABL story: bench to bedside and back. Annu. Rev. Immunol. *22*, 247-306.

Wu,J., Meng,F., Lu,H., Kong,L., Bornmann,W., Peng,Z., Talpaz,M., and Donato,N.J. (2008). Lyn regulates BCR-ABL and Gab2 tyrosine phosphorylation and c-Cbl protein stability in imatinib-resistant chronic myelogenous leukemia cells. Blood *111*, 3821-3829.

Wu,Y. and Engen,J.R. (2004). What mass spectrometry can reveal about protein function. Analyst *129*, 290-296.

Xie,S., Wang,Y., Liu,J., Sun,T., Wilson,M.B., Smithgall,T.E., and Arlinghaus,R.B. (2001). Involvement of Jak2 tyrosine phosphorylation in Bcr-Abl transformation. Oncogene *20*, 6188-6195.

Xiong,X., Cui,P., Hossain,S., Xu,R., Warner,B., Guo,X., An,X., Debnath,A.K., Cowburn,D., and Kotula,L. (2008). Allosteric inhibition of the nonMyristoylated c-Abl tyrosine kinase by phosphopeptides derived from Abi1/Hssh3bp1. Biochim. Biophys. Acta *1783*, 737-747.

Yaish,P., Gazit,A., Gilon,C., and Levitzki,A. (1988). Blocking of EGF-dependent cell proliferation by EGF receptor kinase inhibitors. Science *242*, 933-935.

Yu,H., Rosen,M.K., Sin,T.B., Seidel-Dugan,C., Brugge,J.S., and Schreiber,S.L. (1992). Solution structure of the SH3 domain of Src and identification of its ligand binding site. Science *258*, 1665-1668.

Zha,J., Harada,H., Yang,E., Jockel,J., and Korsmeyer,S.J. (1996). Serine phosphorylation of death agonist BAD in response to survival factor results in binding to 14-3-3 not BCL-X(L). Cell *87*, 619-628.

Zhang,J., Adrian,F.J., Jahnke,W., Cowan-Jacob,S.W., Li,A.G., Iacob,R.E., Sim,T., Powers,J., Dierks,C., Sun,F., Guo,G.R., Ding,Q., Okram,B., Choi,Y., Wojciechowski,A., Deng,X., Liu,G., Fendrich,G., Strauss,A., Vajpai,N., Grzesiek,S., Tuntland,T., Liu,Y., Bursulaya,B., Azam,M., Manley,P.W., Engen,J.R., Daley,G.Q., Warmuth,M., and Gray,N.S. (2010). Targeting Bcr-Abl by combining allosteric with ATP-binding-site inhibitors. Nature *463*, 501-506.

Zhang,J., Yang,P.L., and Gray,N.S. (2009). Targeting cancer with small molecule kinase inhibitors. Nat. Rev. Cancer *9*, 28-39.

Zhao,R.C., Jiang,Y., and Verfaillie,C.M. (2001). A model of human p210(bcr/ABL)-mediated chronic myelogenous leukemia by transduction of primary normal human CD34(+) cells with a BCR/ABL-containing retroviral vector. Blood *97*, 2406-2412.

Zhao,X., Ghaffari,S., Lodish,H., Malashkevich,V.N., and Kim,P.S. (2002). Structure of the Bcr-Abl oncoprotein oligomerization domain. Nat. Struct. Biol. *9*, 117-120.

Zhou,T., Commodore,L., Huang,W.S., Wang,Y., Thomas,M., Keats,J., Xu,Q., Rivera,V.M., Shakespeare,W.C., Clackson,T., Dalgarno,D.C., and Zhu,X. (2011). Structural mechanism of the Pan-BCR-ABL inhibitor ponatinib (AP24534): lessons for overcoming kinase inhibitor resistance. Chem. Biol. Drug Des *77*, 1-11.

Zhuang,C., Tang,H., Dissanaike,S., Cobos,E., Tao,Y., and Dai,Z. (2011). CDK1-mediated phosphorylation of Abi1 attenuates Bcr-Abl-induced F-actin assembly and tyrosine phosphorylation of WAVE complex during mitosis. J. Biol. Chem. *286*, 38614-38626.